Universidade do Estado do Rio de Janeiro

Centro de Ciências e Tecnologia

Instituto de Química
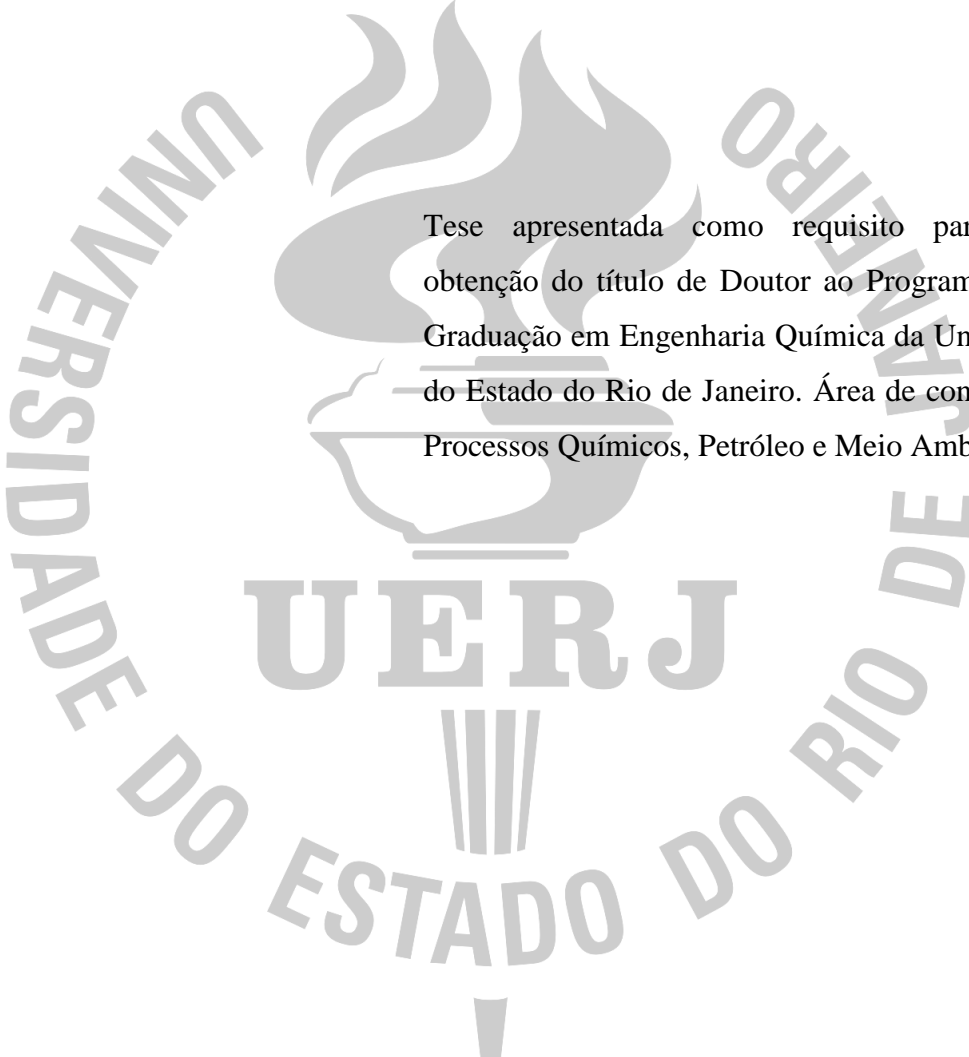
Caroline de Oliveira Gonçalves

Design optimization of shell-and-tube heat exchangers using mathematical programming

Rio de Janeiro

2019

Caroline de Oliveira Gonçalves

Design optimization of shell-and-tube heat exchangers using mathematical programming

Tese apresentada como requisito parcial para obtenção do título de Doutor ao Programa de Pós-Graduação em Engenharia Química da Universidade do Estado do Rio de Janeiro. Área de concentração: Processos Químicos, Petróleo e Meio Ambiente.

Orientadores: Prof. Dr. André Luiz Hemerly Costa e Prof. Dr. Miguel Jorge Bagajewicz

Rio de Janeiro

2019

Autorizo, apenas para fins acadêmicos e científicos, a reprodução total ou parcial desta dissertação, desde que citada a fonte.

_____   _____

      Assinatura   Data

Caroline de Oliveira Gonçalves

Design optimization of shell-and-tube heat exchangers using mathematical programming

> Tese apresentada como requisito parcial para obtenção do título de Doutor ao Programa de Pós-Graduação em Engenharia Química da Universidade do Estado do Rio de Janeiro. Área de concentração: Processos Químicos, Petróleo e Meio Ambiente.

Aprovada em 25 de fevereiro de 2019

Orientadores:

_____
Prof. Dr. André Luiz Hemerly Costa
Instituto de Química – UERJ

_____
Prof. Dr. Miguel Jorge Bagajewicz
Instituto de Química – UERJ

Banca Examinadora:

_____
Prof. Dr. Marco Antonio Gaya de Figueiredo
Instituto de Química – UERJ

_____
Prof. Dr. Eduardo Rocha de Almeida Lima
Instituto de Química – UERJ

_____
Dra. Andressa Nakao
PEQ/COPPE – UFRJ

_____
Prof. Dr. Eduardo Mach Queiroz
Escola de Química – UFRJ

_____
Dr. Sérgio Gregório de Oliveira
CENPES – PETROBRAS

Rio de Janeiro

2019

DEDICATÓRIA

Dedico esta Tese a meus pais, por sempre me apoiarem e incentivarem em todas as circunstâncias, mas principalmente nos estudos.

AGRADECIMENTOS

A Deus pela vida e por tantas bênçãos recebidas.

Ao meu orientador, Prof. André Hemerly, por sua dedicação, sua atenção, sua amizade, sua confiança e seu exemplo como professor e pesquisador não só durante a orientação deste trabalho, mas desde quando comecei como sua aluna de mestrado. Agradeço imensamente você ter dividido uma parte de seu conhecimento comigo, pelo incentivo durante toda a minha vida acadêmica, pela participação direta na minha formação como pesquisadora. Sinto-me muito honrada de ter sido sua aluna por todos esses anos e tenho muita admiração por você.

Ao meu orientador, Prof. Miguel Bagajewicz, pela confiança desde o início do doutorado, por dividir parte do seu conhecimento ajudando imensamente no progresso do meu trabalho, pelo incentivo a publicação de artigos e pela acolhida e oportunidade de realizar parte do meu doutorado na University of Oklahoma.

Ao meu marido, Frederico, pelo apoio e compreensão nesta fase da minha formação. Obrigada por apoiar minhas escolhas e me incentivar a continuar trilhando o caminho da pesquisa e da docência.

Aos meus pais, Carlos e Marytsa, que sempre me mostraram o quanto era importante estudar, buscar conhecimento, fazer o que ama e me apoiaram em todas as minhas escolhas sempre com muito amor.

Aos meus irmãos Carlos e Marcele, por sempre estarem ao meu lado me apoiando, algumas vezes perturbando, algumas vezes aconselhando, mas sempre juntos.

À minha Voninha (*in memoriam*), Zaíra, que sempre esteve ao meu lado e foi grande incentivadora aos estudos e infelizmente faleceu em 2018, mas que tenho certeza estaria vibrando ao meu lado com mais essa etapa conquistada.

À minha querida família, em especial tia Maryse, tio Ronaldo, tio Altair e tia Maysa, por terem me ensinado o que é amar e ser amado e sempre torcerem por mim.

Aos amigos Bruna, Felipe, Susana, Diego, Julyana, Luiz Flávio, pela amizade, pelo apoio e pela alegria compartilhada, sem vocês minha vida acadêmica não seria a mesma!

As minhas amigas desde a Federal de Química, as ciclopentinas, Juliana, Ariane, Thabata e Bianca por estarem ao meu lado nos momentos tristes e felizes.

RESUMO

GONÇALVES, C. de O. *Otimização do projeto de trocadores de calor casco-e-tubo empregando programação matemática.* 2019. 148f. Tese (Doutorado em Engenharia Química) – Instituto de Química, Universidade do Estado do Rio de Janeiro, Rio de Janeiro, 2019.

Trocadores de calor são equipamentos largamente empregados na indústria de processos, sendo responsáveis pelo aquecimento, resfriamento, vaporização ou condensação de correntes materiais. A abordagem clássica de projeto de um trocador de calor consiste em um procedimento de tentativa e erro, onde o projetista, baseado na sua experiência, avalia de forma sequencial as diferentes alternativas de equipamentos, buscando identificar uma solução que atenda às especificações do serviço térmico da melhor forma possível. Entretanto, tal abordagem é fortemente dependente da experiência do engenheiro responsável. Por esta razão, mais modernamente, um grande número de trabalhos de pesquisa foi publicado propondo procedimentos de projeto baseados em algoritmos de otimização capazes de identificar a melhor solução dentro do espaço de busca disponível automaticamente, sem a intervenção direta do projetista. Diante deste quadro, esta tese apresenta uma contribuição inédita à literatura na aplicação de técnicas de otimização via programação matemática para a determinação do ótimo global no projeto de trocadores de calor. Do ponto de vista do escopo, esta proposta de tese será focada em serviços sem mudança de fase. Através da aplicação de técnicas de programação matemática, são propostas formulações do problema levando em conta os métodos de cálculo de Kern e de Bell-Delaware. A primeira formulação resulta em um problema de Programação Linear Inteira (ILP) e a segunda formulação corresponde a um problema de Programação Linear Inteira Mista (MILP). O caráter linear de ambas as formulações permite a identificação do ótimo global, mesmo utilizando algoritmos de otimização convencionais. As formulações propostas são capazes de identificar soluções viáveis para o projeto de trocadores de calor com menor custo que aquelas obtidas através da formulação convencional do projeto.

Palavras-chave: Trocador de calor. Otimização global. Programação matemática.

ABSTRACT

GONÇALVES, C. de O. *Design optimization of shell-and-tube heat exchangers using mathematical programming.* 2019. 148f. Tese (Doutorado em Engenharia Química) – Instituto de Química, Universidade do Estado do Rio de Janeiro, Rio de Janeiro, 2019.

Heat exchangers are widely used equipment in the process industry and are responsible for heating, cooling, vaporizing or condensing material streams. The classic design of a heat exchanger consists of a trial and error procedure, where the designer, based on his experience, evaluates in a sequential way different equipment alternative, aiming to identify a solution that fulfils the specifications of the thermal service in the best possible way. However, such approach is heavily dependent on the experience of the responsible engineer. For this reason, most currently, many research works have been published proposing design procedures based on optimization algorithms capable of identifying the best solution within the available search space automatically, without the direct intervention of the designer. According to this context, this thesis presents an unprecedented contribution to the literature for the application of optimization techniques through mathematical programming for the determination of global optimum in the design of heat exchangers. From the point of view of scope, this thesis proposal will be focused on services without phase change. Through the application of mathematical programming techniques, formulations of the problem are proposed, taking into account the Kern and Bell-Delaware calculation methods. The first formulation results in an integer linear programming (ILP) problem and the second formulation correspond to a mixed integer linear programming (MILP) problem. The linear character of both formulations allows the identification of the global optimum, even using conventional optimization algorithms. The proposed formulations are capable of identifying feasible solutions for the design of heat exchangers with lower costs than those obtained through the conventional design formulation.

Keywords: Heat exchanger. Global optimization. Mathematical programming.

LISTA DE ILUSTRAÇÕES

LISTA DE TABELAS

LISTA DE ABREVIATURAS E SIGLAS

TEMA	Tubular Exchangers Manufacturers Association
ILP	Integer Linear Programing
MILP	Mixed Integer Linear Programing
MINLP	Mixed Integer Nonlinear Programing
GAMS	General Algebraic Modelling System

LISTA DE SÍMBOLOS

- Latin letters

A area, m^2

$\widehat{Aexc}$ excess area, %

$Areq$ required area, m^2

Ar area between adjacent baffles, m^2

a, $a1$, $a2$, $a3$, $a4$ Colburn's heat transfer factor parameters

b, $b1$, $b2$, $b3$, $b4$ friction factor for ideal tube bank flow parameters

Cl tube layout parameter

Cbh Bell-Delaware parameter according to the flow

Cps heat capacity of shell-side fluid

Cpt heat capacity of tube-side fluid

dte outer tube diameter, m

dti inner tube diameter, m

Deq equivalent diameter, m

Ds shell diameter, m

Dw hydraulic diameter, m

fs Darcy friction factor for shell-side

ft Darcy friction factor for tube-side

F LMTD correction factor

FAR free area ratio

Fc fraction of the number of tubes in pure cross flow between baffle tips

Fw fraction of the number of tubes inside one window

$Fsbp$ ratio of the bypass area between the tube bundle and the shell to the cross-flow area

$\widehat{FMP}$ value of the correction factor of the LMTD

$\hat{g}$ gravity acceleration, m/s^2

Gs Mass flux, kg/(m²s)

hi convective heat transfer coefficient ideal for shell-side, W/m^{2}K

hs convective heat transfer coefficient for shell-side, W/m^{2}K

ht convective heat transfer coefficient for tube-side, W/m^{2}K

Jc, Jl, Jb, Jr Bell-Delaware method parameters

$\widehat{ks}$ thermal conductivity of the fluid on shell-side, W/m·K

$\widehat{kt}$	thermal conductivity of the fluid on tube-side, W/m·K
$\widehat{ktube}$	thermal conductivity of the tube wall, W/m·K
lay	layout of the heat exchanger
Lbb	shell-to-tubes clearances (for fixed tubesheet or U tubes), m
lbc	baffle spacing, m
Lsb	shell-to-baffle diametral clearance, m
ltp	tube pitch, m
ltp_{eff}	distance between tubes along the rows perpendicular to the flow, m
Lpl	the effect of the tube lane partition bypass width, m
Lpp	shell parameter
L	tube length, m
$\widehat{ms}$	mass flow rate on shell-side, kg/s
$\widehat{mt}$	mass flow rate on tube-side, kg/s
Nb	number of baffles
Nc	total number of rows crossed along the entire heat exchanger
Npt	number of tube passes
Ntp	number of tubes per pass
Ntt	total number of tubes
$Ntcc$	number of tube rows crossed between baffle tips
$Ntcw$	effective number of tube rows crossed in the baffle window
Ntw	number of tubes from the window area
Nus	Nusselt number for shell-side
Nut	Nusselt number for tube-side
$\widehat{PDs}_{srow}$	standard shell diameter, m
$\widehat{Pdte}_{srow}$	standard outer tube diameter, m
$\widehat{Pdti}_{srow}$	standard inner tube diameter, m
$\widehat{PL}_{srow}$	standard tube length, m
$\widehat{Play}_{srow}$	tube layout
$\widehat{PNb}_{srow}$	number of baffles
$\widehat{PNpt}_{srow}$	number of tube passes
$\widehat{PNtt}_{srow}$	total number of tubes
$\widehat{Prp}_{srow}$	standard tube pitch ratio
$\widehat{Prs}$	Prandtl for shell-side

$\widehat{Prt}$	Prandtl for tube-side
$\hat{Q}$	heat load, W
rlm	ratio of both leakage areas to the cross-flow area
rp	pitch ratio
rs	ratio of the shell-to-baffle leakage area to the sum of this area and the tube-to-baffle leakage area
Rb	by-pass correction factor
Res	Reynolds number for shell-side
Ret	Reynolds number for tube-side
Rfs	fouling factor on shell-side, m^2K/W
Rft	fouling factor on tube-side, m^2K/W
Rl	leakage correction factor
Sb	bypass flow area between the tube bundle and the shell, m²
Sm	the cross-flow area is delimited between adjacent baffles, m²
Stb	area of the flow through the hole leakage area of the baffle, m²
Ssb	the flow area between the shell and the baffle, m²
Sw	the free flow area through the baffle window, m²
Swg	gross window flow area, m²
Swt	the area occupied by the tubes, m²
$\widehat{Tci}$	cold stream inlet temperature, ºC
$\widehat{Tco}$	cold stream outlet temperature, ºC
$\widehat{Thi}$	hot stream inlet temperature, ºC
$\widehat{Tho}$	hot stream outlet temperature, ºC
U	overall heat transfer coefficient, W/m^2 K
vs	shell-side flow velocity, m/s
$\widehat{vsmax}$	maximum shell-side flow velocity, m/s
$\widehat{vsmin}$	minimum shell-side flow velocity, m/s
vt	tube-side flow velocity, m/s
$\widehat{vtmax}$	maximum tube-side flow velocity, m/s
$\widehat{vtmin}$	minimum tube-side low velocity, m/s
w	product of binary variables
x	design variable
$\widehat{xd_i}$	discret option of design variable x

y	binary variable
yd_{sd}	binary variable representing the tube diameter
yDs_{sDs}	binary variable representing the shell diameter
yL_{sL}	binary variable representing the tube length
$ylay_{slay}$	binary variable representing the tube layout
yNb_{sNb}	binary variable representing the number of baffles
$yNpt_{sNpt}$	binary variable representing the number of tube passes
yrp_{srp}	binary variable representing the tube pitch ratio
$yrow_{srow}$	binary variable that represents simultaneously all discrete variables

- Greek letters

ΔPs	pressure drop on shell-side, Pa
ΔPc	pressure drop in the flow through the tube bundle between adjacent baffles in cross flow, Pa
ΔPe	the pressure drop at the end zones, Pa
ΔPbi	the ideal bank pressure drop delimited by one central baffle spacing, Pa
ΔPw	the pressure drop in the baffle windows, Pa
$\widehat{\Delta Psdisp}$	available pressure drop on shell-side, Pa
ΔPt	pressure drop on tube-side, Pa
$\widehat{\Delta Ptdisp}$	available pressure drop on tube-side, Pa
$\widehat{\Delta Tlm}$	logarithmic mean temperature difference, ºC
$\widehat{\mu s}$	viscosity of the fluid on shell-side, Pa·s
$\widehat{\mu t}$	viscosity of the fluid on tube-side, Pa·s
$\widehat{\rho s}$	density of the fluid on the shell-side, kg/m^3
$\widehat{\rho t}$	density of the fluid on the tube-side, kg/m^3
θDs	central angle defined by the intercession of the baffle cut edge with the shell
θctl	central angle delimited by the intercession between the baffle cut edge and the circle associated to the centers of the outer tubes
ψ_n	represents the omission of tubes inside the shell due to the presence of multiple tube passes
$\hat{\varepsilon}$	small positive number

TABLE OF CONTENTS

INTRODUCTION

Heat exchangers are widely used equipment in the process industry and are responsible for heating, cooling, vaporizing or condensing material streams. There are numerous examples of services involving heat exchangers in the chemical process industry, such as heating raw material streams until reaction conditions are reached, separating components of interest through the condensation of vapour streams, supplying energy to fractionation by distillation, cooling of product streams for storage, etc. Faced with the increase in energy costs over the last decades, the interest in the analysis of processes involving thermal exchange has increased considerably.

The classic design of a heat exchanger consists of a trial and error procedure, where the designer, based on his experience, evaluates in a sequential way different equipment alternative, seeking to identify a solution that meets the specifications of the thermal service of the best (KERN, 1950). However, such approach is heavily dependent on the experience of the responsible engineer.

Due to their wide use in various functions, a considerable part of the investment to be made in a process plant is consumed in the acquisition of heat exchangers. In this way, the development of procedures to optimize the design of this type of equipment can bring considerable economic gains. For this reason, most currently, many research works have been published proposing design procedures based on optimization algorithms capable of identifying the best solution within the available search space automatically, without the direct intervention of the designer.

Due to the large diversity of different thermal services, there are several alternatives of types of heat exchangers available, such as, shell-and-tube heat exchangers, double pipe heat exchangers, gasketed-and-plate heat exchangers, etc. However, despite the increasing development of new solutions, the chemical process industry is still heavily based on the use of shell and tube heat exchangers due to their robustness, versatility and reliability.

According to this scenario, this thesis presents the development of optimization algorithms for the minimization of costs in the design of shell-and-tube heat exchangers. For this, we chose to use mathematical programming tools, with special attention to issues involving global optimization. Each solution candidate is described by a set of standard values of the design variables, coherent with industrial practice; each allows the conversion of all the original Mixed Integer Nonlinear Programming (MINLP) models into linear ones.

This thesis is organized as follows: Chapter 1 brings a brief review of the literature with the works that have been developed around the subject of this thesis; Chapter 2 presents the development of the MILP heat exchanger design model, employed with Kern Method; Chapter 3 contains the alternative formulations for shell and tube heat exchanger optimal design with Kern method; Chapter 4 encompasses the mixed integer linear programming considering the Bell Delaware method; and finally, the conclusions and suggestions are presented.

1　**LITERATURE REVIEW**

The review of the literature will encompass the following subjects: heat exchangers calculation and optimization of heat exchanger design.

1.1　**Heat exchanger calculation**

1.1.1　**Logarithmic mean temperature difference method**

The Logarithmic Mean Temperature Difference method (LMTD) is the main method to describe the steady-state behavior of shell-and-tube heat exchangers. The main variable for design purposes is the heat transfer area and for that, we must know the inlet and outlet temperatures of both streams that are exchanging heat. However, the temperature difference can be not uniform inside the equipment and a solution is to use an average temperature difference. According to the LMTD method, the heat transfer area can be calculated by (INCROPERA and DE WITT, 2006):

$$Q = UA\ \Delta Tlm\ F \tag{1}$$

where Q is the heat transfer rate, A is the heat transfer area, U is the overall heat transfer coefficient, ΔTlm is the logarithmic mean temperature difference for the equivalent countercurrent configuration, and F is a correction factor.

The expression of the logarithmic mean temperature difference is:

$$\Delta Tlm = \frac{(Thi-Tco)-(Tho-Tci)}{\ln(\frac{(Thi-Tco)}{(Tho-Tci)})} \tag{2}$$

where T represent the temperature, the subscript h refers to the hot stream, subscript c to the cold stream, o to the outlet and i to the inlet.

The logarithmic temperature difference concept can be directly applied to the countercurrent or the cocurrent flow configurations. The application of the LMTD method for other configurations demands the utilization of the correction factor, F. For example, for

shell-and-tube heat exchangers with multiple even tube-side passes, the expression of the correction factor is:

$$F = \frac{(R^2+1)^{0.5}\ln\left(\frac{(1-P)}{(1-RP)}\right)}{(R-1)\ln\left(\frac{2-P\left(R+1-(R^2+1)^{0.5}\right)}{2-P\left(R+1+(R^2+1)^{0.5}\right)}\right)}$$ (3)

where:

$$R = \frac{Thi-Tho}{Tco-Tci}$$ (4)

$$P = \frac{Tco-Tci}{Thi-Tci}$$ (5)

1.1.2 Tube-side convective heat transfer coefficient and pressure drop

The dimensionless representation of the convective heat transfer coefficient (*ht*) corresponds to the Nusselt number (*Nut*) (INCROPERA and DE WITT, 2006):

$$Nut = \frac{ht\,dti}{kt}$$ (6)

where kt is the tube-side fluid thermal conductivity and *dti* is the inner tube diameter.

The Nusselt number is a dimensionless parameter determined by theoretical models or empirical correlations. The specific model to be applied depends on the flow regime.

One of the correlations that can be used for calculating the Nusselt number for turbulent flow is the Gnielinski correlation (INCROPERA and DE WITT, 2006), that can also be used for the transition region ($2300 < Ret < 5\cdot10^6$):

$$Nut^{Gni} = \frac{\left(ft/8\right)(Ret-1000)Prt}{1+12.7\left(ft/8\right)^{1/2}\left(Prt^{2/3}-1\right)}$$ (7)

where *ft* is the friction factor for the tube-side, *Ret* is the Reynolds number and Prt is the Prandlt number. For the laminar flow ($Ret \leq 2300$), the effects related to the entry region may be relevant. Therefore for $Prt > 5$, the Hausen correlation is employed:

$$Nut^{Hau} = 3.66 + \frac{0.0668\left(dti/L\right)Ret\,Prt}{1+0.04\left[\left(dti/L\right)Ret\,Prt\right]^{2/3}} \qquad (8)$$

For $0.6 \leq Prt \leq 5$, we use the Sieder and Tate correlation:

$$Nut^{S\&T} = 1.86\left(\frac{Ret\,Prt}{L/dti}\right)^{1/3} \qquad (9)$$

However, when the Nusselt falls lower than 3.66 (theoretical result for fully developed flow), then this limit value is used: $Nut^{theo} = 3.66$.

Another correlation used for turbulent flow is Dittus-Boelter (INCROPERA and DE WITT, 2006):

$$Nut^{D\&B} = 0.023\,Ret^{0.8}Prt^{n} \qquad (10)$$

where *n* is a parameter equal to 0.3, if the tube-side fluid is being cooled, and 0.4 if it is being heated.

Despite the Gnielinski correlation gives more accurate results, Dittus-Boelter correlation is simpler, allowing its use in more complex problems, like heat exchanger design optimization problems (MIZUTANI et al., 2003).

1.1.3 **Shell-side convective heat transfer coefficient**

The flow of the shell-side is a complex combination of different flow paths, where the main transversal flow path between adjacent baffles is combined with a set of secondary streams that flows through the constructional clearances and gaps. The next paragraphs describe the main methods available for evaluation of the thermo-fluid dynamic behavior of the shell-side flow: Kern method (KERN, 1950), Bell-Delaware method (BELL, 1960) and the streams method.

1.1.3.1 Kern method (KERN, 1950)

The Kern method is one of the most popular and traditional methods of calculation proposed. It has been used extensively in the design of heat exchangers; however, the error can be high in some cases.

The Kern method has easy application but has limited accuracy. The Kern method analysis does not describe the leakage and bypass streams in its equation.

This method is restricted to baffles that have a 25% window cut-off percentage and is not applicable to laminar flow; however, the method allows a rapid estimation of the pressure drop and the heat transfer coefficient on the shell-side (KERN, 1950). The detailed model and its equations will be shown later.

1.1.3.2   Bell-Delaware method (BELL, 1960)

The Bell-Delaware method arises in the early 60's and is considered a more accurate procedure than the Kern method, since it already recognizes the division of the flow into several streams as shown in Figure 1 in a schematic representation of the shell-side flow. The Bell-Delaware method addresses the effects of flow through windows and by-pass streams and leakage through multiplicative factors applied to cross-flow results. This method uses several correction factors for the transversal flow to consider flow through the windows, leak flows and bypass flows.

Figure 1 - Shell-side flow
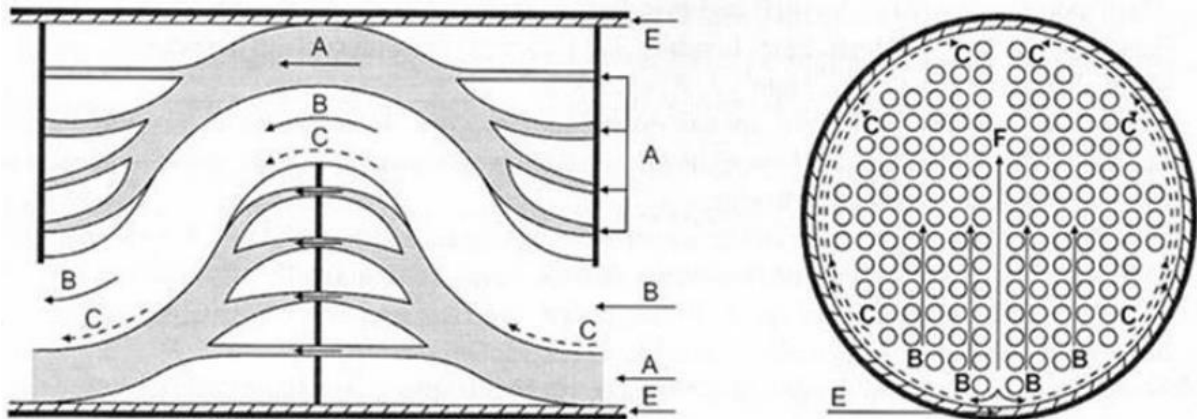
Source: TABOREK, 2008a.

In Figure 1, Stream B is the ideal one, the one that most favors heat transfers. If only stream B existed, the correction factors, shown in Equation 11, would not be necessary:

$$h = h_{ideal} J_c J_l J_b J_r J_s \tag{11}$$

In Equation 11, h_{ideal} is the one calculated for a cross flow through a tube bundle, in which all the stream flows perpendicularly to the tubes. The correction factor J_c is related to the baffle cut and spacing, J_l is the correction factor that considers the shell-baffle and baffle-tube leak streams (streams A and E in Figure 1), J_b is the correction factor due to the different baffle spacing in the inlet and outlet regions of the equipment and J_r is the correction factor for the adverse temperature gradient in laminar flow.

1.1.3.3 Stream analysis method

In the stream analysis method, a hydraulic model is used to calculate the pressure drop and flows in the shell of heat exchangers. These flows are used to calculate the coefficient of heat transfer on the shell-side. This approach, although dependent on empirical parameters, is considered more fundamental than the Bell method because it is based on hydraulic principles that take into account the interactions between the streams on the shell side.

The first approach related to this method was proposed by Tinker (1947) and developed later by others. Due to its more complex structure, computational routines are necessary for its implementation. Wills and Johnston (1984) published a simplified and more complete version of this method, however, the complete version of this method is not available in open literature. The use of this method is only possible through a commercial software.

1.2 Optimization of the exchanger design

Shell and tube heat exchangers are the most common type of thermal equipment in chemical process industries. The wide use of shell-and-tube heat exchangers can be explained by its robustness, versatility and reliability (SAUNDERS, 1988).

The traditional approach for the design of shell-and-tube heat exchangers involves a trial-and-verification procedure where, at each solution candidate, a skilled engineer must identify the constraint violations (e.g. shell-side pressure-drop higher than the allowable value, etc.) and propose modifications to attain a feasible solution (e.g. increase the baffle spacing). The time consumed in the design and the performance of the resulting solution is

highly dependent on the experience of the designer. Because the trial-and-error procedure stops when a feasible exchanger is obtained, the resulting solution is not necessarily optimal and depends on the initial choices.

Modern textbooks (SERTH, 2007; BELL, 2008; CAO, 2010) also presents in essence the same trial-and-error design procedure: first an initial tentative heat exchanger is proposed, then the heat exchanger is rated, and the results are checked to verify if the heat exchanger is acceptable, considering the excess area and the allowable pressure drop. If the proposed heat exchanger does not satisfy the task demands, alterations in the design must be made and followed by a new rating and further examination. The procedure must be repeated until an acceptable solution is found. This traditional approach involves the direct intervention of a skilled engineer and remained somewhat unaltered for a long time. Alternatively, algorithms based on heuristic rules, which could be implemented in a computer code, were also proposed for the identification of a design solution (BELL, 2008; CAO, 2010). However, the heuristic nature of these schemes does not guarantee that the area or the cost are optimal.

More recently, heat exchanger design was considered as an optimization problem with cost being minimized. However, for a given heat transfer task, an accurate assessment of the heat exchanger capital cost would require elaborate costing of parts as well as assembly costs. For this reason, previous works usually employed some substitutes: heat exchanger area or a simplified cost function in relation to the area. Therefore, the objective function used normally is the minimization of the heat exchanger area or the total annualized cost, including capital (area based) and operating costs (pumping costs).

The techniques for design optimization of shell and tube heat exchangers can be organized in three mains classes: heuristic rules based on thermofluidynamic relations, metaheuristic methods and mathematical programming.

The utilization of heuristic rules involves different techniques for the exploration of the search space, such as, graphical analysis and systematic screening of the counting table. Muralikrishna and Shenoy (2000) proposed the analysis of the feasible region of the design problem through a pressure drop graph using geometrical and operational constraints. The insertion of objective function curves in the proposed graph allowed the identification of the best design alternative. Ravagnani et al. (2003) proposed the application of a heuristic algorithm to a crescent sequence of shell diameters in the counting table aiming to identify the smallest heat exchanger according to the pressure drop constraints. Eryener (2006) presented several graphs associated to the baffle spacing aiming to identify the optimal value of this design parameter. Costa and Queiroz (2008) applied a systematic screening of the counting

table, based on discrete alternatives, seeking to identify the heat exchanger with the smallest area for a given thermal task.

Different metaheuristic algorithms were used to solve the optimal design problem: simulated annealing (CHAUDHURI, 1997), genetic algorithms (TAYAL et al., 1999; WILDI-TREMBLAY et al., 2007; PONCE-ORTEGA et al., 2009), particle swarm (RAVAGNANI et al., 2009; PATEL and RAO, 2010), imperialist competitive algorithm (HADIDI et al., 2013), cuckoo-search algorithm (ASADI et al., 2014), firefly algorithm (MOHANTY, 2016), etc. However, there is a lack of organized comparative studies that allow a clear assessment of the best options among the existent alternatives. In addition, none of these techniques guarantees global optimality.

The utilization of mathematical programming based on a more rigorous treatment of optimality conditions was also investigated. Because of the nature of the problem variables, involving continuous (e.g. heat transfer coefficients, pressure drops, etc.) and discrete variables (e.g. tube diameter, number of the tubes, etc.), and the nonlinearity of the thermal and hydraulic model equations, all works use a mixed-integer nonlinear optimization (MINLP) formulation. Mizutani et al. (2003) formulated the design optimization based on general disjunctive programming, which structure is organized as a MINLP problem. The objective function encompasses capital and operating costs, and the heat exchanger model is based on the Bell-Delaware method (TABOREK, 2008c). Ponce-Ortega et al. (2006) employed an MINLP formulation to the design of series of shell and tube heat exchangers with 1 shell pass and 2 tube passes. The dimensioning of the heat exchanger components, however, is not discussed. Ravagnani and Caballero (2007) organized the MINLP problem describing the set of heat exchanger design variables associated to the mechanical components according to their corresponding discrete values and the remaining model variables as continuous ones.

A common feature of all mathematical programming papers in the literature of heat exchanger design is the nonconvexity of the formulations proposed, which does not guarantee global optimality when using local solvers. An exception of all these string of articles in mathematical programming is the early work of Jegede and Polley (1992), who propose a simplified model consisting of three equations involving the heat transfer coefficients of both tube and shell side and the area, as well as the pressure drops on both sides. For fixed pressure drops these equations can be solved and then other parameters can be obtained. Unfortunately, some parameters as the number of tubes may not be integers. In addition, if the diameters of tubes and lengths are standardized and limited to discrete values, the procedure may also

render values that do not match these discrete options. There is no procedure suggested as of how large these mismatches are and how they ought to be handled. When pressure drops are to be optimized in addition to area, the procedure includes pumping/compression costs. Finally, if the pressure drops are to be subject just to a maximum limit, the procedure ought to be different.

2 SHELL AND TUBE HEAT EXCHANGER DESIGN USING MIXED-INTEGER LINEAR PROGRAMMING WITH KERN METHOD

This chapter presents the formulation of the optimization design problem of shell-and-tube heat exchanger in a linear form. The analysis is focused on shell and tube heat exchanger without phase change. We use an E-shell type and the service must be executed in a single shell without loss of generality. The flow regime considered is a turbulent one, as it is common in industrial equipment. The physical properties are assumed constant, according to average values. Because we are focusing on the design procedure and not on the model, we chose the simpler Kern formulation for the shell-side equations (KERN, 1950) and the Dittus-Boelter as well as the Darcy-Weisbach for the tube-side (SAUNDERS, 1988; INCROPERA and DE WITT, 2006).

In this section, the problem parameters, which are fixed prior the optimization, are represented with the symbol "^".

2.1 Heat Exchanger Model

Fluid Allocation: The selection of the tube-side and shell-side streams depends on several factors, e.g., fouling, temperature, pressure, flow rate, etc. Therefore, it will be considered that the stream allocation is established prior the optimization. Thus, the values of the physical properties in the tube-side and shell-side streams are fixed parameters.

Shell-Side Thermal and Hydraulic Equations: The flow velocity in the shell-side (*vs*) depends on the flow area between adjacent baffles (*Ar*):

$$vs = \frac{\widehat{ms}}{\widehat{\rho s}\, Ar} \tag{12}$$

where $\widehat{ms}$ and $\widehat{\rho s}$ are the shell-side stream flow rate and density, respectively.

This flow area corresponds to the area delimited by the shell diameter (*Ds*) and baffle spacing (*lbc*) multiplied by the free area ratio (*FAR*):

$$Ar = Ds\, FAR\, lbc \tag{13}$$

The free area ratio between baffles is given by:

$$FAR = \frac{(ltp - dte)}{ltp} = 1 - \frac{dte}{ltp} = 1 - \frac{1}{rp} \qquad (14)$$

where *ltp* is the tube pitch, *dte* is the outer tube diameter, and *rp* is the ratio between the tube pitch and the tube diameter.

The Reynolds number associated to the shell-side velocity (*Res*) is given by:

$$Res = \frac{Deq \; vs \; \widehat{\rho s}}{\widehat{\mu s}} \qquad (15)$$

where *Deq* is the equivalent diameter, and $\widehat{\mu s}$ is the shell-side fluid viscosity.

The equivalent diameter present in the Reynolds number depends on the tube layout. For a square and triangular pattern, respectively:

$$Deq = \frac{4 \; ltp^2}{\pi \; dte} - dte \qquad \text{(Square pattern)} \qquad (16)$$

$$Deq = \frac{3.46 \; ltp^2}{\pi \; dte} - dte \qquad \text{(Triangular pattern)} \qquad (17)$$

The Nusselt number for the shell-side flow (*Nus*) is a function of the Reynolds and Prandtl numbers (*Res* and $\widehat{Prs}$) (KERN, 1950):

$$Nus = 0.36 \; Res^{0.55} \widehat{Prs}^{1/3} \qquad (18)$$

where the dimensionless groups Nusselt and Prandtl are defined by:

$$Nus = \frac{hs \; Deq}{\widehat{ks}} \qquad (19)$$

$$\widehat{Prs} = \frac{\widehat{Cps} \; \widehat{\mu s}}{\widehat{ks}} \qquad (20)$$

where hs is the shell-side convective heat transfer coefficient, $\widehat{ks}$ is the thermal conductivity, and $\widehat{Cps}$ is the heat capacity.

The head loss in the shell-side flow, dismissing nozzle pressure drop, can be calculated by (KERN, 1950):

$$\frac{\Delta Ps}{\widehat{\rho s}\,\hat{g}} = fs\frac{Ds(Nb+1)}{Deq}\left(\frac{vs^2}{2\,\hat{g}}\right) \tag{21}$$

where ΔPs is the shell-side stream pressure drop, fs is the shell-side friction factor and Nb is the number of baffles.

The expression for evaluation of the shell-side friction factor is:

$$fs = 1.728\,Res^{-0.188} \tag{22}$$

The number of baffles is directly related to the baffle spacing and tube length:

$$Nb = \frac{L}{lbc} - 1 \tag{23}$$

Tube-Side Thermal and Hydraulic Equations: The flow velocity in the tube-side (vt) depends on the number of tubes per pass (Ntp) and the inner tube diameter (dti):

$$vt = \frac{4\,\widehat{mt}}{Ntp\,\pi\,\widehat{\rho t}\,dti^2} \tag{24}$$

where $\widehat{mt}$ and $\widehat{\rho t}$ are the tube-side stream flow rate and density, respectively.

The equation of the Reynolds number related to the tube-side flow rate (Ret) is:

$$Ret = \frac{dti\,vt\,\widehat{\rho t}}{\widehat{\mu t}} \tag{25}$$

where dti is the inner tube diameter, and $\widehat{\mu t}$ is the tube-side fluid viscosity.

The Prandtl number for the tube-side fluid ($\widehat{Prt}$) is:

$$\widehat{Prt} = \frac{\widehat{Cpt}\,\widehat{\mu t}}{\widehat{kt}} \tag{26}$$

where $\widehat{kt}$ and $\widehat{Cpt}$ are the tube-side fluid thermal conductivity, and heat capacity, respectively.

The Reynolds and Prandtl numbers allow the evaluation of the tube-side Nusselt number (*Nut*) through the Dittus-Boelter correlation (INCROPERA and DE WITT, 2006):

$$Nut = 0.023\,Ret^{0.8}\,\widehat{Prt}^n \tag{27}$$

where the parameter n is equal to 0.4 for heating services and 0.3 for cooling services.

The definition of the Nusselt number is:

$$Nut = \frac{ht\,dti}{\widehat{kt}} \tag{28}$$

where *ht* is the tube-side convective heat transfer coefficient.

The head loss in the tube-side flow, dismissing nozzle pressure drop and the variation of the physical properties, is given by (SAUNDERS, 1988):

$$\frac{\Delta Pt}{\widehat{\rho t}\,\hat{g}} = \frac{ft\,Npt\,L\,vt^2}{2\,\hat{g}\,dti} + \frac{K\,Npt\,vt^2}{2\,\hat{g}} \tag{29}$$

where *ΔPt* is the tube-side stream pressure drop, and *ft* is the tube-side friction factor. The first term in the RHS (right hand side) corresponds to the head loss in the tube bundle and the second corresponds to the head loss in the front and rear headers. The parameter *K* is equal to 0.9 for one tube pass and 1.6 for two or more tube passes (SAUNDERS, 1988).

The expression for the Darcy friction factor for turbulent flow can be expressed by (SAUNDERS, 1988):

$$ft = 0.014 + \frac{1.056}{Ret^{0.42}} \tag{30}$$

Overall Heat Transfer Coefficient: The expression of the overall heat transfer coefficient (*U*) is:

$$U = \frac{1}{\frac{dte}{dti\,ht} + \frac{\widehat{Rft}\,dte}{dti} + \frac{dte\ln(\frac{dte}{dti})}{2\,\widehat{ktube}} + \widehat{Rfs} + \frac{1}{hs}} \tag{31}$$

where the $\widehat{ktube}$ is the thermal conductivity of the tube wall, and $\widehat{Rft}$ and $\widehat{Rfs}$ are the fouling factors of the tube-side and shell-side streams, respectively.

Heat Transfer Rate Equation: According to the LMTD method, the heat transfer rate expression is:

$$\widehat{Q} = UAreq\,\widehat{\Delta Tlm}\;F \tag{32}$$

where $\widehat{Q}$ is the heat load, *Areq* is the required area, $\widehat{\Delta Tlm}$ is logarithmic mean temperature difference (LMTD), and *F* is the LMTD correction factor.

The LMTD is given by:

$$\widehat{\Delta Tlm} = \frac{(\widehat{Thi} - \widehat{Tco}) - (\widehat{Tho} - \widehat{Tci})}{\ln(\frac{(\widehat{Thi} - \widehat{Tco})}{(\widehat{Tho} - \widehat{Tci})})} \tag{33}$$

The LMTD correction factor is equal to 1 for one tube pass, and is equal to the following expression for an even number of tube passes:

$$F = \frac{(\widehat{R}^2 + 1)^{0.5}\;\ln\left(\frac{(1 - \widehat{P})}{(1 - \widehat{R}\,\widehat{P})}\right)}{(\widehat{R} - 1)\ln\left(\frac{2 - \widehat{P}\left(\widehat{R} + 1 - (\widehat{R}^2 + 1)^{0.5}\right)}{2 - \widehat{P}\left(\widehat{R} + 1 + (\widehat{R}^2 + 1)^{0.5}\right)}\right)} \tag{34}$$

where:

$$\hat{R} = \frac{\widehat{Thi} - \widehat{Tho}}{\widehat{Tco} - \widehat{Tci}} \tag{35}$$

$$\hat{P} = \frac{\widehat{Tco} - \widehat{Tci}}{\widehat{Thi} - \widehat{Tci}} \tag{36}$$

The heat transfer area (A) is represented by the sum of the area of the surface of each tube:

$$A = Ntt\ \pi\ dte\ L \tag{37}$$

where Ntt is the total number of tubes.

In order to guarantee an adequate design margin, the exchanger area must be higher than the required area according to a certain "excess area" ($\widehat{Aexc}$), specified by the design engineer:

$$A \geq \left(1 + \frac{\widehat{Aexc}}{100}\right) * Areq \tag{38}$$

Therefore, the heat transfer rate equation is reorganized using actual heat exchanger area:

$$UA \geq \left(1 + \frac{\widehat{Aexc}}{100}\right) \frac{\hat{Q}}{\widehat{\Delta Tlm}\ F} \tag{39}$$

Bounds on Pressure Drops, Flow Velocities and Reynolds Numbers: During the process design, allowable pressure drops are imposed according to the pressure profile of the unit. These parameters are related to a trade-off between capital and operating costs. The corresponding constraints are:

$$\Delta Ps \leq \widehat{\Delta Psdisp} \tag{40}$$

$$\Delta Pt \leq \widehat{\Delta Ptdisp} \tag{41}$$

Additionally, lower and upper bounds on flow velocities are also established:

$$vs \geq \widehat{vsmin} \tag{42}$$

$$vs \leq \widehat{vsmax} \tag{43}$$

$$vt \geq \widehat{vtmin} \tag{44}$$

$$vt \leq \widehat{vtmax} \tag{45}$$

Flow velocity lower bounds seek to avoid fouling susceptible conditions. Corresponding upper bounds aims to avoid erosional conditions that could damage the heat exchanger during its operational life.

According to the application range of the convective heat transfer coefficient correlations, there are bounds on the Reynolds numbers in the shell-side and tube-side:

$$Res \geq 2{\cdot}10^3 \tag{46}$$

$$Ret \geq 10^4 \tag{47}$$

Geometric Constraints: The baffle spacing must be limited between 20% and 100% of the shell diameter (TABOREK, 2008d):

$$lbc \geq 0.2\, Ds \tag{48}$$

$$lbc \leq 1.0\, Ds \tag{49}$$

The ratio between the tube length and shell diameter must be between 3 and 15 (TABOREK, 2008b):

$$L \geq 3\, Ds \tag{50}$$

$$L \leq 15\, Ds \tag{51}$$

Objective function: The optimization problem seeks to minimize the heat transfer area, which has a direct impact in the exchanger cost:

$$\min \quad A \tag{52}$$

Other objective functions can be constructed. Normally, capital cost is monotone with area, so minimizing area is somehow equivalent to minimizing the capital cost.

2.2   Model Reformulation Using Discrete Variables

In the proposed problem formulation, each discrete design variable (x) is represented according to their respective standard indexed values. That is, x is now represented by several discrete options $\widehat{xd}_i$, of which one and only one will be chosen. Thus, we introduce a set of binary variables y_i, and write x as follows:

$$x = \sum_i \widehat{xd}_i\, y_i \tag{53}$$

$$\sum_i y_i = 1 \tag{54}$$

According to the engineering practice and Tubular Exchangers Manufactures Association (TEMA) standards (TABOREK, 2008d; TEMA, 2007), these design variables are: inner and outer tube diameter (*dti* and *dte*), tube length (*L*), number of baffles (*Nb*), number of tube passes (*Npt*), pitch ratio (*rp*), shell diameter (*Ds*), and tube layout (*lay*).

Therefore, for our discrete variables, we write:

$$dte = \sum_{sd=1}^{sdmax} \widehat{pdte}_{sd}\, yd_{sd} \tag{55}$$

$$dti = \sum_{sd=1}^{sdmax} \widehat{pdti}_{sd} \, yd_{sd} \tag{56}$$

$$\sum_{sd=1}^{sdmax} yd_{sd} = 1 \tag{57}$$

$$L = \sum_{sL=1}^{sLmax} \widehat{pL}_{sL} \, yL_{sL} \tag{58}$$

$$\sum_{sL=1}^{sLmax} yL_{sL} = 1 \tag{59}$$

$$Nb = \sum_{sNb=1}^{sNbmax} \widehat{pNb}_{sNb} \, yNb_{sNb} \tag{60}$$

$$\sum_{sNb=1}^{sNbmax} yNb_{sNb} = 1 \tag{61}$$

$$Npt = \sum_{sNpt=1}^{sNptmax} \widehat{pNpt}_{sNpt} \, yNpt_{sNpt} \tag{62}$$

$$\sum_{sNpt=1}^{sNptmax} yNpt_{sNpt} = 1 \tag{63}$$

$$rp = \sum_{srp=1}^{srpmax} \widehat{prp}_{srp} \, yrp_{srp} \tag{64}$$

$$\sum_{srp=1}^{srpmax} yrp_{srp} = 1 \tag{65}$$

$$Ds = \sum_{sDs=1}^{sDsmax} \widehat{pDs}_{sDs} \, yDs_{sDs} \tag{66}$$

$$\sum_{sDs=1}^{sDsmax} yDs_{sDs} = 1 \tag{67}$$

$$lay = \sum_{slay=1}^{slaymax} \widehat{play}_{slay} \, ylay_{slay} \tag{68}$$

$$\sum_{slay=1}^{slaymax} ylay_{slay} = 1 \tag{69}$$

Instead of leaving this discrete representation as additional equations to the model, we substitute them in the rest of the equations. After the substitution of the discrete variables by its binary representation, mathematical expressions appear in the heat exchanger model in the form $p^{n1} q^{n2} \cdots z^{nm}$ that are replaced as follows:

$$p^{n1}q^{n2}\cdots z^{nm} = [\textstyle\sum_i \widehat{pd}_i\, yp_i]^{n1}\, [\textstyle\sum_j \widehat{qd}_j\, yq_j]^{n2}\, [\textstyle\sum_k \widehat{zd}_k\, yz_k]^{nm} \tag{70}$$

Because all binary variables assume a value 1 only once in the corresponding set (see Equation 54), it is easy to see that Equation 70 becomes:

$$p^{n1}q^{n2}\cdots z^{nm} = \textstyle\sum_{i,j,..k} \widehat{pd}_i^{\;n1}\, \widehat{qd}_j^{\;n2}\, ...\, \widehat{zd}_k^{\;nm}\, yp_i\, yq_j\, ...\, yz_k \tag{71}$$

Therefore, the reformulated model is now composed by several expressions containing multiple summations of products of binary variables and a few continuous variables. We now show the reformulated model.

Shell-side Thermal and Hydraulic Equations: After the substitution of the discrete variables by their representation through correspondent binaries, the expression of the shell-side flow velocity obtained from Equation 12 becomes:

$$vs = \frac{\widehat{ms}}{\widehat{\rho s}\, \sum_{sDs=1}^{sDsmax} \sum_{srp=1}^{srpmax} \sum_{sL=1}^{sLmax} \sum_{sNb=1}^{sNbmax} \frac{\widehat{pDs}_{sDs}\widehat{pFAR}_{srp}\widehat{pL}_{sL}}{(\widehat{pNb}_{sNb}+1)} yDs_{sDs}\, yrp_{srp}\, yL_{sL}\, yNb_{sNb}} \tag{72}$$

This equation (Equation 72) is derived from the following expression of the flow area originally present in Equation 13:

$$Ar = \sum_{sDs=1}^{sDsmax} \sum_{srp=1}^{srpmax} \sum_{sL=1}^{sLmax} \sum_{sNb=1}^{sNbmax} \frac{\widehat{pDs}_{sDs}\widehat{pFAR}_{srp}\widehat{pL}_{sL}}{(\widehat{pNb}_{sNb}+1)} yDs_{sDs}\, yrp_{srp}\, yL_{sL}\, yNb_{sNb} \tag{73}$$

where:

$$\widehat{pFAR}_{srp} = 1 - \frac{1}{\widehat{prp}_{srp}} \tag{74}$$

The equivalent diameter corresponding to Equations (16) and (17) is given by:

$$Deq = \sum_{srp=1}^{srpmax} \sum_{sd=1}^{sdmax} \sum_{slay=1}^{slaymax} \widehat{pDeq}_{srp,sd,slay}\, yrp_{srp}\, yd_{sd}\, ylay_{slay} \tag{75}$$

where:

$$\widehat{pDeq}_{srp,sd,slay} = \frac{aDeq_{slay}\widehat{prp}_{srp}^2\widehat{pdte}_{sd}^2}{\pi\widehat{pdte}_{sd}} - \widehat{pdte}_{sd} \tag{76}$$

$$aDeq_{slay} = 4 \qquad \text{if } slay = 1 \text{ (square pattern)} \tag{77}$$

$$aDeq_{slay} = 3.46 \qquad \text{if } slay = 2 \text{ (triangle pattern)} \tag{78}$$

The Reynolds number equation, associated to the shell-side flow velocity and equivalent diameter, becomes, after reformulation of Equation (15):

$$Res =$$

$$\frac{\widehat{ms}}{\widehat{\mu s}}\left(\sum_{srp=1}^{srpmax}\sum_{sd=1}^{sdmax}\sum_{slay=1}^{slaymax}\widehat{pDeq}_{srp,sd,slay}yrp_{srp}yd_{sd}ylay_{slay}\right)\cdot$$

$$\left(\sum_{sDs=1}^{sDsmax}\sum_{srp=1}^{srpmax}\sum_{sL=1}^{sLmax}\sum_{sNb=1}^{sNbmax}\frac{(\widehat{pNb}_{sNb}+1)}{\widehat{pDs}_{sDs}\widehat{pFAR}_{srp}\widehat{pL}_{sL}}yDs_{sDs}yrp_{srp}yL_{sL}\,yNb_{sNb}\right) \tag{79}$$

Substituting the expression above of the Reynolds number in to Equation (79), the reformulated form of the Nusselt number for the shell-side flow becomes:

$$Nus = 0.36\left(\frac{\widehat{ms}}{\widehat{\mu s}}\right)^{0.55}SNus_{srp,sd,slay,sDs,sL,sNb}\widehat{Prs}^{1/3} \tag{80}$$

where $SNus_{srp,sd,slay,sDs,sL,sNb}$ represents the following sum of binary variables:

$$SNus_{srp,sd,slay,sDs,sL,sNb} =$$

$$\sum_{srp=1}^{srpmax}\sum_{sd=1}^{sdmax}\sum_{slay=1}^{slaymax}\sum_{sDs=1}^{sDsmax}\sum_{sL=1}^{sLmax}\sum_{sNb=1}^{sNbmax}\left(\frac{\widehat{pDeq}_{srp,sd,slay}(\widehat{pNb}_{sNb}+1)}{\widehat{pDs}_{sDs}\widehat{pFAR}_{srp}\widehat{pL}_{sL}}\right)^{0.55}yrp_{srp}\cdot$$

$$yd_{sd}ylay_{slay}yDs_{sDs}yL_{sL}\,yNb_{sNb} \tag{81}$$

The substitution of Equation (80) in the definition of the Nusselt number in Equation (19) yields the following equation related to the shell-side heat transfer coefficient:

$$hs = \frac{\widehat{ks}0.36\left(\frac{\widehat{ms}}{\widehat{\mu s}}\right)^{0.55} SNus_{srp,sd,slay,sDs,sL,sNb}\widehat{Prs}^{1/3}}{\sum_{srp=1}^{srpmax}\sum_{sd=1}^{sdmax}\sum_{slay=1}^{slaymax}\widehat{pDeq}_{srp,sd,slay}yrp_{srp}yd_{sd}ylay_{slay}} \tag{82}$$

The reformulation of Equation (21) of the head loss in the shell-side flow yields:

$$\Delta Ps =$$

$$\sum_{sDs=1}^{sDsmax}\sum_{sNb=1}^{sNbmax}\sum_{srp=1}^{srpmax}\sum_{sL=1}^{sLmax}\sum_{sd=1}^{srpmax}\sum_{slay=1}^{slaymax}\widehat{p\Delta Ps}_{sDs,sNb,srp,sL,sd,slay}\, yDs_{sDs}yNb_{sNb}\cdot$$

$$yrp_{srp}\,yL_{sL}\,yd_{sd}ylay_{slay} \tag{83}$$

where:

$$\widehat{p\Delta Ps}_{sDs,sNb,srp,sL,sd,slay} =$$

$$0.864\frac{\widehat{ms}^{1.812}\widehat{\mu s}^{0.188}}{\widehat{\rho s}}\left(\frac{\widehat{\mu s}}{\widehat{\mu w}}\right)^{-0.14}\left(\frac{(\widehat{pNb}_{sNb}+1)^{2.812}}{\widehat{pDs}_{sDs}{}^{0.812}(\widehat{pFAR}_{srp}\widehat{pL}_{sL})^{1.812}(\widehat{pDeq}_{srp,sd,slay})^{1.188}}\right) \tag{84}$$

Tube-side Thermal and Hydraulic Equations: The reformulation of the flow velocity in the tube-side is obtained from Equation (24):

$$vt = 4\,\widehat{mt}/(\pi\,\widehat{\rho t}\sum_{sDs=1}^{sDsmax}\sum_{sd=1}^{sdmax}\sum_{sNpt=1}^{sNptmax}\sum_{srp=1}^{srpmax}\sum_{slay=1}^{slaymax}\frac{\widehat{pNtt}_{sDs,sd,sNpt,srp,slay}\widehat{pdt\iota}_{sd}^{2}}{\widehat{pNpt}_{sNpt}}\cdot$$

$$yDs_{sDs}\,yd_{sd}yNpt_{sNpt}yrp_{srp}ylay_{slay}\,) \tag{85}$$

The Reynolds number expression (Equation (25)) is now as follows:

$$Ret = \frac{4\,\widehat{mt}}{\pi\,\widehat{\mu t}}\sum_{sDs=1}^{sDsmax}\sum_{sd=1}^{sdmax}\sum_{sNpt=1}^{sNptmax}\sum_{srp=1}^{srpmax}\sum_{slay=1}^{slaymax}\frac{\widehat{pNpt}_{sNpt}}{\widehat{pNtt}_{sDs,sd,sNpt,srp,slay}\widehat{pdt\iota}_{sd}}\cdot$$

$$yDs_{sDs}\,yd_{sd}yNpt_{sNpt}yrp_{srp}ylay_{slay} \tag{86}$$

The insertion of Equation (86) into Equation (27) yields the reformulated form of the Nusselt number for tube-side flow:

$$Nut = 0.023\left(\frac{4\,\widehat{mt}}{\pi\,\widehat{\mu t}}\right)^{0.8} SNut_{srp,sd,slay,sDs,sNpt}\widehat{Prt}^{n} \tag{87}$$

where $SNut_{srp,sd,slay,sDs,sNpt}$ represents a sum of binary variables:

$$SNut_{srp,sd,slay,sDs,sL,sNb} =$$

$$\sum_{srp=1}^{srpmax} \sum_{sd=1}^{sdmax} \sum_{slay=1}^{slaymax} \sum_{sDs=1}^{sDsmax} \sum_{sL=1}^{sLmax} \sum_{sNb=1}^{sNbmax} \left(\frac{\widehat{pNpt}_{sNpt}}{\widehat{pNtt}_{sDs,sd,sNpt,srp,slay}\widehat{pdt}_{sd}} \right)^{0.8} \cdot$$

$$yDs_{sDs} \, yd_{sd} yNpt_{sNpt} yrp_{srp} ylay_{slay} \tag{88}$$

According the definition of the Nusselt number in Equation (28), the tube-side heat transfer coefficient equation becomes:

$$ht = \frac{\widehat{kt} 0.023 \left(\frac{4\,\widehat{mt}}{\pi\,\widehat{\mu t}} \right)^{0.8} SNut_{srp,sd,slay,sDs,sNpt} \widehat{Prt}^n}{\sum_{sd=1}^{sdmax} \widehat{pdt}_{sd} yd_{sd}} \tag{89}$$

The reformulation of Equation 29 of the head loss in the tube-side flow yields:

$$\Delta Pt =$$

$$\frac{\widehat{\rho t} \; \sum_{sNpt=1}^{sNptmax} \widehat{pNpt}_{sNpt} \, yNpt_{sNpt} \sum_{sL=1}^{sLmax} \widehat{pL}_{sL} \, yL_{sL}}{2 \; \sum_{sd=1}^{sdmax} \widehat{pdt}_{sd} \, yd_{sd}} \cdot$$

$$\left(0.014 + 1.056 \left(\frac{4\,\widehat{mt}}{\pi\,\widehat{\mu t}} \frac{\widehat{pNpt}_{sNpt}}{\widehat{pNtt}_{sDs,sd,sNpt,srp,slay}\widehat{pdt}_{sd}} \right)^{-0.42} \cdot \right.$$

$$\left. \sum_{sDs=1}^{sDsmax} \sum_{sd=1}^{sdmax} \sum_{sNpt=1}^{sNptmax} \sum_{srp=1}^{srpmax} \sum_{slay=1}^{slaymax} yDs_{sDs} \, yd_{sd} \cdot yNpt_{sNpt} yrp_{srp} ylay_{slay} \right) \cdot$$

$$\left(\frac{4\,\widehat{mt}}{\pi\,\widehat{\rho t}} \frac{\widehat{pNpt}_{sNpt}}{\widehat{pNtt}_{sDs,sd,sNpt,srp,slay}\widehat{pdt}_{sd}^2} \right)^2 \cdot$$

$$\sum_{sDs=1}^{sDsmax} \sum_{sd=1}^{sdmax} \sum_{sNpt=1}^{sNptmax} \sum_{srp=1}^{srpmax} \sum_{slay=1}^{slaymax} yDs_{sDs} \, yd_{sd} \cdot yNpt_{sNpt} yrp_{srp} ylay_{slay} +$$

$$\frac{\widehat{\rho t} \left(\widehat{K1P} \, yNpt_{sNpt1} + \widehat{KMP} \, (1 - yNpt_{sNpt1}) \right) \sum_{sNpt=1}^{sNptmax} \widehat{pNpt}_{sNpt} \, yNpt_{sNpt}}{2} \cdot$$

$$\left(\frac{4\,\widehat{mt}}{\pi\,\widehat{\rho t}} \frac{\widehat{pNpt}_{sNpt}}{\widehat{pNtt}_{sDs,sd,sNpt,srp,slay}\widehat{pdt}_{sd}^2} \right)^2 \cdot$$

$$\sum_{sDs=1}^{sDsmax} \sum_{sd=1}^{sdmax} \sum_{sNpt=1}^{sNptmax} \sum_{srp=1}^{srpmax} \sum_{slay=1}^{slaymax} yDs_{sDs} \, yd_{sd} \cdot yNpt_{sNpt} yrp_{srp} ylay_{slay}$$

$$\tag{90}$$

Overall Heat Transfer Coefficient: The reformulation of the overall heat transfer coefficient in Equation (31) yields:

$$\frac{1}{U} =$$

$$\frac{1}{\left(\sum_{sDs=1}^{sDsmax} \sum_{sd=1}^{sdmax} \sum_{sNpt=1}^{sNptmax} \sum_{srp=1}^{srpmax} \sum_{slay=1}^{slaymax} \widehat{pht}_{sDs,sd,sNpt,srp,slay}\, yDs_{sDs}\, yd_{sd}yNpt_{sNpt}yrp_{srp}ylay_{slay} \right)} \cdot$$

$$\frac{\sum_{sd=1}^{sdmax} \widehat{pdte}_{sd}\, yd_{sd}}{\sum_{sd=1}^{sdmax} \widehat{pdti}_{sd}\, yd_{sd}} + \widehat{Rft}\, \frac{\sum_{sd=1}^{sdmax} \widehat{pdte}_{sd}\, yd_{sd}}{\sum_{sd=1}^{sdmax} \widehat{pdti}_{sd}\, yd_{sd}} + \frac{\sum_{sd=1}^{sdmax} \widehat{pdte}_{sd}\, yd_{sd}\, \ln\left(\frac{\sum_{sd=1}^{sdmax} \widehat{pdte}_{sd}\, yd_{sd}}{\sum_{sd=1}^{sdmax} \widehat{pdti}_{sd}\, yd_{sd}}\right)}{2\, \widehat{Ktube}} + \widehat{Rfs} +$$

$$\frac{1}{\left(\sum_{srp=1}^{srpmax} \sum_{sd=1}^{sdmax} \sum_{slay=1}^{slaymax} \sum_{sDs=1}^{sDsmax} \sum_{sL=1}^{sLmax} \sum_{sNb=1}^{sNbmax} \widehat{phs}_{srp,sd,slay,sDs,sL,sNb} yrp_{srp}yd_{sd}ylay_{slay}yDs_{sDs}yL_{sL}\, yNb_{sNb} \right)} \tag{91}$$

Heat Transfer Rate Equation: The heat transfer area related to Equation (37) is given by:

$$A = \pi \sum_{sDs=1}^{sDsmax} \sum_{sd=1}^{sdmax} \sum_{sNpt=1}^{sNptmax} \sum_{srp=1}^{srpmax} \sum_{slay=1}^{slaymax} \sum_{sL=1}^{sLmax} \widehat{pNtt}_{sDs,sd,sNpt,srp,slay} \cdot$$

$$\widehat{pdte}_{sd}\, \widehat{pL}_{sL}\, yDs_{sDs}\, yd_{sd}yNpt_{sNpt}yrp_{srp}ylay_{slay}yL_{sL} \tag{92}$$

The correction factor of the LMTD assumes the following form:

$$F = yNpt_{sNpt1} + \widehat{FMP}\,(1 - yNpt_{sNpt1}) \tag{93}$$

where $\widehat{FMP}$ is the value of the correction factor of the LMTD for a configuration with a single shell pass and an even number of tube passes (Equation (34)).

The substitution of these expressions in Equation (39) yields the reformulated form of the heat transfer rate equation:

$$\frac{1}{\left(\sum_{sDs=1}^{sDsmax}\sum_{sd=1}^{sdmax}\sum_{sNpt=1}^{sNptmax}\sum_{srp=1}^{srpmax}\sum_{slay=1}^{slaymax}\widehat{pht}_{sDs,sd,sNpt,srp,slay}\,yDs_{sDs}\,yd_{sd}yNpt_{sNpt}yrp_{srp}ylay_{slay}\right)}\cdot$$

$$\frac{\sum_{sd=1}^{sdmax}\widehat{pdte}_{sd}\,yd_{sd}}{\sum_{sd=1}^{sdmax}\widehat{pdti}_{sd}\,yd_{sd}}+\widehat{Rft}\;\frac{\sum_{sd=1}^{sdmax}\widehat{pdte}_{sd}\,yd_{sd}}{\sum_{sd=1}^{sdmax}\widehat{pdti}_{sd}\,yd_{sd}}+\frac{\sum_{sd=1}^{sdmax}\widehat{pdte}_{sd}\,yd_{sd}\ln\!\left(\frac{\sum_{sd=1}^{sdmax}\widehat{pdte}_{sd}\,yd_{sd}}{\sum_{sd=1}^{sdmax}\widehat{pdti}_{sd}\,yd_{sd}}\right)}{2\,\widehat{ktube}}+\widehat{Rfs}+$$

$$\frac{1}{\left(\sum_{srp=1}^{srpmax}\sum_{sd=1}^{sdmax}\sum_{slay=1}^{slaymax}\sum_{sDs=1}^{sDsmax}\sum_{sL=1}^{sLmax}\sum_{sNb=1}^{sNbmax}\widehat{phs}_{srp,sd,slay,sDs,sL,sNb}\,yrp_{srp}yd_{sd}ylay_{slay}yDs_{sDs}yL_{sL}\,yNb_{sNb}\right)}\leq$$

$$\frac{1}{\widehat{Q}\left(1+\frac{\widehat{Aexc}}{100}\right)}\left(\pi\sum_{sDs=1}^{sDsmax}\sum_{sd=1}^{sdmax}\sum_{sNpt=1}^{sNptmax}\sum_{srp=1}^{srpmax}\sum_{slay=1}^{slaymax}\sum_{sL=1}^{sLmax}\widehat{pNtt}_{sDs,sd,sNpt,srp,slay}\,\widehat{pdte}_{sd}\,\widehat{pL}_{sL}\cdot\right.$$

$$\left.yDs_{sDs}\,yd_{sd}yNpt_{sNpt}yrp_{srp}ylay_{slay}yL_{sL}\right)\widehat{\Delta Tlm}\;\left(yNpt_{sNpt1}+\widehat{FMP}\,(1-yNpt_{sNpt1})\right)\;(94)$$

Bounds on Pressure Drops, Flow Velocities and Reynolds Numbers: These inequality

constraints become:

$$\sum_{sDs=1}^{sDsmax}\sum_{sNb=1}^{sNbmax}\sum_{srp=1}^{srpmax}\sum_{sL=1}^{sLmax}\sum_{sd=1}^{srpmax}\sum_{slay=1}^{slaymax}\widehat{p\Delta Ps}_{sDs,sNb,srp,sL,sd,slay}\,yDs_{sDs}yNb_{sNb}\cdot$$

$$yrp_{srp}\,yL_{sL}\,yd_{sd}ylay_{slay}\;\leq\;\widehat{\Delta Psdisp}\tag{95}$$

$$\frac{\widehat{\rho t}}{2}\left(0.014\;+1.056\cdot\right.$$

$$\left(\frac{\pi\,\widehat{\mu t}}{4\,\widehat{mt}}\frac{\sum_{sDs=1}^{sDsmax}\sum_{sd=1}^{sdmax}\sum_{sNpt=1}^{sNptmax}\sum_{srp=1}^{srpmax}\sum_{slay=1}^{slaymax}\widehat{pNtt}_{sDs,sd,sNpt,srp,slay}yDs_{sDs}\,yd_{sd}yNpt_{sNpt}yrp_{srp}ylay_{slay}}{\sum_{sNpt=1}^{sNptmax}\widehat{pNpt}_{sNpt}\,yNpt_{sNpt}}\cdot\right.$$

$$\left.\left.\sum_{sd=1}^{sdmax}\widehat{pdti}_{sd}\,yd_{sd}\right)^{-0.42}\right)\cdot$$

$$\sum_{sNpt=1}^{sNptmax}\widehat{pNpt}_{sNpt}\,yNpt_{sNpt}\;\sum_{sL=1}^{sLmax}\widehat{pL}_{sL}\,yL_{sL}\cdot$$

$$\left(\frac{4\,\widehat{mt}}{\pi\,\widehat{\rho t}}\frac{\sum_{sNpt=1}^{sNptmax}\widehat{pNpt}_{sNpt}\,yNpt_{sNpt}}{\sum_{sDs=1}^{sDsmax}\sum_{sd=1}^{sdmax}\sum_{sNpt=1}^{sNptmax}\sum_{srp=1}^{srpmax}\sum_{slay=1}^{slaymax}\widehat{pNtt}_{sDs,sd,sNpt,srp,slay}yDs_{sDs}\,yd_{sd}yNpt_{sNpt}yrp_{srp}ylay_{slay}}\cdot\right.$$

$$\left.\frac{1}{\left(\sum_{sd=1}^{sdmax}\widehat{pdti}_{sd}\,yd_{sd}\right)^2}\right)^2\cdot\frac{1}{\sum_{sd=1}^{sdmax}\widehat{pdti}_{sd}\,yd_{sd}}+$$

$$\frac{\widehat{\rho t}}{2}\left(\widehat{K1P}\,yNpt_{sNpt1}+\widehat{KMP}\,(1-yNpt_{sNpt1})\right)\;\sum_{sNpt=1}^{sNptmax}\widehat{pNpt}_{sNpt}\,yNpt_{sNpt}\cdot$$

$$\left(\frac{4\,\widehat{mt}}{\pi\,\widehat{\rho t}}\frac{\sum_{sNpt=1}^{sNptmax}\widehat{pNpt}_{sNpt}\,yNpt_{sNpt}}{\sum_{sDs=1}^{sDsmax}\sum_{sd=1}^{sdmax}\sum_{sNpt=1}^{sNptmax}\sum_{srp=1}^{srpmax}\sum_{slay=1}^{slaymax}\widehat{pNtt}_{sDs,sd,sNpt,srp,slay}yDs_{sDs}\,yd_{sd}yNpt_{sNpt}yrp_{srp}ylay_{slay}}\cdot\right.$$

$$\left.\frac{1}{\left(\sum_{sd=1}^{sdmax}\widehat{pdti}_{sd}\,yd_{sd}\right)^2}\right)^2\;\leq\;\widehat{\Delta Ptdisp}\tag{96}$$

$$\frac{\widehat{ms}}{\widehat{\rho s}\;\sum_{sDs=1}^{sDsmax}\sum_{srp=1}^{srpmax}\sum_{sL=1}^{sLmax}\sum_{sNb=1}^{sNbmax}\frac{\widehat{pDs}_{sDs}\,\widehat{pFAR}_{srp}\,\widehat{pL}_{sL}}{(\widehat{pNb}_{sNb}+1)}yDs_{sDs}yrp_{srp}yL_{sL}\,yNb_{sNb}}\;\geq\;\widehat{vsmin}\tag{97}$$

$$\frac{\widehat{ms}}{\widehat{\rho s} \sum_{sDs=1}^{sDsmax} \sum_{srp=1}^{srpmax} \sum_{sL=1}^{sLmax} \sum_{sNb=1}^{sNbmax} \frac{\widehat{pDs}_{sDs}\widehat{pFAR}_{srp}\widehat{pL}_{sL}}{(\widehat{pNb}_{sNb}+1)} yDs_{sDs}yrp_{srp}yL_{sL}\, yNb_{sNb}} \leq \widehat{vsmax} \tag{98}$$

$$4\,\widehat{mt}/$$

$$(\pi\,\widehat{\rho t}\sum_{sDs=1}^{sDsmax}\sum_{sd=1}^{sdmax}\sum_{sNpt=1}^{sNptmax}\sum_{srp=1}^{srpmax}\sum_{slay=1}^{slaymax}\frac{\widehat{pNtt}_{sDs,sd,sNpt,srp,slay}\widehat{pdtl}^2_{sd}}{\widehat{pNpt}_{sNpt}}yDs_{sDs}\,yd_{sd}\cdot$$

$$yNpt_{sNpt}yrp_{srp}ylay_{slay}\,)\geq \widehat{vtmin} \tag{99}$$

$$4\,\widehat{mt}/$$

$$(\pi\,\widehat{\rho t}\sum_{sDs=1}^{sDsmax}\sum_{sd=1}^{sdmax}\sum_{sNpt=1}^{sNptmax}\sum_{srp=1}^{srpmax}\sum_{slay=1}^{slaymax}\frac{\widehat{pNtt}_{sDs,sd,sNpt,srp,slay}\widehat{pdtl}^2_{sd}}{\widehat{pNpt}_{sNpt}}yDs_{sDs}\,yd_{sd}\cdot$$

$$yNpt_{sNpt}yrp_{srp}ylay_{slay}\,)\leq \widehat{vtmax} \tag{100}$$

$$\frac{\widehat{ms}}{\widehat{\mu s}}\left(\sum_{srp=1}^{srpmax}\sum_{sd=1}^{sdmax}\sum_{slay=1}^{slaymax}\widehat{pDeq}_{srp,sd,slay}yrp_{srp}yd_{sd}ylay_{slay}\right)\cdot$$

$$\left(\sum_{sDs=1}^{sDsmax}\sum_{srp=1}^{srpmax}\sum_{sL=1}^{sLmax}\sum_{sNb=1}^{sNbmax}\frac{(\widehat{pNb}_{sNb}+1)}{\widehat{pDs}_{sDs}\widehat{pFAR}_{srp}\widehat{pL}_{sL}}yDs_{sDs}yrp_{srp}yL_{sL}\,yNb_{sNb}\right)\geq 2\cdot10^3$$

$$\tag{101}$$

$$\frac{4\,\widehat{mt}}{\pi\,\widehat{\mu t}}\sum_{sDs=1}^{sDsmax}\sum_{sd=1}^{sdmax}\sum_{sNpt=1}^{sNptmax}\sum_{srp=1}^{srpmax}\sum_{slay=1}^{slaymax}\frac{\widehat{pNpt}_{sNpt}}{\widehat{pNtt}_{sDs,sd,sNpt,srp,slay}\widehat{pdtl}_{sd}}yDs_{sDs}\,yd_{sd}\cdot$$

$$yNpt_{sNpt}yrp_{srp}ylay_{slay}\,\geq 10^4 \tag{102}$$

Geometric Constraints: These constraints are modified according to the discrete nature of the design variables:

$$\frac{\sum_{sL=1}^{sLmax}\widehat{pL}_{sL}\,yL_{sL}}{\sum_{sNb=1}^{sNbmax}\widehat{pNb}_{sNb}\,yNb_{sNb}+1}\geq 0.2\,\sum_{sDs=1}^{sDsmax}\widehat{pD s}_{sDs}\,yDs_{sDs} \tag{103}$$

$$\frac{\sum_{sL=1}^{sLmax}\widehat{pL}_{sL}\,yL_{sL}}{\sum_{sNb=1}^{sNbmax}\widehat{pNb}_{sNb}\,yNb_{sNb}+1}\leq 1.0\,\sum_{sDs=1}^{sDsmax}\widehat{pD s}_{sDs}\,yDs_{sDs} \tag{104}$$

$$\sum_{sL=1}^{sLmax} \widehat{pL}_{sL} \, yL_{sL} \geq 3 \sum_{sDs=1}^{sDsmax} \widehat{pDs}_{sDs} \, yDs_{sDs} \tag{105}$$

$$\sum_{sL=1}^{sLmax} \widehat{pL}_{sL} \, yL_{sL} \leq 15 \sum_{sDs=1}^{sDsmax} \widehat{pDs}_{sDs} \, yDs_{sDs} \tag{106}$$

Objective function: The objective function in relation to the binary variables assumes the following form:

$$Min \ \pi \ \sum_{sDs=1}^{sDsmax} \sum_{sd=1}^{sdmax} \sum_{sNpt=1}^{sNptmax} \sum_{srp=1}^{srpmax} \sum_{slay=1}^{slaymax} \sum_{sL=1}^{sLmax} \widehat{pNtt}_{sDs,sd,sNpt,srp,slay} \cdot$$

$$\widehat{pdte}_{sd} \, \widehat{pL}_{sL} \, yDs_{sDs} \, yd_{sd} yNpt_{sNpt} yrp_{srp} ylay_{slay} yL_{sL} \tag{107}$$

2.3 Conversion to a Linear Model

The previous reformulation of the heat exchanger model using binary variables contains several expressions with products of binaries. Therefore, at this stage, the problem is a nonlinear one, which could present multiple local optima with different values of objective function.

Aiming at providing a linear formulation of the optimization problem, thus suppressing the nonconvexity drawback, a rigorous linear alternative for these binary expressions is used, according to the procedure shown as follows. It is important to mention that the proposed procedure does not involve any numerical approximation, i.e., the solution of the resultant formulation rigorously guarantees the global optimum of the design problem.

The product of binary variables in an expression like the one shown in equation (71) can be grouped in a continuous variable $w_{i,j,\dots,k}$ as follows:

$$w_{i,j,\dots,k} = yp_j \, yq_j \dots yz_k \tag{108}$$

Then (Equation 71) can be rewritten as follows

$$p^{n1}q^{n2}\cdots z^{nm} = \sum_{i,j,..k} \widehat{pd}_i^{\,n1}\widehat{qd}_j^{\,n2}\,.....\,\widehat{zd}_k^{\,nm}\,w_{i,j,...k} \tag{109}$$

Besides (Equation 108) can be substituted by

$$w_{i,j,...,k} \leq yp_i \tag{110}$$

$$w_{i,j,...,k} \leq yq_j \tag{111}$$

...

$$w_{i,j,...,k} \leq yz_k \tag{112}$$

$$w_{i,j,...,k} \geq yp_i + yq_j + \cdots + yz_k - (m-1) \tag{113}$$

where *m* is the number of binary variables in the product. Consequently, the original nonlinear term related to the product of binaries is substituted by linear constraints.

2.4   **Final Linear Model**

After the application of the technique described above, the problem becomes a mixed-integer linear programming (MILP). Aiming to decrease the computational effort, additional constraints are included to reduce the search space, as described at the end of this section.

The MILP equations of the heat exchanger design problem are shown below.

Binary Variables Equality Constraints: The following constraints guarantee that in the solution only one of the integer values will be selected:

$$\sum_{sd=1}^{sdmax} yd_{sd} = 1 \tag{114}$$

$$\sum_{sL=1}^{sLmax} yL_{sL} = 1 \tag{115}$$

$$\sum_{sNb=1}^{sNbmax} yNb_{sNb} = 1 \tag{116}$$

$$\sum_{sNpt=1}^{sNptmax} yNpt_{sNpt} = 1 \tag{117}$$

$$\sum_{srp=1}^{srpmax} yrp_{srp} = 1 \tag{118}$$

$$\sum_{sDs=1}^{sDsmax} yDs_{sDs} = 1 \tag{119}$$

$$\sum_{slay=1}^{slaymax} ylay_{slay} = 1 \tag{120}$$

Heat Transfer Rate Equation: The heat transfer rate equation in the MILP formulation contains all the expressions related to the heat transfer coefficients and heat transfer area:

$$\widehat{Q} \left(\sum_{sDs=1}^{sDsmax} \sum_{sd=1}^{sdmax} \sum_{sNpt=1}^{sNptmax} \sum_{srp=1}^{srpmax} \sum_{slay=1}^{slaymax} \frac{\widehat{pdte}_{sd}}{\widehat{pht}_{sDs,sd,sNpt,srp,slay}\widehat{pdti}_{sd}} wvt_{sDs,sd,sNpt,srp,slay} \; + \right.$$

$$\widehat{Rft} \sum_{sd=1}^{sdmax} \frac{\widehat{pdte}_{sd}}{\widehat{pdti}_{sd}} yd_{sd} + \frac{\sum_{sd=1}^{sdmax} \widehat{pdte}_{sd} \ln(\frac{\widehat{pdte}_{sd}}{\widehat{pdti}_{sd}}) yd_{sd}}{2 \, \widehat{ktube}} + \widehat{Rfs} \; +$$

$$\left. \sum_{srp=1}^{srpmax} \sum_{sd=1}^{sdmax} \sum_{slay=1}^{slaymax} \sum_{sDs=1}^{sDsmax} \sum_{sL=1}^{sLmax} \sum_{sNb=1}^{sNbmax} \frac{1}{\widehat{phs}_{srp,sd,slay,sDs,sL,sNb}} whs_{sDs,srp,sL,sNb,sd,slay} \right) \le$$

$$\left(\pi \sum_{sDs=1}^{sDsmax} \sum_{sd=1}^{sdmax} \sum_{sNpt=1}^{sNptmax} \sum_{srp=1}^{srpmax} \sum_{slay=1}^{slaymax} \sum_{sL=1}^{sLmax} \widehat{pNtt}_{sDs,sd,sNpt,srp,slay} \; \widehat{pdte}_{sd} \; \widehat{pL}_{sL} \cdot \right.$$

$$\left. wA1P_{sDs,sd,sNpt,srp,slay,sL} \right) \left(\frac{100}{100+\widehat{Aexc}} \right) \widehat{\Delta Tlm} \; +$$

$$\left(\pi \, \widehat{FMP} \sum_{sDs=1}^{sDsmax} \sum_{sd=1}^{sdmax} \sum_{sNpt=1}^{sNptmax} \sum_{srp=1}^{srpmax} \sum_{slay=1}^{slaymax} \sum_{sL=1}^{sLmax} \widehat{pNtt}_{sDs,sd,sNpt,srp,slay} \; \widehat{pdte}_{sd} \; \widehat{pL}_{sL} \cdot \right.$$

$$\left. wA_{sDs,sd,sNpt,srp,slay,sL} \right) \left(\frac{100}{100+\widehat{Aexc}} \right) \widehat{\Delta Tlm} \; -$$

$$\left(\pi \, \widehat{FMP} \sum_{sDs=1}^{sDsmax} \sum_{sd=1}^{sdmax} \sum_{sNpt=1}^{sNptmax} \sum_{srp=1}^{srpmax} \sum_{slay=1}^{slaymax} \sum_{sL=1}^{sLmax} \widehat{pNtt}_{sDs,sd,sNpt,srp,slay} \; \widehat{pdte}_{sd} \; \widehat{pL}_{sL} \cdot \right.$$

$$\left. wA1P_{sDs,sd,sNpt,srp,slay,sL} \right) \left(\frac{100}{100+\widehat{Aexc}} \right) \widehat{\Delta Tlm} \tag{121}$$

The constraint in Equation (121) has continuous variables: $wvt_{sDs,sd,sNpt,srp,slay}$, $whs_{sDs,srp,sL,sNb,sd,slay}$, $wA1P_{sDs,sd,sNpt,srp,slay,sL}$ and $wA_{sDs,sd,sNpt,srp,slay,sL}$. The relations of these variables and the corresponding binary variables are:

$$wvt_{sDs,sd,sNpt,srp,slay} \leq yDs_{sDs} \tag{122}$$

$$wvt_{sDs,sd,sNpt,srp,slay} \leq yd_{sd} \tag{123}$$

$$wvt_{sDs,sd,sNpt,srp,slay} \leq yNpt_{sNpt} \tag{124}$$

$$wvt_{sDs,sd,sNpt,srp,slay} \leq yrp_{srp} \tag{125}$$

$$wvt_{sDs,sd,sNpt,srp,slay} \leq ylay_{slay} \tag{126}$$

$$wvt_{sDs,sd,sNpt,srp,slay} \geq yDs_{sDs} + yd_{sd} + yNpt_{sNpt} + yrp_{srp} + ylay_{slay} - 4 \tag{127}$$

$$whs_{sDs,srp,sL,sNb,sd,slay} \leq yrp_{srp} \tag{128}$$

$$whs_{sDs,srp,sL,sNb,sd,slay} \leq yd_{sd} \tag{129}$$

$$whs_{sDs,srp,sL,sNb,sd,slay} \leq ylay_{slay} \tag{130}$$

$$whs_{sDs,srp,sL,sNb,sd,slay} \leq yDs_{sDs} \tag{131}$$

$$whs_{sDs,srp,sL,sNb,sd,slay} \leq yL_{sL} \tag{132}$$

$$whs_{sDs,srp,sL,sNb,sd,slay} \leq yNb_{sNb} \tag{133}$$

$$whs_{sDs,srp,sL,sNb,sd,slay} \geq yrp_{srp} + yd_{sd} + ylay_{slay} + yDs_{sDs} + yL_{sL} + yNb_{sNb} - 5 \tag{134}$$

$$wA1P_{sDs,sd,sNpt,srp,slay,sL} \leq wA_{sDs,sd,sNpt,srp,slay,sL} \tag{135}$$

$$wA1P_{sDs,sd,sNpt,srp,slay,sL} \leq yNpt_{sNpt1} \tag{136}$$

$$wA1P_{sDs,sd,sNpt,srp,slay,sL} \geq wA_{sDs,sd,sNpt,srp,slay,sL} + yNpt_{sNpt1} - 1 \tag{137}$$

$$wA_{sDs,sd,sNpt,srp,slay,sL} \leq yDs_{sDs} \tag{138}$$

$$wA_{sDs,sd,sNpt,srp,slay,sL} \leq yd_{sd} \tag{139}$$

$$wA_{sDs,sd,sNpt,srp,slay,sL} \leq yNpt_{sNpt} \tag{140}$$

$$wA_{sDs,sd,sNpt,srp,slay,sL} \leq yrp_{srp} \tag{141}$$

$$wA_{sDs,sd,sNpt,srp,slay,sL} \leq ylay_{slay} \tag{142}$$

$$wA_{sDs,sd,sNpt,srp,slay,sL} \leq yL_{sL} \tag{143}$$

$$wA_{sDs,sd,sNpt,srp,slay,sL} \geq yDs_{sDs} + yd_{sd} + yNpt_{sNpt} + yrp_{srp} + ylay_{slay} + yL_{sL} - 5 \tag{144}$$

Bounds on Pressure Drops, Flow Velocities and Reynolds Numbers: The linear form of the bound on the shell-side pressure drop is:

$$\sum_{sDs=1}^{sDsmax} \sum_{sNb=1}^{sNbmax} \sum_{srp=1}^{srpmax} \sum_{sL=1}^{sLmax} \sum_{sd=1}^{srpmax} \sum_{slay=1}^{slaymax} \widehat{p\Delta Ps}_{sDs,sNb,srp,sL,sd,slay} \cdot$$

$$wDPs_{sDs,sNb,srp,sL,sd,slay} \leq \widehat{\Delta Psdisp} \tag{145}$$

The constraints relating the $wDPs_{sDs,sNb,srp,sL,sd,slay}$ continuous variable and the respective binary variables are:

$$wDPs_{sDs,sNb,srp,sL,sd,slay} \leq yDs_{sDs} \tag{146}$$

$$wDPs_{sDs,sNb,srp,sL,sd,slay} \leq yNb_{sNb} \tag{147}$$

$$wDPs_{sDs,sNb,srp,sL,sd,slay} \leq yrp_{srp} \tag{148}$$

$$wDPs_{sDs,sNb,srp,sL,sd,slay} \leq yL_{sL} \tag{149}$$

$$wDPs_{sDs,sNb,srp,sL,sd,slay} \leq yd_{sd} \tag{150}$$

$$wDPs_{sDs,sNb,srp,sL,sd,slay} \leq ylay_{slay} \tag{151}$$

$$wDPs_{sDs,sNb,srp,sL,sd,slay} \geq yDs_{sDs} + yNb_{sNb} + yrp_{srp} + yL_{sL} + yd_{sd} + ylay_{slay} - 5 \tag{152}$$

The tube-side pressure drop constraint is:

$$\sum_{sDs=1}^{sDsmax} \sum_{sd=1}^{sdmax} \sum_{sNpt=1}^{sNptmax} \sum_{srp=1}^{srpmax} \sum_{slay=1}^{slaymax} \sum_{sL=1}^{sLmax} p\widehat{\Delta Ptturb1}_{sNpt.sL,sDs,sd,srp,slay} \cdot$$

$$wvtturb_{sDs,sd,sNpt,srp,slay,sL} +$$

$$\sum_{sDs=1}^{sDsmax} \sum_{sd=1}^{sdmax} \sum_{sNpt=1}^{sNptmax} \sum_{srp=1}^{srpmax} \sum_{slay=1}^{slaymax} \sum_{sL=1}^{sLmax} p\widehat{\Delta Ptturb2}_{sNpt,sL,sDs,sd,srp,slay} \cdot$$

$$wvtturb_{sDs,sd,sNpt,srp,slay,sL} +$$

$$\sum_{sDs=1}^{sDsmax} \sum_{sd=1}^{sdmax} \sum_{sNpt=1}^{sNptmax} \sum_{srp=1}^{srpmax} \sum_{slay=1}^{slaymax} p\widehat{\Delta Ptcab}_{sNpt,sDs,sd,srp,slay} \cdot$$

$$(\widehat{K1P}\, wvt1P_{sDs,sd,sNpt,srp,slay} + \widehat{KMP}\, wvt_{sDs,sd,sNpt,srp,slay} -$$

$$\widehat{KMP}\, wvt1P_{sDs,sd,sNpt,srp,slay}) \leq \widehat{\Delta Ptdisp} \tag{153}$$

The constraints relating the $wvtturb_{sDs,sd,sNpt,srp,slay,sL}$ and $wvt1P_{sDs,sd,sNpt,srp,slay}$ continuous variables and the respective binary variables are:

$$wvtturb_{sDs,sd,sNpt,srp,slay,sL} \leq wvt_{sDs,sd,sNpt,srp,slay} \tag{154}$$

$$wvtturb_{sDs,sd,sNpt,srp,slay,sL} \leq yNpt_{sNpt} \tag{155}$$

$$wvtturb_{sDs,sd,sNpt,srp,slay,sL} \leq yL_{sL} \tag{156}$$

$$wvtturb_{sDs,sd,sNpt,srp,slay,sL} \leq yd_{sd} \tag{157}$$

$$wvtturb_{sDs,sd,sNpt,srp,slay,sL} \geq wvt_{sDs,sd,sNpt,srp,slay} + yNpt_{sNpt} + yL_{sL} + yd_{sd} - 3 \tag{158}$$

$$wvt1P_{sDs,sd,sNpt,srp,slay} \leq wvt_{sDs,sd,sNpt,srp,slay} \tag{159}$$

$$wvt1P_{sDs,sd,sNpt,srp,slay} \leq yNpt_{sNpt1} \tag{160}$$

$$wvt1P_{sDs,sd,sNpt,srp,slay} \geq wvt_{sDs,sd,sNpt,srp,slay} + yNpt_{sNpt1} - 1 \tag{161}$$

The linear form of the bounds on the shell-side flow velocity is:

$$\widehat{vsmin} \leq \frac{\widehat{ms}}{\widehat{\rho s}} \sum_{sDs=1}^{sDsmax} \sum_{srp=1}^{srpmax} \sum_{sL=1}^{sLmax} \sum_{sNb=1}^{sNbmax} \frac{(\widehat{pNb}_{sNb}+1)}{\widehat{pDs}_{sDs}\widehat{pFAR}_{srp}\widehat{pL}_{sL}} wvs_{sDs,srp,sL,sNb} \tag{162}$$

$$\widehat{vsmax} \geq \frac{\widehat{ms}}{\widehat{\rho s}} \sum_{sDs=1}^{sDsmax} \sum_{srp=1}^{srpmax} \sum_{sL=1}^{sLmax} \sum_{sNb=1}^{sNbmax} \frac{(\widehat{pNb}_{sNb}+1)}{\widehat{pDs}_{sDs}\widehat{pFAR}_{srp}\widehat{pL}_{sL}} wvs_{sDs,srp,sL,sNb} \tag{163}$$

The constraints relating the $wvs_{sDs,srp,sL,sNb}$ continuous variable and the corresponding binary variables are:

$$wvs_{sDs,srp,sL,sNb} \leq yDs_{sDs} \tag{164}$$

$$wvs_{sDs,srp,sL,sNb} \leq yrp_{srp} \tag{165}$$

$$wvs_{sDs,srp,sL,sNb} \leq yL_{sL} \tag{166}$$

$$wvs_{sDs,srp,sL,sNb} \leq yNb_{sNb} \tag{167}$$

$$wvs_{sDs,srp,sL,sNb} \geq yDs_{sDs} + yrp_{srp} + yL_{sL} + yNb_{sNb} - 3 \tag{168}$$

The bounds on the tube-side flow velocity are:

$$\widehat{vtmin} \leq \frac{4\ \widehat{mt}}{\pi\ \widehat{\rho t}} \sum_{sDs=1}^{sDsmax} \sum_{sd=1}^{sdmax} \sum_{sNpt=1}^{sNptmax} \sum_{srp=1}^{srpmax} \sum_{slay=1}^{slaymax} \frac{\widehat{pNpt}_{sNpt}}{\widehat{pNtt}_{sDs,sd,sNpt,srp,slay} \widehat{pdti}_{sd}^{\ 2}} \cdot$$

$$wvt_{sDs,sd,sNpt,srp,slay} \quad (169)$$

$$\widehat{vtmax} \geq \frac{4\ \widehat{mt}}{\pi\ \widehat{\rho t}} \sum_{sDs=1}^{sDsmax} \sum_{sd=1}^{sdmax} \sum_{sNpt=1}^{sNptmax} \sum_{srp=1}^{srpmax} \sum_{slay=1}^{slaymax} \frac{\widehat{pNpt}_{sNpt}}{\widehat{pNtt}_{sDs,sd,sNpt,srp,slay} \widehat{pdti}_{sd}^{\ 2}} \cdot$$

$$wvt_{sDs,sd,sNpt,srp,slay} \quad (170)$$

The bounds on the Reynolds numbers are:

$$\frac{\widehat{ms}}{\widehat{\mu s}} \sum_{srp=1}^{srpmax} \sum_{sd=1}^{sdmax} \sum_{slay=1}^{slaymax} \sum_{sDs=1}^{sDsmax} \sum_{sL=1}^{sLmax} \sum_{sNb=1}^{sNbmax} \frac{\widehat{pDeq}_{srp,sd,slay}(\widehat{pNb}_{sNb}+1)}{\widehat{pDs}_{sDs} \widehat{pFAR}_{srp} \widehat{pL}_{sL}} \cdot$$

$$whs_{sDs,srp,sL,sNb,sd,slay} \geq 2 \cdot 10^3 (171)$$

$$\frac{4\ \widehat{mt}}{\pi\ \widehat{\mu t}} \sum_{sDs=1}^{sDsmax} \sum_{sd=1}^{sdmax} \sum_{sNpt=1}^{sNptmax} \sum_{srp=1}^{srpmax} \sum_{slay=1}^{slaymax} \frac{\widehat{pNpt}_{sNpt}}{\widehat{pNtt}_{sDs,sd,sNpt,srp,slay} \widehat{pdti}_{sd}} \cdot$$

$$wvt_{sDs,sd,sNpt,srp,slay} \geq 10^4 \ (172)$$

Geometric Constraints: The constraints related to the maximum and minimum baffle spacing are:

$$\sum_{sL=1}^{sLmax} \sum_{sNb=1}^{sNbmax} \frac{\widehat{pL}_{sL}}{(\widehat{pNb}_{sNb}+1)} wlbc_{sL,sNb} \leq 1.0 \sum_{sDs=1}^{sDsmax} \widehat{pDs}_{sDs}\ yDs_{sDs} \quad (173)$$

$$\sum_{sL=1}^{sLmax} \sum_{sNb=1}^{sNbmax} \frac{\widehat{pL}_{sL}}{(\widehat{pNb}_{sNb}+1)} wlbc_{sL,sNb} \geq 0.2 \sum_{sDs=1}^{sDsmax} \widehat{pDs}_{sDs}\ yDs_{sDs} \quad (174)$$

The constraints relating the $wlbc_{sL,sNb}$ continuous variable and the corresponding binary variables are:

$$wlbc_{sL,sNb} \leq yL_{sL} \quad (175)$$

$$wlbc_{sL,sNb} \leq yNb_{sNb} \quad (176)$$

$$wlbc_{sL,sNb} \geq yL_{sL} + yNb_{sNb} - 1 \tag{177}$$

The constraints associated to ratio between the tube length and shell diameter are:

$$\sum_{sL=1}^{sLmax} \widehat{pL}_{sL} \, yL_{sL} \geq 3 \sum_{sDs=1}^{sDsmax} \widehat{pDs}_{sDs} \, yDs_{sDs} \tag{178}$$

$$\sum_{sL=1}^{sLmax} \widehat{pL}_{sL} \, yL_{sL} \leq 15 \sum_{sDs=1}^{sDsmax} \widehat{pDs}_{sDs} \, yDs_{sDs} \tag{179}$$

Objective function: The objective function is:

$$\text{Min } \pi \sum_{sDs=1}^{sDsmax} \sum_{sd=1}^{sdmax} \sum_{sNpt=1}^{sNptmax} \sum_{srp=1}^{srpmax} \sum_{slay=1}^{slaymax} \sum_{sL=1}^{sLmax} \widehat{pNtt}_{sDs,sd,sNpt,srp,slay} \cdot$$

$$\widehat{pdte}_{sd} \, \widehat{pL}_{sL} wA_{sDs,sd,sNpt,srp,slay,sL} \tag{180}$$

Additional Constraints to Convergence Acceleration

Velocity bounds: The analysis of the feasible set allows the introduction of additional constraints, which can accelerate the solution algorithm. Bounds on flow velocities are imposed by the constraints in the Equations (162), (163), (169) and (170), but the analysis of these conditions indicates that an extra set of constraints can also be added to the problem formulation:

$$wvs_{sDs,srp,sL,sNb} = 0 \qquad \text{for } (sDs, srp, sL, sNb) \in (Svsminout \cup Svsmaxout) \tag{181}$$

$$wvt_{sDs,sd,sNpt,srp,slay} = 0 \quad \text{for } (sDs, srp, sL, sNb) \in (Svtminout \cup Svtmaxout) \tag{182}$$

The sets *Svsminout*, *Svsmaxout*, *Svtminout*, and *Svtmaxout* are established prior to the optimization, based on the values of the set of problem parameters, as follows:

$$Svsminout = \{(sDs, srp, sL, sNb) \, / \, \widehat{pvs}_{sDs,srp,sL,sNb} \leq \widehat{vsmin} - \hat{\varepsilon}\} \tag{183}$$

$$Svsmaxout = \{(sDs, srp, sL, sNb) \mid \widehat{pvs}_{sDs,srp,sL,sNb} \geq \widehat{vsmax} + \hat{\varepsilon}\} \tag{184}$$

$$Svtminout = \{(sDs, sd, sNpt, srp, slay) \mid \widehat{pvt}_{sDs,sd,sNpt,srp,slay} \leq \widehat{vtmin} - \hat{\varepsilon}\} \tag{185}$$

$$Svtmaxout = \{(sDs, sd, sNpt, srp, slay) \mid \widehat{pvt}_{sDs,sd,sNpt,srp,slay} \geq \widehat{vsmax} + \hat{\varepsilon}\} \tag{186}$$

where $\hat{\varepsilon}$ is a small positive number.

Shell-side pressure upper bound: The same logic can be employed in relation to the upper bound on the shell-side pressure drop in Equation (145), thus yielding:

$$wDPs_{sDs,sNb,srp,sL,sd,slay} = 0 \qquad \text{for } (sDs, sNb, srp, sL, sd, slay) \in SDPsmaxout \tag{187}$$

$$SDPsmaxout = \{(sDs, sNb, srp, sL, sd, slay) \mid \widehat{p\Delta Ps}_{sDs,sNb,srp,sL,sd,slay} \geq \widehat{\Delta Psdisp} + \hat{\varepsilon}\} \tag{188}$$

Baffle spacing: The baffle spacing constraints in Equations (173) and (174) yield the following additional constraints:

$$yL_{sL} + yNb_{sNb} + yDs_{sDs} \leq 2 \quad \text{for } (sL, sNb, sDs) \in (SLNbminout \cup SLNbmaxout) \tag{189}$$

$$SLNbminout = \{(sL, sNb, sDs) \mid \frac{\widehat{pL}_{sL}}{\widehat{pNb}_{sNb}+1} \leq 0.2\widehat{PDs}_{sDs} - \hat{\varepsilon}\} \tag{190}$$

$$SLNbmaxout = \{(sL, sNb, sDs) \mid \frac{\widehat{pL}_{sL}}{\widehat{pNb}_{sNb}+1} \geq 1.0\widehat{PDs}_{sDs} + \hat{\varepsilon}\} \tag{191}$$

Tube length / shell diameter: The ratio between the tube length and shell diameter in Equations (180) and (181) yield the following additional constraints:

$$yL_{sL} + yDs_{sDs} \leq 1 \qquad \text{for } (sL, sDs) \in (SLDminout \cup SLDmaxout) \tag{192}$$

$$SLDminout = \{(sL, sDs) \mid \widehat{pL}_{sL} \leq 3\widehat{PDs}_{sDs} - \hat{\varepsilon}\} \tag{193}$$

$$SLDmaxout = \{(sL, sDs) \mid \widehat{pL}_{sL} \geq 15\widehat{PDs}_{sDs} + \hat{\varepsilon}\} \tag{194}$$

Heat transfer area: The heat transfer area is the objective function and, a priori, does not have a bound constraint. However, based on maximum velocity limits, it is possible to determine maximum values for the convective heat transfer coefficients and, therefore, to evaluate a maximum value for the overall heat transfer coefficients. Finally, based on this parameter, it is possible to establish a minimum value for the heat transfer area. The expression of the additional constraint is:

$$wA_{sDs,sd,sNpt,srp,slay,sL} = 0 \qquad \text{for } (sDs,sd,sNpt,srp,slay,sL) \in SAminout \qquad (195)$$

where the set of heat exchangers with area lower than the minimum possible is given by:

$$SAminout = \{(sDs,sd,sNpt,srp,slay,sL) \, / \pi \, \widehat{pNtt}_{sDs,sd,sNpt,srp,slay} \widehat{pdte}_{sd} \widehat{pL}_{sL} \leq \widehat{Amin} - \hat{\varepsilon}\} \qquad (196)$$

The lower bound on the heat transfer area can be determined through the following set of equations:

$$Amin = \frac{\hat{Q}}{\widehat{Umax}\,\widehat{\Delta Tlm}} \qquad (197)$$

$$Umax = \frac{1}{\frac{1}{\widehat{htmax}}\widehat{drmin} + \widehat{Rft}\cdot\widehat{drmin} + \frac{\widehat{pdte}_{sd1}\ln(\widehat{drmin})}{2\,\widehat{ktube}} + \widehat{Rfs} + \frac{1}{\widehat{hsmax}}} \qquad (198)$$

$$\widehat{htmax} = \max(\widehat{pht}_{sDs,sd,sNpt,srp,slay}) \qquad (199)$$

$$\widehat{hsmax} = \max(\widehat{phs}_{srp,sd,slay,sDs,sL,sNb}) \qquad (200)$$

$$\widehat{drmin} = \min(\widehat{pdte}_{sd}/\widehat{pdti}_{sd}) \qquad (201)$$

2.5 **Results**

The application of the proposed MILP approach is illustrated by its utilization in the solution of a typical design task described in Table 1. The physical properties of the streams

are shown in Table 2. The standard values of the design variables are displayed in Table 3; related to a fixed tubesheet type exchanger with E-shell, single segmental baffles, tube wall thickness of 1.65 mm (BWG 16) and thermal conductivity of the tube wall equal to 50 W/m K. The minimum excess area is 11% and the tube count data is based on Kakaç et al. (2012).

Table 1 - Design Data

	Hot stream	Cold stream
Fluid	Crude oil	Cooling water
Stream allocation	Shell side	Tube side
Mass flow rate (kg/s)	110	228.8
Inlet temperature (ºC)	90	30
Outlet temperature (ºC)	50	40
Fouling factor (m^2K/W)	0.0002	0.0004
Allowable pressure drop (kPa)	100	100
Flow velocity bounds (m/s)	[1.0 3.0]	[0.5 2.0]

Table 2 - Physical Properties of the Streams

	Hot stream	Cold stream
Density (kg/m^3)	786.4	995
Heat capacity (J/(kg·K))	2177	4187
Viscosity (Pa·s)	$1.89 \cdot 10^{-3}$	$0.72 \cdot 10^{-3}$
Thermal conductivity (W/(m·K))	0.122	0.59

Table 3 - Standard Values of the Discrete Design Variables

Variable	Values
Outer tube diameter $\widehat{pdte}_{sd}$ (m)	0.019, 0.025, 0.032, 0.038, 0.051
Tube length, $\widehat{pL}_{sL}$ (m)	1.220, 1.829, 2.439, 3.049, 3.659, 4.877, 6.098
Number of baffles, $\widehat{pNb}_{sNb}$	1, 2, ... , 20
Number of tube passes, $\widehat{pNpt}_{sNpt}$	1, 2, 4, 6
Tube pitch ratio, $\widehat{prp}_{srp}$	1.25, 1.33, 1.50
Shell diameter, $\widehat{pDs}_{sDs}$ (m)	0.787, 0.838, 0.889, 0.940, 0.991, 1.067, 1.143, 1.219, 1.372, 1.524
Tube layout, $\widehat{play}_{slay}$	1 = square, 2 = triangular

Source: The author.

The design task was solved using the MILP formulation implemented in the optimization software General Algebraic Modelling System (GAMS) using the solver CPLEX. The objective function and the design and thermo-fluid dynamic variables in the solution obtained are shown in Tables 4 and 5.

Table 4 - Heat Exchanger Design Results

	MILP
Area (m^2)	624
Outer tube diameter (m)	0.019
Tube length (m)	4.9
Number of baffles	7
Number of tube passes	4
Tube pitch ratio	1.25
Shell diameter (m)	1.219
Tube layout	triangular
Total number of tubes	2139
Baffle spacing (m)	0.610
Tube pitch (m)	0.024

Table 5 - Thermo-fluid dynamic Results

	MILP
Shell-side flow velocity (m/s)	0.94
Tube-side flow velocity (m/s)	2.2
Shell-side heat transfer coefficient (W/m^2K)	1163
Tube-side heat transfer coefficient (W/m^2K)	9206
Overall heat transfer coefficient (W/m^2K)	584
Shell-side pressure drop (kPa)	84.9
Tube-side pressure drop (kPa)	91.9

The analysis of the results indicates that the optimal solution is coherent with general optimization trends employed in heat exchanger design. The pressure drops in the shell and tube sides are close to the allowable values, i.e. the optimal solution promotes a good exploration of the available pressure drop aiming to increase the overall heat transfer coefficient and, consequently, to diminish the heat transfer area.

Performance Analysis: Aiming to provide a clearer assessment of the performance of the proposed approach when compared to conventional nonlinear alternatives (MINLP), a set of 10 different design tasks were tested (the problem discussed previously is the first example of the sample). These tasks involve streams typically found in heat exchanger design problems: methanol, ethanol, acetone, sucrose solution, crude oil, cooling water, and hot water (KAKAÇ etl al., 2012; TOWLER and SINNOT, 2008). The standard values of the design variables are equal to the data displayed in Table 3 and the properties and flows of the fluids for each example are shown in Table 6, 7 and 8.

Table 6 - Heat Exchanger Examples

Example	1	2	3	4	5
Service	Crude oil cooler	Crude oil cooler	Methanol cooler	Methanol cooler	Methanol heater
Hot stream	Crude oil	Crude oil	Methanol	Methanol	Hot water
Cold stream	Cooling water	Cooling water	Cooling water	Cooling water	Methanol
Tube-side stream	Cold	Cold	Hot	Hot	Hot
Example	6	7	8	9	10
Service	Ethanol cooler	Sucrose solution heater	Sucrose solution cooler	Acetone ethanol exchanger	Acetone ethanol exchanger
Hot stream	Ethanol	Hot water	Sucrose solution	Ethanol	Ethanol
Cold stream	Cooling water	Sucrose solution	Cooling water	Acetone	Acetone
Tube-side stream	Cold	Hot	Cold	Cold	Hot

Table 7 - Hot Stream Data

Example	1	2	3	4	5	6	7	8	9	10
$\hat{m}$ (kg/s)	110.0	50.0	27.8	69.4	40.0	55.6	40.0	83.3	111.1	111.1
Inlet $\hat{T}$ (°C)	90.0	100.0	70.0	100.0	220.0	150.0	220.0	90.0	190.0	190.0
Outlet $\hat{T}$ (°C)	50.0	50.0	40.0	40.0	110.2	60.0	80.8	40.0	120.0	120.0
max ΔP (kPa)	100	60	70	70	70	70	70	100	100	100
ρ (kg/m^3)	786	786	750	750	888	789	888	1080	789	789
$\hat{\mu}$ (mPa·s)	1.89	1.89	0.34	0.34	0.15	0.67	0.15	1.30	0.67	0.67
$\widehat{cp}$ (J/kg·K)	2177	2177	2840	2840	4312	2470	4312	3601	2470	2470
$\hat{k}$ (W/m·K)	0.12	0.12	0.19	0.19	0.70	0.17	0.70	0.58	0.17	0.17
$\widehat{Rf}$ (m^{2}K/W)	0.0002	0.0002	0.0002	0.0002	0.0001	0.0002	0.0001	0.0001	0.0002	0.0002

Table 8 - Cold Stream Data

Example	1	2	3	4	5	6	7	8	9	10
$\hat{m}$ (kg/s)	228.8	130.0	56.6	353.3	133.3	295.0	133.3	358.3	166.7	166.7
Inlet $\hat{T}$ (°C)	30.0	30.0	30.0	32.0	30.0	30.0	30.0	30.0	30.0	30.0
Outlet $\hat{T}$ (°C)	40.0	40.0	40.0	40.0	80.0	40.0	80.0	40.0	79.7	79.7
max ΔP (kPa)	100	50	100	70	70	70	70	100	100	100
ρ (kg/m^3)	995	995	995	995	750	995	1080	995	736	736
$\hat{\mu}$ (mPa·s)	0.72	0.72	0.72	0.72	0.34	0.72	1.30	0.80	0.21	0.21
$\widehat{cp}$ (J/kg·K)	4187	4187	4187	4187	2840	4187	3601	4187	2320	2320
$\hat{k}$ (W/m·K)	0.59	0.59	0.59	0.59	0.19	0.59	0.58	0.59	0.14	0.14
$\widehat{Rf}$ (m^{2}K/W)	0.0004	0.0003	0.0002	0.0004	0.0001	0.0004	0.0001	0.0004	0.0002	0.0002

The problem sample was solved using the MILP formulation and compared to the original nonlinear model (Equations 12-52, 55-69) using an MINLP approach with two different solvers: DICOPT and SBB. The DICOPT algorithm is the outer approximation with equality relaxation and augmented penalty algorithm (OA/ER/AP) and the SBB is a branch-and-bound algorithm (BB). The MINLP formulation employed for the performance analysis is composed of the constraints in Equations (12) through (51), objective function in Equation (52), and the description of the discrete variables in Equations (55) to (69). An initialization procedure was provided for initial estimates of the thermal variables based on the flow velocity bounds in the MINLP algorithms. No initial estimates were employed in the MILP runs.

The heat transfer area of the solutions and the computational time employed are displayed in Table 9. The computational times were measured using a computer with a processor Intel Core i7 3.40 GHz with 12.0 GB RAM memory.

Table 9 - Performance Comparison

Example	Heat transfer area (m^2)			Solution time (s)		
	MILP	MINLP DICOPT	MINLP SBB	MILP	MINLP DICOPT	MINLP SBB
1	624	NC	NC	1772	NC	NC
2	319	319	319	1606	8.8	1.3
3	199	NC	NC	211	NC	NC
4	872	872	872	153	87	0.4
5	144	NC	NC	931	NC	NC
6	332	355	341	2824	5061	1.8
7	207	225	207	2529	1.5	0.9
8	914	914	914	171	19	0.7
9	287	287	287	2058	9.3	0.9
10	327	NC	NC	2329	NC	NC

Note: NC = non-convergence

The results displayed in Table 9 indicate a considerable number of occasions where the MINLP algorithms failed to converge. This problem has occurred in 40% of the problems when using the solvers DICOPT and SBB. The analysis of the converged results also indicates that the MINLP algorithms may be trapped in local optima. This problem has occurred in 33% of the converged runs of the DICOPT solver and 17% of the solutions when using the SBB solver. The comparison of the solution time (evaluated using the elapsed time command in GAMS) indicates that the MILP approach is usually much slower than the

MINLP algorithms. However, the observed solution times of the MILP approach do not compromise its use in practical applications, varying between about 3 min to 45 min.

Effect of Pressure Drop: As mentioned before, the objective function can be formulated differently. One of the issues is the pressure drop as it is associated to pumping costs. In this case one could construct an objective function that is a linear combination of the amortized cost of area, and the pressure drops. Because the coefficients of such cost function depend a lot on the context, that is, whether the exchanger is alone needing (or not) pumping for a source pressure to a delivery pressure, or is part of a network, we believe that it is better to study the effect of the pressure drop on the final design. To do this we prepared three runs related to the design task described in Table 1, one limiting the pressure drop on tubes to an 80% smaller value. We do the same for the shell and finally, for completeness we add both. The results of these runs, together with the original design are shown in Table 10.

Table 10 - Effect of the Allowable Pressure Drop in the Optimal Design

	MILP without changes	Lower pressure drop on tubes	Lower pressure drop on shell	Lower pressure drop on tubes and shell
Area (m^2)	624	684	855	855
Tube length (m)	4.9	4.9	6.1	6.1
Number of baffles	7	8	5	5
Number of tube passes	4	2	4	2
Shell diameter (m)	1.219	1.372	1.372	1.372
Tube layout	triangular	square	square	square
Total number of tubes	2139	2344	2344	2344
Baffle spacing (m)	0.610	0.542	1.016	1.016
Shell-side flow velocity (m/s)	0.94	0.94	0.50	0.50
Tube-side flow velocity (m/s)	2.2	1.0	2.0	1.0
Shell-side heat transfer coefficient (W/m^{2}K)	1163	1009	714	714
Tube-side heat transfer coefficient (W/m^{2}K)	9206	4914	8556	4914
Overall heat transfer coefficient (W/m^{2}K)	584	511	442	422
Shell-side pressure drop (kPa)	84.9	73.7	15.7	15.7
Tube-side pressure drop (kPa)	91.9	10.9	93.8	13.3

The analysis of the results indicates that the reduction of the allowable pressure drop determined a reduction in the flow velocity, which causes a decrease of the corresponding heat transfer coefficient. Consequently, the smaller value of the overall heat transfer coefficient implies an increase of the area necessary to fulfill the design task. Because the heat transfer coefficient in the shell-side is lower than in the tube-side, the area increase is more pronounced when the allowable shell-side pressure drop is reduced. The allowable tube-side pressure drop reduction determines an area increase of 10% and the equivalent shell-side

pressure drop reduction determines an increase of 40%, equivalent to the increase when both parameters are reduced.

2.6 **Partial Conclusions**

A MILP model for the design of shell and tube heat exchangers was presented. The model is linear, thanks to the fact that several geometric design variables are discrete and therefore amenable to be expressed in terms of binary variables. When these expressions are substituted in the model, the resulting equations are nonlinear expressions containing binary variables. We therefore reformulate the problem as a linear one without losing any rigor.

The comparison of the MILP model with an MINLP formulation through the solution of the same sample of heat exchanger design problems shows drawbacks in the MINLP approach in relation to non-convergence and local optima. Due to its linear nature, the MILP model proposed here is immune to these obstacles, always reaching the global optimum.

The computational time for the MILP model is remarkable higher than the required by others, but it is still satisfactory for its use in practice. In the next chapter, it is explored alternative techniques to reduce the computational effort. An important aspect that must also be noted is that the linear nature of the proposed model makes it amenable to be easier to add to other broader models (i.e. HEN synthesis with simultaneous heat exchanger design).

3   ALTERNATIVE MILP FORMULATIONS FOR SHELL AND TUBE HEAT EXCHANGER OPTIMAL DESIGN

This chapter presents the exploration of alternative techniques to reduce the computational effort for the identification of the global optimum of the design of shell-and-tube heat exchangers. The scope and the original nonlinear model employed corresponds to the same set of equations presented in the previous chapter.

MILP Model: After the substitution of the discrete variables is made, the model results in a complex mixed integer nonlinear programming (MINLP) model that contains products of binaries and continuous variables. In the previous chapter, we converted this rigorous MINLP model into a rigorous linear model (MILP), making no simplifying assumptions. Thus, a rigorous solution of the MILP is also a rigorous solution of the MINLP. Moreover, because of its linearity, the MILP model renders a global solution. As we shown, solving the MINLP model using local solvers many times rendered a non-global local solution.

MILP Model Performance: After testing several options of binary variable prioritizations in the MILP branch and bound, we came up with one option that rendered solutions in the range from 153 to 2824 seconds, with an average of 1458 seconds for 10 test problems (computer with a processor Intel Core i7 3.40 GHz with 12.0 GB RAM memory). This performance time is more than acceptable for a stand-alone run, even if the number of geometric options is increased. However, this computational time is high when, for example, repeated runs are needed to handle uncertainty, and when the model becomes a sub-model of others, like the simultaneous design of a heat exchanger network with detailed heat exchanger design. We now explore different rigorous alternatives of binary variable aggregation, all having different computational efficiency still rendering the same result.

3.1   Alternatives of binary variables organization

We present five different aggregations of binary variables leading to MILP formulations, which render the same result each with its own computational efficiency.

Alternative 1: This alternative corresponds to the linear formulation presented in the previous chapter.

Alternative 2: A counting table structure can be employed to organize the discrete values of the shell diameter, tube diameter, tube layout, number of tube passes, and tube pitch ratio, where only one set of binary variables, $yrow_{srow}$, is employed to represent these discrete values. In this context, $srow$ is a multi-index set, i.e. $srow = (sd, sDs, slay, sNpt, srp)$. The tube length and the number of baffles remain represented by the original sets of binary variables yL_{sL} and yNb_{sNb}.

Alternative 3: This alternative represents the discrete values in two tables. The first one corresponds to the counting table, as shown in the previous alternative, where the corresponding set of binaries is $yrow1_{srow1}$ with $srow1 = (sd, sDs, slay, sNpt, srp)$. The second table contains all pairs of discrete values of tube length and number of baffles. The set of binaries which represent these discrete values is $yrow2_{srow2}$ with $srow2 = (sNb\ sL)$.

Alternative 4: Another possible combination was the use of two set of binary variables: $yrow1_{srow1}$ with $srow1 = (sd, sDs, slay, sNpt, srp, sL)$, representing all variables but the number of baffles, which is represented by the original binary yNb_{sNb}.

Alternative 5: The last alternative investigated in this work is the use of a unique set of binary variables, $yrow_{srow}$, which corresponds to all discrete variables, $srow = (sd, sDs, slay, sNpt, srp, sL, sNb)$.

Table 11 contains an overview of the different combinations between binary variables and the original discrete variables.

Table 11 - Alternatives investigated of binary variables

alternative	binary variable {original discrete variable}
1	yd_{sd} {dt}, yDs_{sDs} {Ds}, $ylay_{slay}$ {lay}, $yNpt_{sNpt}$ {Npt} yrp_{srp} {rp}, yL_{sL} {L}, yNb_{sNb} {Nb}
2	$yrow_{srow}$ {dt, Ds, lay, Npt, rp}, yL_{sL} {L}, yNb_{sNb} {Nb}
3	$yrow1_{srow1}$ {dt, Ds, lay, Npt, rp}, $yrow2_{srow2}$ {L, Nb}
4	$yrow_{srow}$ {dt, Ds, lay, Npt, rp, L}, yNb_{sNb} {Nb}
5	$yrow_{srow}$ {$dt, Ds, lay, Npt, rp, L, Nb$}

Source: The author.

3.2 Development of The Alternative Linear Formulations

The new linear formulations are built starting from the MINLP model (Equations 13-53 through three main steps: the organization of the data table of the discrete variables, the model reformulation, and the conversion to a linear model. For reasons of space and because the procedure is very similar when aggregates of binary variables is made, we only illustrate Alternative 5 in detail (this alternative is associated to the highest reduction of the computational time consumed by the MILP solver, as it will be shown in the results). Alternative 1 is identical of the original proposal presented in the previous chapter and the equations of Alternatives 2, 3 and 4 can be found in the Appendix A.

Organization of the Data Table of the Discrete Variables: The original relation between the discrete variables and the corresponding binaries is given by (as it is employed in Alternative 1):

$$dte = \sum_{sd=1}^{sdmax} \widehat{pdte}_{sd}\, yd_{sd} \tag{202}$$

$$dti = \sum_{sd=1}^{sdmax} \widehat{pdti}_{sd} \, yd_{sd} \tag{203}$$

$$Ds = \sum_{sDs=1}^{sDsmax} \widehat{pDs}_{sDs} \, yDs_{sDs} \tag{204}$$

$$lay = \sum_{slay=1}^{slaymax} \widehat{play}_{slay} \, ylay_{slay} \tag{205}$$

$$Npt = \sum_{sNpt=1}^{sNptmax} \widehat{pNpt}_{sNpt} \, yNpt_{sNpt} \tag{206}$$

$$rp = \sum_{srp=1}^{srpmax} \widehat{prp}_{srp} yrp_{srp} \tag{207}$$

$$L = \sum_{sL=1}^{sLmax} \widehat{pL}_{sL} \, yL_{sL} \tag{208}$$

$$Nb = \sum_{sNb=1}^{sNbmax} \widehat{pNb}_{sNb} \, yNb_{sNb} \tag{209}$$

with the following equations needed to guarantee only one choice among many:

$$\sum_{sd=1}^{sdmax} yd_{sd} = 1 \tag{210}$$

$$\sum_{sDs=1}^{sDsmax} yDs_{sDs} = 1 \tag{211}$$

$$\sum_{slay=1}^{slaymax} ylay_{slay} = 1 \tag{212}$$

$$\sum_{sNpt=1}^{sNptmax} yNpt_{sNpt} = 1 \tag{213}$$

$$\sum_{srp=1}^{srpmax} yrp_{srp} = 1 \tag{214}$$

$$\sum_{sL=1}^{sLmax} yL_{sL} = 1 \tag{215}$$

$$\sum_{sNb=1}^{sNbmax} yNb_{sNb} = 1 \tag{216}$$

According to the aggregation strategy employed in the development of the new MILP formulations, the parameters that represent the discrete values can be grouped in one or more tables. Therefore, several discrete values of the design variables are identified by the same index (a multi-index related to the corresponding original indices). For example, in Alternative 5, the multi-index *srow* represents the discrete values of all design variables. The corresponding set of parameters which compose the table are defined from the original ones, as follows

$$\widehat{Pdte}_{srow} = \widehat{pdte}_{sd} \tag{217}$$

$$\widehat{Pdti}_{srow} = \widehat{pdti}_{sd} \tag{218}$$

$$\widehat{PDs}_{srow} = \widehat{pDs}_{sDs} \tag{219}$$

$$\widehat{Play}_{srow} = \widehat{play}_{slay} \tag{220}$$

$$\widehat{PNpt}_{srow} = \widehat{pNpt}_{sNpt} \tag{221}$$

$$\widehat{Prp}_{srow} = \widehat{prp}_{srp} \tag{222}$$

$$\widehat{PL}_{srow} = \widehat{pL}_{sL} \tag{223}$$

$$\widehat{PNb}_{srow} = \widehat{pNb}_{sNb} \tag{224}$$

Consequently, different discrete variables become associated to the same set of binaries. In Alternative 5, all discrete variables are described by the set of binaries $yrow_{srow}$, thus yielding:

$$dte = \sum_{srow} \widehat{Pdte}_{srow}\, yrow_{srow} \tag{225}$$

$$dti = \sum_{srow} \widehat{Pdti}_{srow}\, yrow_{srow} \tag{226}$$

$$Ds = \sum_{srow} \widehat{PDs}_{srow}\, yrow_{srow} \tag{227}$$

$$lay = \sum_{srow} \widehat{Play}_{srow}\, yrow_{srow} \tag{228}$$

$$Npt = \sum_{srow} \widehat{PNpt}_{srow}\, yrow_{srow} \tag{229}$$

$$rp = \sum_{srow} \widehat{Prp}_{srow} yrow_{srow} \tag{230}$$

$$L = \sum_{srow} \widehat{PL}_{srow}\, yrow_{srow} \tag{231}$$

$$Nb = \sum_{srow} \widehat{PNb}_{srow}\, yrow_{srow} \tag{232}$$

$$\sum_{srow} yrow_{srow} = 1 \tag{233}$$

Model Reformulation: In this step, the model equations are modified through the substitution of the discrete variables by their binary representation. This reformulation step also involves a procedure for the organization of the resultant expressions containing binary variables, as described in Chapter 2.

3.3 MILP Formulation with a Single Set of Binaries

This section presents the complete linear formulation of the optimal heat exchanger design problem based on a unique set of binary variables to represent the discrete options of the design variables (Alternative 5).

Binary Variables Equality Constraints: This constraint imposes that only one design alternative must be chosen:

$$\sum_{srow} yrow_{srow} = 1 \tag{234}$$

Heat Transfer Rate Equation: The expressions of all heat transfer coefficients and the heat transfer area are inserted into the heat transfer equation, thus yielding:

$$\hat{Q}\left(\sum_{srow} \frac{\widehat{Pdte}_{srow}}{\widehat{Pht}_{srow}\,\widehat{Pdti}_{srow}} yrow_{srow} + \widehat{Rft} \sum_{srow} \frac{\widehat{Pdte}_{srow}}{\widehat{Pdti}_{srow}} yrow_{srow} + \right.$$

$$\frac{\sum_{srow} \widehat{Pdte}_{srow}\, yrow_{srow} \ln\left(\frac{\widehat{Pdte}_{srow}}{\widehat{Pdti}_{srow}}\right)}{2\,\widehat{ktube}} + \widehat{Rfs} + \left. \sum_{srow} \frac{1}{\widehat{Phs}_{srow}} yrow_{srow} \right) \le$$

$$\left(\frac{100}{100+\widehat{Aexc}}\right)\left(\pi \sum_{srow} \widehat{PNtt}_{srow}\, \widehat{Pdte}_{srow}\, \widehat{PL}_{srow} yrow_{srow} \right) \widehat{\Delta Tlm}\ \hat{F}_{srow} \tag{235}$$

where $\widehat{PNtt}_{srow}$ is the total number of tubes and:

$$\widehat{Pht}_{srow} = \frac{\widehat{kt}\,0.023\left(\frac{4\,\widehat{mt}}{\pi\,\widehat{\mu t}}\right)^{0.8}\widehat{Prt}^{n}}{\widehat{Pdti}_{srow}^{1.8}}\left(\frac{\widehat{PNpt}_{srow}}{\widehat{PNtt}_{srow}}\right)^{0.8} \tag{236}$$

$$\widehat{Phs}_{srow} = \frac{\widehat{ks}\,0.36\left(\frac{\widehat{ms}}{\widehat{\mu s}}\right)^{0.55}\widehat{Prs}^{1/3}}{\widehat{pDeq}_{srow}^{\;0.45}}\left(\frac{(\widehat{PNb}_{srow}+1)}{\widehat{PDs}_{srow}\,\widehat{PFAR}_{srow}\,\widehat{PL}_{srow}}\right)^{0.55} \tag{237}$$

$$\widehat{PFAR}_{srow} = 1 - \frac{1}{\widehat{Prp}_{srow}} \tag{238}$$

$$\widehat{pDeq}_{srow} = \frac{\widehat{aDeq}_{srow}\widehat{Prp}_{srow}^2\widehat{Pdte}_{srow}^2}{\pi\widehat{Pdte}_{srow}} - \widehat{Pdte}_{srow} \tag{239}$$

$$\widehat{aDeq}_{srow} = \begin{cases} 4 & \text{if } \widehat{Play}_{srow} = 1 \\ \\ 3.46 & \text{if } \widehat{Play}_{srow} = 2 \end{cases} \tag{240}$$

$$\widehat{F}_{srow} = \begin{cases} \dfrac{(\widehat{R}^2+1)^{0.5} \ \ln\left(\frac{(1-\widehat{P})}{(1-\widehat{R}\,\widehat{P})}\right)}{(\widehat{R}-1)\ln\left(\dfrac{2-\widehat{P}\left(\widehat{R}+1-(\widehat{R}^2+1)^{0.5}\right)}{2-\widehat{P}\left(\widehat{R}+1+(\widehat{R}^2+1)^{0.5}\right)}\right)} & \text{if } \widehat{PNpt}_{srow} \neq 1 \\[2em] 1 & \text{if } \widehat{PNpt}_{srow} = 1 \end{cases} \tag{241}$$

Bounds on Pressure Drops, Flow Velocities and Reynolds Numbers: The bounds on the shell-side and tube-side pressure drops are expressed by:

$$\sum_{srow} \widehat{P\Delta Ps}_{srow} yrow_{srow} \leq \Delta \widehat{Psdisp} \tag{242}$$

$$\sum_{srow} P\Delta\widehat{Ptturb1}_{srow} yrow_{srow} + \sum_{srow} P\Delta\widehat{Ptturb2}_{srow} yrow_{srow} +$$

$$\sum_{srow} P\Delta\widehat{Ptcab}_{srow} \widehat{K}_{srow} yrow_{srow} \leq \Delta\widehat{Ptdisp} \tag{243}$$

where:

$$\widehat{P\Delta Ps}_{srow} = 0.864 \frac{\widehat{ms}^{1.812}\widehat{\mu s}^{0.188}}{\widehat{\rho s}} \left(\frac{(\widehat{PNb}_{srow}+1)^{2.812}}{\widehat{PDs}_{srow}{}^{0.812}(\widehat{PFAR}_{srow}\widehat{PL}_{srow})^{1.812}(\widehat{PDeq}_{srow})^{1.188}} \right) \tag{244}$$

$$P\Delta\widehat{Ptturb1}_{srow} = \left(\frac{0.112\ \widehat{mt}^2}{\pi^2 \rho t} \right) \left(\frac{\widehat{PNpt}_{srow}^3 \widehat{PL}_{srow}}{\widehat{PNtt}_{srow}^2 \widehat{Pdt\iota}_{srow}{}^5} \right) \tag{245}$$

$$P\Delta\widehat{Ptturb2}_{srow} = (0.528)\left(\frac{4^{1.58}\ \widehat{mt}^{1.58}\ \widehat{\mu t}^{0.42}}{\pi^{1.58}\ \widehat{\rho t}} \right) \frac{\widehat{PNpt}_{srow}^{2.58} \widehat{PL}_{srow}}{\widehat{PNtt}_{srow}^{1.58}\widehat{Pdt\iota}_{srow}^{4.58}} \tag{246}$$

$$P\Delta\widehat{Ptcab}_{srow} = \left(\frac{8\ \widehat{mt}^2}{\pi^2\ \widehat{\rho t}} \right) \frac{\widehat{PNpt}_{srow}^3}{\widehat{PNtt}_{srow}^2 \widehat{Pdt\iota}_{srow}{}^4} \tag{247}$$

The bounds on the shell-side and tube-side flow velocities are:

$$\widehat{vsmin} \leq \frac{\widehat{ms}}{\widehat{\rho s}} \sum_{srow} \frac{(\widehat{PNb}_{srow}+1)}{\widehat{PDs}_{srow}\ \widehat{PFAR}_{srow}\ \widehat{PL}_{srow}} yrow_{srow} \tag{248}$$

$$\widehat{vsmax} \geq \frac{\widehat{ms}}{\widehat{\rho s}} \sum_{srow} \frac{(\widehat{PNb}_{srow}+1)}{\widehat{PDs}_{srow}\ \widehat{PFAR}_{srow}\ \widehat{PL}_{srow}} yrow_{srow} \tag{249}$$

$$\widehat{vtmin} \leq \frac{4\ \widehat{mt}}{\pi\ \widehat{\rho t}} \sum_{srow} \frac{\widehat{PNpt}_{srow}}{\widehat{PNtt}_{srow}\ \widehat{Pdt\iota}_{srow}{}^2} yrow_{srow} \tag{250}$$

$$\widehat{vtmax} \geq \frac{4\ \widehat{mt}}{\pi\ \widehat{\rho t}} \sum_{srow} \frac{\widehat{PNpt}_{srow}}{\widehat{PNtt}_{srow}\ \widehat{Pdt\iota}_{srow}{}^2} yrow_{srow} \tag{251}$$

The bounds on the Reynolds numbers are:

$$\frac{\widehat{ms}}{\widehat{\mu s}} \sum_{srow} \frac{\widehat{PDeq}_{srow}(\widehat{PNb}_{srow}+1)}{\widehat{PDs}_{srow}\ \widehat{PFAR}_{srow}\ \widehat{PL}_{srow}} yrow_{srow} \geq 2 \cdot 10^3 \tag{252}$$

$$\frac{4\,\widehat{mt}}{\pi\,\widehat{\mu t}}\sum_{srow}\frac{\widehat{PNpt}_{srow}}{\widehat{PNtt}_{srow}\,\widehat{Pdtt}_{srow}}\,yrow_{srow} \geq 10^4 \tag{253}$$

Geometric Constraints: The maximum and minimum baffle spacing constraints are:

$$\sum_{srow}\frac{\widehat{PL}_{srow}}{(\widehat{PNb}_{srow}+1)}\,yrow_{srow} \leq 1.0\;\sum_{srow}\widehat{PDs}_{srow}\,yrow_{srow} \tag{254}$$

$$\sum_{srow}\frac{\widehat{PL}_{srow}}{(\widehat{PNb}_{srow}+1)}\,yrow_{srow} \geq 0.2\;\sum_{srow}\widehat{PDs}_{srow}\,yrow_{srow} \tag{255}$$

The constraints related to the ratio between the tube length and the shell diameter are:

$$\sum_{srow}\widehat{PL}_{srow}\,yrow_{srow} \leq 15\;\sum_{srow}\widehat{PDs}_{srow}\,yrow_{srow} \tag{256}$$

$$\sum_{srow}\widehat{PL}_{srow}\,yrow_{srow} \geq 3\;\sum_{srow}\widehat{PDs}_{srow}\,yrow_{srow} \tag{257}$$

Objective Function: The expression of the objective function in relation to the binary variables is given by:

$$\text{Min } \pi\;\sum_{srow}\widehat{PNtt}_{srow}\,\widehat{Pdte}_{srow}\,\widehat{PL}_{srow}yrow_{srow} \tag{258}$$

Additional Constraints for the Convergence Acceleration: These extra sets of constraints aim to accelerate the search and are derived from the bounds on velocities, shell-side pressure drop, and tube length/shell diameter ratio. A lower bound on the heat transfer area is also included based on maximum flow velocities (see Chapter 2 for further details).

Flow Velocities Bounds.

$$yrow_{srow} = 0 \qquad \text{for } srow \in (Svsminout \cup Svsmaxout) \tag{259}$$

$$yrow_{srow} = 0 \qquad \text{for } srow \in (Svtminout \cup Svtmaxout) \tag{260}$$

The sets *Svsminout, Svsmaxout, Svtminout,* and *Svtmaxout* are given by:

$$Svsminout = \{srow\;/\frac{\widehat{ms}}{\widehat{\rho s}}\;\frac{(\widehat{PNb}_{srow}+1)}{\widehat{PDs}_{srow}\,\widehat{PFAR}_{srow}\,\widehat{PL}_{srow}} \leq \widehat{vsmin}-\widehat{\varepsilon}\} \tag{261}$$

$$Svsmaxout = \{srow \ / \ \frac{\widehat{ms}}{\widehat{\rho s}} \ \frac{(\widehat{PNb}_{srow}+1)}{\widehat{PDs}_{srow} \ \widehat{PFAR}_{srow} \ \widehat{PL}_{srow}} \geq \widehat{vsmax} + \hat{\varepsilon}\} \tag{262}$$

$$Svtminout = \{srow \ / \ \frac{4 \ \widehat{mt}}{\pi \ \widehat{\rho t}} \ \frac{\widehat{PNpt}_{srow}}{\widehat{PNtt}_{srow} \ \widehat{Pdti}_{srow}^2} \leq \widehat{vtmin} - \hat{\varepsilon}\} \tag{263}$$

$$Svtmaxout = \{srow \ / \ \frac{4 \ \widehat{mt}}{\pi \ \widehat{\rho t}} \ \frac{\widehat{PNpt}_{srow}}{\widehat{PNtt}_{srow} \ \widehat{Pdti}_{srow}^2} \geq \widehat{vtmax} + \hat{\varepsilon}\} \tag{264}$$

where $\hat{\varepsilon}$ is a small positive number.

Shell-Side Pressure Upper Bound.

$$yrow_{srow} = 0 \qquad \text{for } srow \in SDPsmaxout \tag{265}$$

where the set *SDPsmaxout* is given by:

$$SDPsmaxout = \{srow \ / \ \widehat{P\Delta Ps}_{srow} \geq \widehat{\Delta Psdisp} + \hat{\varepsilon}\} \tag{266}$$

Baffle Spacing.

$$yrow_{srow} = 0 \qquad \text{for } srow \in (SLNbminout \cup SLNbmaxout) \tag{267}$$

where the sets *SLNbminout* and *SLNbmaxout* are given by:

$$SLNbminout = \{srow \ / \ \frac{\widehat{PL}_{srow}}{\widehat{PNb}_{srow}+1} \leq 0.2\widehat{PDs}_{srow} - \hat{\varepsilon}\} \tag{268}$$

$$SLNbmaxout = \{srow \ / \ \frac{\widehat{PL}_{srow}}{\widehat{PNb}_{srow}+1} \geq 1.0\widehat{PDs}_{srow} + \hat{\varepsilon}\} \tag{269}$$

Tube Length / Shell Diameter Ratio.

$$yrow_{srow} = 0 \text{ for } srow \in (SLDminout \cup SLDmaxout) \tag{270}$$

where the sets *SLDminout* and *SLDmaxout* are given by:

$$SLDminout = \{srow \ / \ \widehat{PL}_{srow} \leq 3\widehat{PDs}_{srow} - \hat{\varepsilon}\} \tag{271}$$

$$SLDmaxout = \{srow \ / \ \widehat{PL}_{srow} \geq 15\widehat{PDs}_{srow} + \hat{\varepsilon}\} \tag{272}$$

Heat Transfer Area.

$$yrow_{srow} = 0 \qquad \text{for } srow \in SAminout \tag{273}$$

where the set of heat exchangers with area lower than the minimum possible is:

$$SAminout = \{srow \,/\pi\, \widehat{PNtt}_{srow}\widehat{Pdte}_{srow}\widehat{PL}_{srow} \leq \widehat{Amin} - \hat{\varepsilon}\} \tag{274}$$

The lower bound on the heat transfer area can be determined by:

$$\widehat{Amin} = \frac{\hat{Q}}{\widehat{Umax}\,\Delta \widehat{Tlm}} \tag{275}$$

$$\widehat{Umax} = \frac{1}{\frac{1}{\widehat{htmax}}\widehat{drmin} + \widehat{Rft}\cdot\widehat{drmin} + \frac{\widehat{Pdte}_{srow}\ln(\widehat{drmin})}{2\,\widehat{ktube}} + \widehat{Rfs} + \frac{1}{\widehat{hsmax}}} \tag{276}$$

$$\widehat{htmax} = \max(\widehat{Pht}_{srow}) \tag{277}$$

$$\widehat{hsmax} = \max(\widehat{Phs}_{srow}) \tag{278}$$

$$\widehat{drmin} = \min(\widehat{Pdte}_{srow}/\widehat{Pdti}_{srow}) \tag{279}$$

3.4 Results

The five aggregation alternatives of the discrete variables were applied to the sample of ten thermal tasks proposed in Chapter 2, involving different heating and cooling services. The complete description of each problem is available at the Tables 6, 7 and 8. The standard values of the discrete variables employed in the solutions are shown in Table 3, related to a fixed tubesheet type exchanger with tube thickness of 1.65 mm (BWG 16) and thermal conductivity of the tube wall equal to 50 W/m K. The minimum excess area is 11% and the tube count data is based on Kakaç et al. (2012).

These problems were solved using the five alternatives of MILP formulations described in Table 8, implemented in the optimization software GAMS using the solver CPLEX.

The comparison of the solution time demanded by each alternative (elapsed time) and the time consumed by the solver itself are shown in Table 12, together with the optimal value

of the objective function (since all alternatives are MILP problems, the solution found is always the same, corresponding to the global optimum). The computational times were measured using a computer with a processor Intel Core i7 3.40 GHz with 12.0 GB RAM memory. The details of each design solution are available at the Tables 13, 14, 15 and 16.

Table 12 - Performance Comparison

example	heat transfer area (m^2)	solution time (s) solver time (s)				
		1	2	3	4	5
1	624	1730	19	13	11	12
		1726	13	6	4	3
2	319	1574	44	12	10	11
		1571	39	6	4	3
3	199	212	10	11	9	11
		208	5	5	3	3
4	872	139	11	11	9	12
		136	5	5	3	3
5	144	869	19	11	10	12
		865	13	6	4	3
6	332	2755	49	12	9	11
		2751	44	6	4	3
7	207	2535	15	12	9	12
		2532	9	5	4	3
8	914	173	11	13	9	12
		169	6	7	3	3
9	287	2077	53	31	11	12
		2073	47	25	6	3
10	327	2342	43	25	10	12
		2338	37	19	4	3
Average	-	1440.6	27.4	15.1	9.7	11.7
		1436.9	21.8	9.0	3.9	3.0

Source: The author.

Table 13 - Heat Exchanger Results – Examples 1 to 5

	Example 1	Example 2	Example 3	Example 4	Example 5
Area (m^2)	624	319	199	872	144
Tube diameter (m)	0.019	0.019	0.019	0.019	0.019
Tube length (m)	4.877	6.098	4.877	6.098	3.049
Number of baffles	7	12	18	5	5
Number of tube passes	4	2	6	6	6
Tube pitch ratio	1.25	1.25	1.33	1.33	1.33
Shell diameter (m)	1.219	0.838	0.787	1.372	0.787
Tube layout	triangular	square	square	triangular	triangular
Total number of tubes	2139	875	682	2391	788
Baffle spacing (m)	0.610	0.469	0.257	1.016	0.508
Tube pitch (m)	0.024	0.024	0.025	0.025	0.025

Source: The author.

Table 14 - Heat Exchanger Results – Examples 6 to 10

	Example 6	Example 7	Example 8	Example 9	Example 10
Area (m^2)	332	207	914	287	327
Tube diameter (m)	0.019	0.019	0.025	0.019	0.019
Tube length (m)	4.877	3.049	6.098	4.877	4.877
Number of baffles	10	4	15	8	7
Number of tube passes	2	6	4	2	4
Tube pitch ratio	1.25	1.25	1.25	1.25	1.33
Shell diameter (m)	0.889	0.889	1.524	0.889	0.940
Tube layout	triangular	triangular	triangular	square	triangular
Total number of tubes	1137	1137	1880	985	1122
Baffle spacing (m)	0.443	0.610	0.381	0.542	0.610
Tube pitch (m)	0.024	0.024	0.032	0.024	0.025

Source: The author.

Table 15 - Thermo-fluid Dynamic Results – Examples 1 to 5

	Example 1	Example 2	Example 3	Example 4	Example 5
Shell-side flow velocity (m/s)	0.941	0.809	1.133	1.027	1.791
Tube-side flow velocity (m/s)	2.208	1.534	1.673	1.193	1.761
Shell-side heat transfer coefficient (W/m^{2}K)	1163	928	4902	5262	3039
Tube-side heat transfer coefficient (W/m^{2}K)	9206	6877	2928	2234	14846
Overall heat transfer coefficient (W/m^{2}K)	584	561	913	709	1498
Shell-side pressure drop (kPa)	84.88	49.46	97.41	62.36	66.41
Tube-side pressure drop (kPa)	91.87	28.48	57.93	37.54	46.48

Source: The author.

Table 16 - Thermo-fluid Dynamic Results – Examples 6 to 10

	Example 6	Example 7	Example 8	Example 9	Example 10
Shell-side flow velocity (m/s)	0.893	1.139	0.664	1.462	1.593
Tube-side flow velocity (m/s)	2.678	1.221	1.999	2.361	2.578
Shell-side heat transfer coefficient (W/m²K)	1845	5579	3644	2098	2388
Tube-side heat transfer coefficient (W/m²K)	10299	11072	7616	4162	2723
Overall heat transfer coefficient (W/m²K)	725	1833	980	803	746
Shell-side pressure drop (kPa)	63.89	65.91	96.73	87.61	76.91
Tube-side pressure drop (kPa)	66.65	23.19	67.08	33.89	99.39

Source: The author.

The solution times in Table 12 for the Alternative 1 differs slightly of those reported in Chapter 2, due to eventual computer performance fluctuations (the registered times are wall times from new independent runs conducted for the same problems).

The analysis of Table 12 indicates that the proposed procedure of aggregation of the binary variables (Alternatives 2 to 5) allows large reductions of the computational effort in relation to the original formulation (Alternative 1). The average time consumed by the solver is associated to reductions ranging from 98.50% to 99.79%. The corresponding reductions of the total elapsed time are similar, ranging from 98.10% to 99.33%.

Comparing the time consumed by the solver in the different alternatives, it is possible to observe that there is a reduction trend from Alternative 1 to Alternative 5, i.e. the increase of the binary variables aggregation decreases the solver time. The behavior of the total

elapsed time is similar, but the demand for processing larger data sets associated to the variable aggregation procedure implies in slightly higher computing times before the solver starts in these alternatives. Therefore, the lowest solver time is associated to the Alternative 5, but the lowest elapsed time corresponds to Alternative 4 (however, the difference is only 2 s).

3.5 Partial Conclusions

This chapter presented an investigation aiming at the reduction of the computational effort for the solution of the MILP problem for the design of shell and tube heat exchangers. Several linear formulations were proposed based on different alternatives of aggregation of the discrete values of the design variables in relation to the binary variables.

In the original MILP formulation developed in Chapter 2, each discrete value corresponds to a binary variable. The alternatives explored here tried to aggregate the discrete alternatives in tables, where each group of discrete values becomes an individual binary variable.

The results showed that the aggregation of the binary variables allows a considerable reduction of the computational effort to solve the MILP problem. Considering a sample of 10 design problems, the best aggregation alternative demanded only 0.21% of the total solver time in comparison of the original MILP.

This performance gain is important because it allows further investigations for the inclusion of this model into more complex problems, such as, the insertion of the detailed heat exchanger design into the heat exchanger network synthesis problem.

4 LINEAR METHOD FOR THE DESIGN OF SHELL AND TUBE HEAT EXCHANGERS USING THE BELL-DELAWARE METHOD

This chapter presents the optimization of shell-and-tube heat exchanger design using the Bell-Delaware method. This model is the most accurate method available in the open literature, but its mathematical structure is quite complex, which demands additional mathematical techniques for the presentation of a linear model. The proposed formulation also extends the tube-side heat transfer model including correlations to encompass laminar, transitional and turbulent flows.

4.1 Non-linear Heat Exchanger Design Model

We consider single E-type shell, single phase on both sides, single segmental baffles uniformly distributed without sealing strips and several tube passes, fixed fouling factors and we ignore pressure drops in the nozzles and the tube lane partition bypass stream. Eight design variables characterize each candidate solution: number of passes on the tube-side (*Npt*), tube diameter (outer and inner: *dte* and *dti*), tube layout (*lay*), tube pitch ratio (*rp*), number of baffles (*Nb*), shell diameter (*Ds*), tube length (*L*), and baffle cut ratio (*Bc*). The tube pitch ratio is the ratio between the tube pitch and the outer tube diameter. The baffle cut ratio is the ratio between the baffle cut and the inner shell diameter. We show model parameters using the symbol "^" on the top. The discrete nature of the design variables is represented by the following generic constraints for *dte*.

$$dte = \sum_{sd=1}^{sdmax} \widehat{pdte}_{sd}\, yd_{sd} \tag{280}$$

$$\sum_{sd=1}^{sdmax} yd_{sd} = 1 \tag{281}$$

The rest of the discrete variables are *dti, Ds, lay, Npt, rp, L, Nb* and *Bc*. The corresponding parameters are $\widehat{pdti}_{sd}$, $\widehat{pDs}_{sDs}$, $\widehat{play}_{slay}$, $\widehat{pNpt}_{sNpt}$, $\widehat{prp}_{srp}$, $\widehat{pL}_{sL}$, $\widehat{pNb}_{sNb}$,

and $\widehat{pBc}_{sBc}$ respectively. The set of constraints is accompanied by a summation of binaries $(yDs_{sDs}, ylay_{slay}, yNpt_{sNpt}, yrp_{srp}, yL_{SL}, yNb_{sNb} \text{ and } yBc_{sBc})$ equal to 1 so that only one option is chosen.

The clearances and diameters are illustrated by Figure 2: *Dctl* is the diameter of the circle delimited by the centers of the outer tubes of the bundle, and *Dotl* is the tube bundle diameter. They are related to other variables by:

$$Dctl = Ds - Lbb - dte \qquad (282)$$

$$Dotl = Ds - Lbb \qquad (283)$$

where *Lbb* is the diametral clearance between the shell and the tube bundle. Two angles associated to the model are also defined: θDs is the central angle defined by the intercession of the baffle cut edge with the shell and θctl is the central angle delimited by the intercession between the baffle cut edge and the circle associated to the centers of the outer tubes. They are related to other variables as follows:

$$\theta Ds = 2\arccos[1 - (2Bc)] \qquad (284)$$

$$\theta ctl = 2\arccos\left\{\frac{Ds}{Dctl}[1 - (2\,Bc)]\right\} \qquad (285)$$

Figure 2 - Geometry for (a) diameters *Dctl*, *Dotl*, and *Ds* and (b) angles θDs and θctl

(a)   (b)
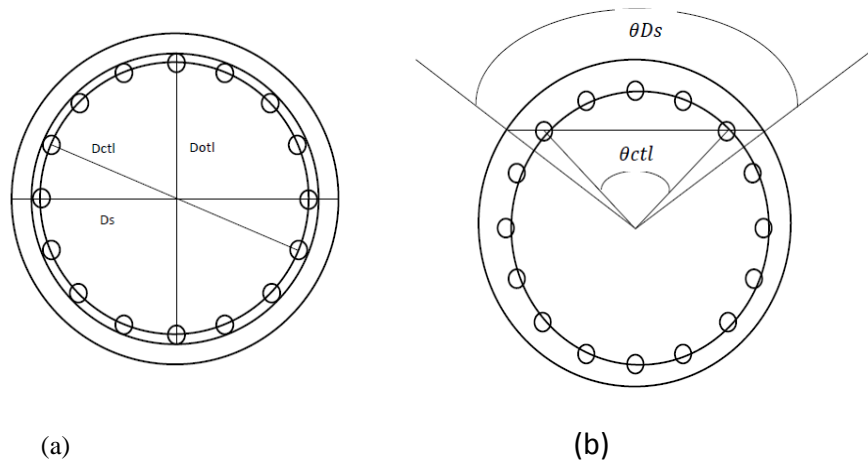
Source: The author.

The total number of tubes in a given shell (*Ntt*) and their relation to diameters and other variables are available in tube count tables with mathematical equations and algorithms for its evaluation (LUDWIG, 2001). In the proposed formulation, we use a set of equations from Taborek (2008d), organized as mathematical constraints of the optimization problem, as follows:

$$Ntt = \frac{0.78 Dctl^2}{C1\, ltp^2}(1 - \psi_n) \tag{286}$$

The parameter *C*1 is equal to 0.866 for a 30° layout or 1.00 for 45° and 90° layouts. Therefore:

$$C1 = 0.866 ylay_1 + 1.00(ylay_2 + ylay_3) \tag{287}$$

The correction factor ψ_n represents the omission of tubes inside the shell due to the presence of multiple tube passes. Based on a graph published by Taborek (2008d), this parameter can be represented by a set of values, which depends on the number of tube passes and the shell diameter (for the sake of simplification the dependence on the tube diameter was dismissed):

$$\psi_n = \sum_{sNpt=1}^{sNptmax} \sum_{sDs=1}^{sDsmax} \left(\overline{P\psi_n}\right)_{sNpt,sDs} yNpt_{sNpt} yDs_{sDs} \tag{288}$$

where the values of the parameter $\left(\overline{P\psi_n}\right)_{sNpt,sDs}$ are displayed in the Appendix B.

Next, *Ntcc* is the number of tube rows crossed between baffle tips and *Ntcw* is the effective number of tube rows crossed in the baffle window:

$$Ntcc = \frac{Ds}{Lpp}[1 - (2\,Bc)] \tag{289}$$

$$Ntcw = \frac{0.8}{Lpp}\left[(Ds\,Bc) - \frac{(Ds - Dctl)}{2}\right] \tag{290}$$

where *Lpp* is equal to 0.866*ltp* for 30° layout (*slay* = 1), *ltp* for 90° layout (*slay* = 2), and 0.707*ltp* for 45° layout (*slay* = 3). This relation is represented by:

$$Lpp = 0.866\,ltp\,ylay_1 + ltp\,ylay_2 + 0.707\,ltp\,ylay_3 \tag{291}$$

The total number of rows crossed along the entire heat exchanger (*Nc*) is given by:

$$Nc = (Ntcc + Ntcw)(Nb + 1) \tag{292}$$

where *Nb* is the number of baffles. For a uniform distribution of the baffles along the tube length, the relation between the baffle spacing (*lbc*) and the number of baffles is:

$$Nb = L/lbc - 1 \tag{293}$$

The fraction of the number of tubes inside one window (*Fw*) is:

$$Fw = \frac{\theta ctl - \sin\theta ctl}{2\pi} \tag{294}$$

Consequently, the fraction of the number of tubes in pure cross flow between baffle tips (*Fc*) is:

$$Fc = 1 - 2Fw \tag{295}$$

The cross-flow area is delimited between adjacent baffles and it is evaluated at the shell center line:

$$Sm = lbc\left[Lbb + \frac{Dctl}{ltp_{eff}}(ltp - dte)\right] \tag{296}$$

where *ltp* is the tube pitch, and ltp_{eff} is the distance between tubes along the rows perpendicular to the flow. The value of ltp_{eff} depends on the tube layout, it is equal to *ltp* for 30° and 90° layouts and it is equal to $0.707 ltp$ for 45° layout:

$$ltp_{eff} = ltp(ylay_1 + ylay_2 + 0.707\ ylay_3) \tag{297}$$

According to the definition of the tube pitch ratio:

$$ltp = rp\ dte \tag{298}$$

The flow through the baffle window is associated to the free flow area in that region (*Sw*), that is calculated by the difference between the gross window flow area (*Swg*), i.e. excluding the presence of the tubes, and the area occupied by the tubes (*Swt*):

$$Sw = Swg - Swt \tag{299}$$

$$Swg = \frac{\pi}{4}Ds^2\left(\frac{\theta Ds - \sin\theta Ds}{2\pi}\right) \tag{300}$$

$$Swt = Ntw\left(\frac{\pi}{4}dte^2\right) \tag{301}$$

where *Ntw* is the number of tubes in the window, which is equivalent by the total number of

tubes (*Ntt*) multiplied by the fraction of the number of tubes in one window (*Fw*):

$$Ntw = Ntt\ Fw \tag{302}$$

The flow area between the shell and the baffle (*Ssb*) is:

$$Ssb = \pi Ds \left(\frac{Lsb}{2}\right)\left(1 - \frac{\theta Ds}{2\pi}\right) \tag{303}$$

where *Lsb* is the shell-to-baffle diametral clearance.

The area of the flow through the hole leakage area of the baffle (*Stb*) is:

$$Stb = Ntt(1 - Fw)\left\{\frac{\pi}{4}[(dte + Ltb)^2 - dte^2]\right\} \tag{304}$$

where *Ltb* is the tube-to-baffle clearance. The bypass flow area between the tube bundle and

the shell is given by:

$$Sb = lbc[(Ds - Dotl) + Lpl] \tag{305}$$

where *Lpl* expresses the effect of the tube lane partition bypass width (in the proposed model,

this gap was dismissed, then *Lpl* = 0).

The model also contains factors related to the area ratios: *rs* is the ratio of the shell-to-

baffle leakage area to the sum of this area and the tube-to-baffle leakage area, *rlm* is the ratio

of both leakage areas to the cross-flow area, *Fsbp* is the ratio of the bypass area between the

tube bundle and the shell to the cross-flow area:

$$rs = \frac{Ssb}{Ssb + Stb} \tag{306}$$

$$rlm = \frac{Ssb + Stb}{Sm} \tag{307}$$

$$Fsbp = \frac{Sb}{Sm} \tag{308}$$

Expressions for evaluation of the clearances *Lbb* (for fixed tubesheet or U tubes) and

Lsb (based on TEMA standards (TEMA, 2007)) are given by Taborek (2008d), respectively:

$$Lbb = 12.8 \cdot 10^{-3} + 4.8 \cdot 10^{-3} Ds \tag{309}$$

$$Lsb = 3.1 \cdot 10^{-3} + 4 \cdot 10^{-3}\ Ds \tag{310}$$

The diametral clearance between the outer tube diameter and the baffle hole is also established by TEMA standards, as follows:

$$dte > 0.03175 \text{ m} \rightarrow Ltb = 0.008 \text{ m} \tag{311}$$

$$dte \leq 0.03175 \text{ m and } lbmax \leq 0.900\text{m} \rightarrow Ltb = 0.008 \text{ m} \tag{312}$$

$$dte \leq 0.03175 \text{ m and } lbmax > 0.900 \text{ m} \rightarrow Ltb = 0.004 \text{ m} \tag{313}$$

where *lbmax* is the maximum unsupported span of the tubes, calculated according to TEMA recommended values (see Equation 372). In the optimization problem, the relations related to Equations 311-313 are represented by a set of values that can be calculated previously depending on the design alternatives:

$$Ltb = \sum_{sd=1}^{sdmax} \sum_{sL=1}^{sLmax} \sum_{sNb=1}^{sNbmax} \widehat{pLtb}_{sDs,sL,sNb} \; yd_{sd} \; yL_{sL} \; yNb_{sNb} \tag{314}$$

Shell-side thermal and hydraulic equations

There are some slightly different variations in the literature of the Bell-Delaware method (SERTH, 2007). We employ equations based on Taborek (2008d).

The heat transfer coefficient is calculated using the Reynolds ($Res=dte \; Gs/\widehat{\mu s}$) and Prandtl numbers ($\widehat{Prs} = \widehat{Cps} \; \widehat{\mu s}/\widehat{ks}$) for the shell-side stream, associated to the mass flux $Gs = \widehat{ms}/Sm$. The shell-side heat transfer coefficient corresponds to the ideal tube bank coefficient (*hi*) multiplied by a series of factors that account the by-pass and leakage streams:

$$hs = hi(Jc \; Jl \; Jb \; Jr) \tag{315}$$

where *Jc* is the segmental baffle window correction factor, *Jl* is the correction factor for baffle leakage effects, *Jb* is the correction factor for bundle to shell bypass effects, *Jr* is the correction factor for adverse temperature gradient in laminar flow. The original Bell Delaware method also uses a correction factor for unequal baffle spacing at the inlet or outlet (we do not include it here; we use uniform distribution of the baffle spacing). In turn, the shell-side heat transfer coefficient for ideal tube bank is given by:

$$hi = ji \; \widehat{Cps} \; Gs \; \widehat{Prs}^{-2/3} \tag{316}$$

where ji is the Colburn's heat transfer factor for ideal tube bank flow:

$$ji = a1 \left(\frac{1.33}{rp}\right)^a Res^{a2} \tag{317}$$

The parameters a, $a1$, $a2$, and $a3$ are given by:

$$a = \frac{a3}{1+0.14Res^{a4}} \tag{318}$$

$$a1 = \sum_{sRes=1}^{sResmax} \sum_{slay=1}^{slaymax} \widehat{Pa1}_{sRes,slay} yRes_{sRes} ylay_{slay} \tag{319}$$

$$a2 = \sum_{sRes=1}^{sResmax} \sum_{slay=1}^{slaymax} \widehat{Pa2}_{sRes,slay} yRes_{sRes} ylay_{slay} \tag{320}$$

$$a3 = \sum_{sRes=1}^{sResmax} \sum_{slay=1}^{slaymax} \widehat{Pa3}_{sRes,slay} yRes_{sRes} ylay_{slay} \tag{321}$$

$$a4 = \sum_{sRes=1}^{sResmax} \sum_{slay=1}^{slaymax} \widehat{Pa4}_{sRes,slay} yRes_{sRes} ylay_{slay} \tag{322}$$

where the values of the parameters $\widehat{Pa1}_{sRes,slay}$, $\widehat{Pa2}_{sRes,slay}$, $\widehat{Pa3}_{sRes,slay}$, and $\widehat{Pa4}_{sRes,slay}$ are displayed in the Appendix B.

The binary variables $yRes_{sRes}$ allow the regime choice through:

$$Res \leq 10yRes_1 + 20yRes_2 + 10^2 yRes_3 + 10^3 yRes_4 + 10^4 yRes_5 + 10^5 yRes_6 \tag{323}$$

$$Res \geq 10yRes_2 + 20yRes_3 + 10^2 yRes_4 + 10^3 yRes_5 + 10^4 yRes_6 + \hat{\varepsilon} \tag{324}$$

$$\sum_{sRes=1}^{sResmax} yRes_{sRes} = 1 \tag{325}$$

where $\hat{\varepsilon}$ is a small positive number and is required to identify when the variable is related to another range.

The correction factors that contribute to calculate hs are given by:

$$Jc = 0.55 + 0.72Fc \tag{326}$$

$$Jl = 0.44(1 - rs) + [1 - 0.44(1 - rs)]\exp(-2.2rlm) \tag{327}$$

$$Jb = \exp[-Cbh \; Fsbp] \tag{328}$$

$$Jr = Jr1 \; (yRes_1 + yRes_2) + Jr2 \; yRes_3 + Jr3 \; (yRes_4 + yRes_6 + yRes_6) \tag{329}$$

where Cbh is equal to 1.35 for laminar flow (Res $\leq$ 100) and 1.25 for turbulent and transition flow (Res $>$ 100), thus Cbh corresponds to:

$$Cbh = 1.35(yRes_1 + yRes_2 + yRes_3) + 1.25(yRes_4 + yRes_5 + yRes_6) \tag{330}$$

The different values of the heat transfer correction factor for adverse temperature gradient in laminar flow is given by:

$$Jr1 = \left(\frac{10}{Nc}\right)^{0.18} \qquad\qquad \text{for } Res \leq 20 \tag{331}$$

$$Jr2 = Jr1 + \left(\frac{20-Res}{80}\right)[Jr1 - 1] \qquad \text{for } 20 < Res \leq 100 \tag{332}$$

$$Jr3 = 1 \qquad\qquad \text{for } Res > 100 \tag{333}$$

The shell-side pressure drop (ΔPs) includes the pressure drop in the flow through the tube bundle between adjacent baffles in cross flow (ΔPc), the pressure drop in the baffle windows (ΔPw), and the pressure drop at the end zones (ΔPe):

$$\Delta Ps = \Delta Pc + \Delta Pw + \Delta Pe \tag{334}$$

In turn, the pressure drop of the cross flow between baffle tips is given by:

$$\Delta Pc = \Delta Pbi\ (Nb - 1)\ Rb\ Rl \tag{335}$$

where ΔPbi is the ideal bank pressure drop delimited by one central baffle spacing, Rb is the by-pass correction factor, and Rl is the leakage correction factor. Finally, the ideal bank pressure drop between baffle tips is given by:

$$\Delta Pbi = 2\ fs\ Ntcc\ \frac{Gs^2}{\widehat{\rho}s} \tag{336}$$

where fs is the friction factor for ideal tube bank flow, given by:

$$fs = b1\left(\frac{1.33}{rp}\right)^b Res^{b2} \tag{337}$$

The values of b, $b1$, $b2$, $b3$, and $b4$ are represented by the following expressions:

$$b = \frac{b3}{1+0.14Res^{b4}} \tag{338}$$

$$b1 = \sum_{sRes=1}^{sResmax} \sum_{slay=1}^{slaymxa} \widehat{Pb1}_{sRes,slay} yRes_{sRes} ylay_{slay} \tag{339}$$

$$b2 = \sum_{sRes=1}^{sResmax} \sum_{slay=1}^{slaymxa} \widehat{Pb2}_{sRes,slay} yRes_{sRes} ylay_{slay} \tag{340}$$

$$b3 = \sum_{sRes=1}^{sResmax} \sum_{slay=1}^{slaymxa} \widehat{Pb3}_{sRes,slay} yRes_{sRes} ylay_{slay} \tag{341}$$

$$b4 = \sum_{sRes=1}^{sResmax} \sum_{slay=1}^{slaymxa} \widehat{Pb4}_{sRes,slay} yRes_{sRes} ylay_{slay} \tag{342}$$

where the values of the parameters $\widehat{Pb1}_{sRes,slay}$, $\widehat{Pb2}_{sRes,slay}$, $\widehat{Pb3}_{sRes,slay}$, and $\widehat{Pb4}_{sRes,slay}$ are displayed in the Appendix B.

The correction factor *Rb* is given by, considering the hypothesis that there is no sealing strips, is given by:

$$Rb = \exp[-Cbp\, Fsbp] \tag{343}$$

where *Cbp* is equal to 4.5 for laminar flow and is equal to 3.7 for transition and turbulent flow and, for the optimization problem, is expressed by:

$$Cbp = 4.5(yRes_1 + yRes_2 + yRes_3) + 3.7(yRes_4 + yRes_5 + yRes_6) \tag{344}$$

The correction factor *Rl* is given by:

$$Rl = \exp[-1.33(1+rs)(rlm)^p] \tag{345}$$

where:

$$p = -0.15(1+rs) + 0.8 \tag{346}$$

The pressure drop in the baffle windows depends on the mass flux in relation to the geometric mean of the cross-flow area and the window area ($Gw = \widehat{ms}/\sqrt{SmSw}$). Therefore, the pressure drop expression (*Res* < 100) for laminar flow is equal to:

$$\Delta Pw^{lam} = Nb\, Rl\left\{26\frac{Gw\,\widehat{\mu s}}{\widehat{\rho s}}\left[\frac{Ntcw}{Ltp-dte} + \frac{lbc}{Dw^2}\right] + \left[2\frac{Gw^2}{\widehat{\rho s}}\right]\right\} \tag{347}$$

where the hydraulic diameter (*Dw*) is equal to:

$$Dw = \frac{4\,Sw}{\pi\, dte\, Ntw + \pi\, Ds\left(\frac{\theta Ds}{2\pi}\right)} \tag{348}$$

The corresponding expression for turbulent flow (*Res* ≥ 100) is:

$$\Delta Pw^{turb} = Nb\, Rl\left[(2 + 0.6Ntcw)\frac{Gw^2}{2\widehat{\rho s}}\right] \tag{349}$$

Thus, the pressure drop in the baffle windows for the optimization problem is:

$$\Delta Pw = \Delta Pw^{lam}(yRes_1 + yRes_2 + yRes_3) + \Delta Pw^{turb}(yRes_4 + yRes_5 + yRes_6) \tag{350}$$

The pressure drop at both end zones is equal to:

$$\Delta Pe = \Delta Pbi \left(1 + \frac{Ntcw}{Ntcc}\right) Rb\, Rs \tag{351}$$

where *Rs* is the end zone correction factor:

$$Rs = \left(\frac{lbc}{lbo}\right)^{2-n} + \left(\frac{lbc}{lbi}\right)^{2-n} \tag{352}$$

where $n = 1$ for laminar ($Res < 100$) and $n = 0.2$ for turbulent ($Res \geq 100$). However, according to the assumption that all baffle spacings are equal, this expression becomes equal to 2.

Tube-side thermal and hydraulic equations

The Reynolds ($Ret = dti\, vt\, \widehat{\rho t}\, /\, \widehat{\mu t}$) and Prandtl numbers ($\widehat{Prt} = \widehat{Cpt}\,\widehat{\mu t}/\widehat{kt}$) of the tube-side flow compose the heat transfer correlations for the determination of the Nusselt number ($Nut = ht\, dti\, /\, \widehat{kt}$), where $\widehat{\rho t}$ is the density, $\widehat{Cpt}$ is the heat capacity, $\widehat{\mu t}$ is the viscosity, and $\widehat{kt}$ is the thermal conductivity. The flow velocity is given by:

$$vt = \frac{4\,\widehat{mt}}{Ntp\, \pi\, \widehat{\rho t} dti^2} \tag{353}$$

where $\widehat{mt}$ is the mass flow rate and *Ntp* is the number of tubes per pass (calculated by the ratio between the total number of tubes, *Ntt*, and the number of passes in the tubes, *Npt*).

The adopted modelling for the evaluation of the convective heat transfer coefficient in the tube-side contemplates laminar, transitional, and turbulent flow according to the proposal of Incropera and De Witt (2006). The evaluation of the Nusselt number for the turbulent and transition regimes employs the Gnielinski correlation ($2300 < Ret < 5 \cdot 10^6$):

$$Nut^{Gni} = \frac{\left(ft/8\right)(Ret-1000)\widehat{Prt}}{1+12.7\left(ft/8\right)^{1/2}\left(\widehat{Prt}^{2/3}-1\right)} \tag{354}$$

where *ft* is tube-side Darcy friction factor. For the laminar flow ($Ret \leq 2300$), the effects related to the entry region may be relevant. Therefore for $\widehat{Prt} > 5$, the Hausen correlation is employed:

$$Nut^{Hau} = 3.66 + \frac{0.0668\left(dti/_L\right) Ret \, \widehat{Prt}}{1+0.04\left[\left(dti/_L\right) Ret \, \widehat{Prt}\right]^{2/3}} \tag{355}$$

For $0.6 \leq \widehat{Prt} \leq 5$, for the calculation of the number of Nusselt we use the Sieder and Tate correlation:

$$Nut^{S\&T} = 1.86\left(\frac{Ret\widehat{Prt}}{L/_{dti}}\right)^{1/3} \tag{356}$$

However, when the Nusselt falls lower than 3.66 (theoretical result for fully developed flow), then this limit value is used ($Nut^{theo} = 3.66$).

The head loss in the tube-side flow is (SAUNDERS, 1988):

$$\Delta Pt = \widehat{\rho t} \, ft \frac{L \, Npt}{dti} \frac{vt^2}{2} + \frac{\widehat{\rho t} \, K \, Npt \, vt^2}{2} \tag{357}$$

where the parameter K, associated with the head loss in the heads, is equal to 0.9 for one tube pass and 1.6 for multiple passes. Considering all flow regimes, the friction factor is given by (SAUNDERS, 1988):

$$ft^{lam} = \frac{64}{Ret} \qquad \text{for} \quad Ret \leq 1311 \tag{358}$$

$$ft^{trans} = 0.0488 \qquad \text{for} \quad 1311 < Ret < 3380 \tag{359}$$

$$ft^{turb} = 0.014 + \frac{1.056}{Ret^{0.42}} \qquad \text{for} \quad Ret \geq 3380 \tag{360}$$

The evaluation of the Nusselt number and the friction factor associated to the selection of the proper regime can be expressed using binary variables:

$$Nut = Nut^{theo}(yRet_1 + yRet_2) \, yNut_1 + Nut^{S\&T}(yRet_1 + yRet_2) \, \widehat{PyPrt} \, yNut_2 +$$
$$Nut^{Hau}(yRet_1 + yRet_2)(1 - \widehat{PyPrt}_1)yNut_2 + Nut^{Gni}(yRet_3 + yRet_4) \tag{361}$$

$$ft = ft^{lam}yRet_1 + ft^{trans}(yRet_2 + yRet_3) + ft^{turb}yRet_4 \tag{362}$$

where the parameter $\widehat{PyPrt}$ is equal to 1 if $\widehat{Prt} \leq 5$, otherwise it is zero. The ranges of the Reynolds number associated to the binary variables are: < 1311 ($sRet = 1$), 1311 to 2300 ($sRet = 2$), 2300 to 3380 ($sRet = 3$), and > 3380 ($sRet = 4$). Thus,

$$Ret \leq 1311 \, yRet_1 + 2300 \, yRet_2 + 3380 \, yRet_3 + \widehat{URet} \, yRet_4 \tag{363}$$

$$Ret \geq 1311 yRet_2 + 2300 yRet_3 + 3380\ yRet_4 + \hat{\varepsilon} \tag{364}$$

$$\sum_{sRet=1}^{sRetmax} yRet_{sRet} = 1 \tag{365}$$

$$Nut < 3.66\ yNut_1 + \widehat{UNut}\ yNut_2 \tag{366}$$

$$Nut \geq 3.66\ yNut_2 + \hat{\varepsilon} \tag{367}$$

where $\hat{\varepsilon}$ is a small positive number. The parameter $\widehat{URet} = 5 \cdot 10^6$ is an upper bond on the Reynolds number, consistent with the validity range of the Gnielinski correlation. The upper bound parameter $\widehat{UNut}$ is assumed equal to $4 \cdot 10^4$, calculated accordingly the value of $\widehat{URet}$.

Heat transfer rate equation and overall heat transfer coefficient

For the area equation, we use a design margin ("excess area", $\widehat{Aexc}$):

$$UA \geq \left(1 + \frac{\widehat{Aexc}}{100}\right)\frac{\hat{Q}}{\Delta\widehat{Tlm}\ F} \tag{368}$$

The overall heat transfer coefficient is:

$$U = \cfrac{1}{\cfrac{dte}{dti\ ht} + \cfrac{\widehat{Rft}\ dte}{dti} + \cfrac{dte\ \ln(\frac{dte}{dti})}{2\ \widehat{ktube}} + \widehat{Rfs} + \cfrac{1}{hs}} \tag{369}$$

The area of the heat exchanger is the sum of the area of each individual tube:

$$A = Ntt\ \pi\ dte\ L \tag{370}$$

where $\widehat{ktube}$ is the thermal conductivity of the tube wall, and $\widehat{Rft}$ and $\widehat{Rfs}$ are the tube-side and shell-side fouling factors. The LMTD correction factor is 1 for countercurrent flow and, for an even number of tube passes, depends on the end temperatures ($\widehat{Fmp}$) (see Equation 394 for the corresponding expression):

$$F = 1\ yNpt_1 + \widehat{Fmp} \sum_{sNpt=2}^{SNptmax} yNpt_{sNpt} \tag{371}$$

Bounds on pressure drops, flow velocities and geometric constraints

Lower and upper bounds constraints on pressure drops and flow velocities are added and because design recommendations impose that the baffle spacing must be between 20%

and 100% of the shell diameter (TABOREK, 2008d) we use $lbc \geq 0.2\ Ds$ and $lbc \leq 1.0\ Ds$.

We use TEMA standards upper bound on the maximum unsupported span of the tubes (*lbmax*), which prevents sagging and vibration, is dependent on the nature of the material and the outer tube diameter (TEMA, 2007):

$$lbmax = \widehat{plbmax}1\ dte + \widehat{plbmax}2 \tag{372}$$

where, for tube diameters higher than 19 mm (3/4 in), $\widehat{plbmax}1 = 52$ and $\widehat{plbmax}2 = 0.532$ m for steel and steel alloys, and $\widehat{plbmax}1 = 46$ and $\widehat{plbmax}2 = 0.436$ m, for aluminum and copper alloys.

The maximum unsupported span is related to the window region, then the constraint involving the baffle spacing is $lbc \leq lbmax/2$. Finally, the ratio between exchanger length and shell diameter must be between 3 and 5 ($L \geq 3\ Ds$ and $L \leq 15\ Ds$) (TABOREK, 2008d).

Objective function

Two alternative objective functions are considered: the first is the minimization of the area associated to given values of maximum pressure drops, and the second is the minimization of the total annualized cost (capital and operating costs in a yearly basis). According to Mizutani et al. (2003), this alternative of objective function can be represented by:

$$\text{Min } \widehat{a_{cost}} A^{\widehat{b_{cost}}} + P_{cost} \tag{373}$$

where $\widehat{a_{cost}}$ and $\widehat{b_{cost}}$ are parameters for the evaluation of the annualized capital cost of the heat exchanger and P_{cost} is the pumping cost:

$$P_{cost} = \widehat{c_{cost}} \left(\frac{\Delta Pt\ \widehat{mt}}{\widehat{\rho t}} + \frac{\Delta Ps\ \widehat{ms}}{\widehat{\rho s}} \right) \tag{374}$$

4.2 Development of the MILP Formulation

The same technique employed in Chapter 3 was use to obtain a MILP formulation. Instead of representing each discrete alternative of each variable by an individual index, a single index, *srow*, is associated to each set of discrete values which compose a candidate solution.

4.3 MILP Formulation

This section presents the complete linear formulation of the optimal heat exchanger design problem resultant of the application of the techniques described before.

Heat transfer rate equations

$$\hat{Q}\left[\sum_{srow=1}^{srowmax} \frac{\widehat{Pdte}_{srow}}{\widehat{kt}} \left\{ \frac{1}{\widehat{PNut1}} wyrowNut1Ret1_{srow} + \frac{\widehat{PyPrt}}{\widehat{PNut2}_{srow}} wyrowNut2Ret1_{srow} + \right.\right.$$

$$\frac{1-\widehat{PyPrt}}{\widehat{PNut3}_{srow}} wyrowNut2Ret1_{srow} + \frac{1}{\widehat{PNut1}} wyrowNut1Ret2_{srow} +$$

$$\frac{\widehat{PyPrt}}{\widehat{PNut2}_{srow}} wyrowNut2Ret2_{srow} + \frac{1-\widehat{PyPrt}}{\widehat{PNut3}_{srow}} wyrowNut2Ret2_{srow} +$$

$$\left. \frac{1}{\widehat{PNut4}_{srow}} wyrowRet3_{srow} + \frac{1}{\widehat{PNut5}_{srow}} wyrowRet4_{srow} \right\} +$$

$$\sum_{srow=1}^{srowmax} \frac{\widehat{Rft}\,\widehat{Pdte}_{srow}}{\widehat{Pdti}_{srow}} yrow_{srow} + \sum_{srow=1}^{srowmax} \frac{\widehat{Pdte}_{srow}\ln\left(\frac{\widehat{Pdte}_{srow}}{\widehat{Pdti}_{srow}}\right)}{2\,\widehat{ktube}} yrow_{srow} + \widehat{Rfs} +$$

$$\left. \sum_{sRes=1}^{sResmax} \sum_{srow=1}^{srowmax} \frac{1}{\widehat{Phs}_{srow,sRes}} wyrowRes_{srow,sRes} \right] \le$$

$$\sum_{srow=1}^{srowmax} \pi \widehat{PNtt}_{srow} \widehat{Pdte}_{srow} \widehat{PL}_{srow} \left(\frac{100}{100+\widehat{Aexc}} \right) \widehat{\Delta Tlm}\ (\hat{F}_{srow}) yrow_{srow}) \quad (375)$$

where $\widehat{PNtt}_{srow}$ is the total number of tubes that can be calculated prior to the optimization using Equations 286-288. The expressions related to the other parameters are:

$$\widehat{PDctl}_{srow} = \widehat{PDs}_{srow} - \widehat{PLbb}_{srow} - \widehat{Pdte}_{srow} \quad (376)$$

$$\widehat{P\theta ctl}_{srow} = 2\left(\cos^{-1}\left\{\left(\frac{\widehat{PDs}_{srow}}{\widehat{PDctl}_{srow}}\right)\left[1 - 2\left(\widehat{PBc}_{srow}\right)\right]\right\}\right) \tag{377}$$

$$\widehat{PFw}_{srow} = \frac{\widehat{P\theta ctl}_{srow} - \sin(\widehat{P\theta ctl}_{srow})}{2\pi} \tag{378}$$

$$\widehat{Pltp}_{srow} = \widehat{Prp}_{srow}\widehat{Pdte}_{srow} \tag{379}$$

$$\widehat{pC1}_{srow} = 0.866 \quad \text{if lay} = 30° \tag{380}$$

$$\widehat{pC1}_{srow} = 1 \qquad \text{if lay} = 45° \text{ or } 90° \tag{381}$$

$$\widehat{PNtt1}_{srow} = \left(\frac{0.78\left(\widehat{PDctl}_{srow}\right)^2}{\widehat{PC1}_{srow}\left(\widehat{Pltp}_{srow}\right)^2}\right) \tag{382}$$

$$\widehat{PNtt}_{srow} = \left(\widehat{PNtt1}_{srow}\right)\left(1 - \widehat{P\psi n}_{srow}\right) \tag{383}$$

$$\widehat{Pvt}_{srow} = \frac{4\,\widehat{mt}}{\pi\,\widehat{\rho t}}\frac{\widehat{PNpt}_{srow}}{\widehat{PNtt}_{srow}\left(\widehat{Pdtl}_{srow}\right)^2} \tag{384}$$

$$\widehat{Plbc}_{srow} = \frac{\widehat{PL}_{srow}}{\left(\widehat{PNb}_{srow}+1\right)} \tag{385}$$

$$\widehat{Paltp, eff}_{srow} = 1 \quad \text{if } lay = 30° \tag{386}$$

$$\widehat{Paltp, eff}_{srow} = 1 \quad \text{if } lay = 90° \tag{387}$$

$$\widehat{Paltp, eff}_{srow}0.707 \quad \text{if } lay = 45° \tag{388}$$

$$\widehat{Pltp, eff}_{srow} = \widehat{Paltp, eff}_{srow}\widehat{Prp}_{srow}\widehat{Pdte}_{srow} \tag{389}$$

$$\widehat{PSm}_{srow} = \widehat{Plbc}_{srow}\left[\widehat{PLbb}_{srow} + \frac{\widehat{PDctl}_{srow}}{\widehat{Pltp,eff}_{srow}}\left(\widehat{Pltp}_{srow} - \widehat{Pdte}_{srow}\right)\right] \tag{390}$$

$$\widehat{Pvs}_{srow} = \frac{\widehat{ms}}{(\widehat{PSm}_{srow})} \tag{391}$$

$$\hat{R} = \frac{\widehat{Thi}-\widehat{Tho}}{\widehat{Tco}-\widehat{Tci}} \tag{392}$$

$$\hat{P} = \frac{\widehat{Tco}-\widehat{Tci}}{\widehat{Thi}-\widehat{Tci}} \tag{393}$$

$$\widehat{Fmp} = \frac{(\hat{R}^2+1)^{0.5}\ \ln\left(\frac{(1-\hat{P})}{(1-\hat{R}\hat{P})}\right)}{(\hat{R}-1)\ln\left(\frac{2-\hat{P}\left(\hat{R}+1-(\hat{R}^2+1)^{0.5}\right)}{2-\hat{P}\left(\hat{R}+1+(\hat{R}^2+1)^{0.5}\right)}\right)} \qquad \text{if sNpt} > 1 \tag{394}$$

$$\widehat{PLbb}_{srow} = 0.0048\ \widehat{PDs}_{srow} + 0.0128 \tag{395}$$

$$\hat{\varepsilon} = 10^{-6} \tag{396}$$

$$\widehat{URet} = 5.\,10^6 \tag{397}$$

$$\widehat{UNut} = 4.\,10^4 \tag{398}$$

$$\widehat{PRet}_{srow} = \frac{\widehat{\rho t}}{\widehat{\mu t}}\ \widehat{Pdti}_{srow}\widehat{Pvt}_{srow} \tag{399}$$

$$\widehat{Pft1}_{srow} = \frac{64}{\widehat{PRet}_{srow}} \tag{400}$$

$$\widehat{Pft2}_{srow} = 0.014 + \left[\frac{1.056}{\widehat{PRet}_{srow}^{0.42}}\right] \tag{401}$$

$$\widehat{PftRet2}_{srow} = 0.0488\ \widehat{PRet}_{srow} \tag{402}$$

$$\widehat{PftRet3}_{srow} = \widehat{Pft2}_{srow}\widehat{PRet}_{srow} \tag{403}$$

$$\widehat{PNut1} = 3.66 \tag{404}$$

$$\widehat{PNut2}_{srow} = 1.86 \left(\frac{\widehat{PRet}_{srow}\widehat{Prt}}{\widehat{PL}_{srow}/\widehat{Pdt\iota}_{srow}} \right)^{\frac{1}{3}}$$

(405)

$$\widehat{PNut3}_{srow} = 3.66 + \frac{0{,}0668 \left(\widehat{Pdt\iota}_{srow}/\widehat{PL}_{srow} \right) \widehat{PRet}_{srow}\,\widehat{Prt}}{1+0.04 \left[\left(\widehat{Pdt\iota}_{srow}/\widehat{pL}_{srow} \right) \widehat{PRet}_{srow}\,\widehat{Prt} \right]^{2/3}}$$

(406)

$$\widehat{PNut4}_{srow} = \frac{\frac{\widehat{Prt}}{8}\left((Pf\widehat{tRet2}_{srow})-1000\,(0.0488)\right)}{1+\frac{12,7}{8^{1/2}}\left(\widehat{Prt}^{2/3}-1\right)\left(0.0488^{1/2}\right)}$$

(407)

$$\widehat{PNut5}_{srow} = \frac{\frac{\widehat{Prt}}{8}\left((Pf\widehat{tRet3}_{srow})-1000\,(\widehat{Pft2}_{srow})\right)}{1+\frac{12,7}{8^{1/2}}\left(\widehat{Prt}^{2/3}-1\right)\widehat{Pft2}_{srow}^{1/2}}$$

(408)

$$\widehat{P\Delta Pt1}_{srow} = \frac{\widehat{\rho t}}{2}\frac{\widehat{PL}_{srow}\widehat{PNpt}_{srow}}{\widehat{Pdt\iota}_{srow}}\left(\widehat{Pvt}_{srow}\right)^2$$

(409)

$$\widehat{PK_{srow}} = 0.9 \quad \text{if sNpt =1}$$

(410)

$$\widehat{PK_{srow}} = 1.6 \quad \text{if sNpt >1}$$

(411)

$$P\Delta\widehat{Phead}_{srow,sRet} = \frac{\widehat{PK_{srow}}\widehat{\rho t}\widehat{PNpt}_{srow}(\widehat{Pvt}_{srow})^2}{2}$$

(412)

$$P\Delta\widehat{Pttube}_{srow,sRet} = \widehat{P\Delta Pt1}_{srow}\widehat{Pft1}_{srow} \text{ if sRet =1}$$

(413)

$$P\Delta\widehat{Pttube}_{srow,sRet} = 0.0488\,\widehat{P\Delta Pt1}_{srow} \quad \text{if sRet =2}$$

(414)

$$P\Delta\widehat{Pttube}_{srow,sRet} = 0.0488\,\widehat{P\Delta Pt1}_{srow} \quad \text{if sRet =3}$$

(415)

$$P\Delta\widehat{Pttube}_{srow,sRet} = \widehat{P\Delta Pt1}_{srow}\widehat{Pft2}_{srow} \text{ if sRet =4}$$

(416)

$$\widehat{PRes}_{srow} = \frac{1}{\widehat{\mu s}}\ \widehat{Pdte}_{srow}\widehat{Pvs}_{srow} \tag{417}$$

$$\widehat{PJ\iota}_{srow,sRes} =$$

$$\widehat{a1}_{srow,sRes}\left(\frac{\widehat{ms}}{\widehat{\mu s}}\right)^{\widehat{a2}_{srow,sRes}}\left(\frac{1.33}{\widehat{Prp}_{srow}}\right)^{\left[\frac{\widehat{a3}_{srow}}{1+0.14\left(\frac{\widehat{ms}}{\widehat{\mu s}}\right)^{\widehat{a4srow}}\left(\frac{\widehat{pdte}_{srow}}{PS\widehat{m}_{srow}}\right)^{\widehat{a4srow}}}\right]}\left(\frac{\widehat{Pdte}_{srow}}{PS\widehat{m}_{srow}}\right)^{\widehat{a2}_{srow,sRes}} \tag{418}$$

$$\widehat{Pfs}_{srow,sRes} =$$

$$\widehat{b1}_{srow,sRes}\left(\frac{\widehat{ms}}{\widehat{\mu s}}\right)^{\widehat{b2}_{srow,sRes}}\left(\frac{1.33}{\widehat{Prp}_{srow}}\right)^{\left[\frac{\widehat{b3}_{srow}}{1+0.14\left(\frac{\widehat{ms}}{\widehat{\mu s}}\right)^{\widehat{b4srow}}\left(\frac{\widehat{pdte}_{srow}}{PS\widehat{m}_{srow}}\right)^{\widehat{b4srow}}}\right]}\left(\frac{\widehat{Pdte}_{srow}}{PS\widehat{m}_{srow}}\right)^{\widehat{b2}_{srow,sRes}} \tag{419}$$

$$\widehat{PFc}_{srow} = 1 - 2\ \widehat{PFw}_{srow} \tag{420}$$

$$\widehat{P\theta ds}_{srow} = 2\cos^{-1}\left[1 - 2\widehat{PBc}_{srow}\right] \tag{421}$$

$$\widehat{PLsb}_{srow} = \left(\frac{3.1+0.004\widehat{PDs}_{srow}10^3}{10^3}\right) \tag{422}$$

$$\widehat{PSsb}_{srow} = \left(\pi\ \widehat{PDs}_{srow}\frac{(\widehat{PLsb}_{srow})}{2}\left(\frac{2\pi-\widehat{P\theta ds}_{srow}}{2\pi}\right)\right) \tag{423}$$

$$\widehat{PStb}_{srow} = (\widehat{PNtt}_{srow})(1 - \widehat{PFw}_{srow})\left\{\frac{\pi}{4}\left[\left(\widehat{Pdte}_{srow} + \widehat{Pltb}_{srow}\right)^2 - \left(\widehat{Pdte}_{srow}\right)^2\right]\right\} \tag{424}$$

$$\widehat{PJc}_{srow} = \left[0.55 + 0.72(\widehat{PFc}_{srow})\right] \tag{425}$$

$$\widehat{PPrs}_{srow} = \frac{\widehat{PSsb}_{srow}}{\widehat{PSsb}_{srow}+\widehat{PStb}_{srow}} \tag{426}$$

$$\widehat{PPrlm}_{srow} = \frac{\widehat{PSsb}_{srow}+\widehat{PStb}_{srow}}{PS\widehat{m}_{srow}} \tag{427}$$

$$\widehat{PJl}_{srow} = \left[0.44(1 - \widehat{PPrs}_{srow})\right] + \left[\left[1 - 0.44(1 - \widehat{PPrs}_{srow})\right]\exp(-2.2\ \widehat{PPrlm}_{srow})\right] \tag{428}$$

$$\widehat{PDotl}_{srow} = \left(\widehat{PDs}_{srow} - \widehat{PLbb}_{srow}\right) \tag{429}$$

$$\widehat{PSb}_{srow} = \widehat{Plbc}_{srow}\left(\widehat{PDs}_{srow} - \widehat{PDotl}_{srow}\right) \tag{430}$$

$$\widehat{PFsbp}_{srow} = \frac{\widehat{PSb}_{srow}}{\widehat{PSm}_{srow}} \tag{431}$$

$$\widehat{PaLpp}_{srow} = 0.866 \quad \text{if } lay = 30° \tag{432}$$

$$\widehat{PaLpp}_{srow} = 1 \qquad \text{if } lay = 90° \tag{433}$$

$$\widehat{PaLpp}_{srow} = 0.707 \quad \text{if lay} = 45° \tag{434}$$

$$\widehat{PLpp}_{srow} = \widehat{PaLpp}_{srow}\widehat{Prp}_{srow}\widehat{Pdte}_{srow} \tag{435}$$

$$\widehat{PNtcc}_{srow} = \frac{\widehat{PDs}_{srow}}{\widehat{PLpp}_{srow}}\left[1 - \left(2\widehat{PBc}_{srow}\right)\right] \tag{436}$$

$$\widehat{Prss}_{srow} = \frac{\widehat{PNss}_{srow}}{\widehat{PNtcc}_{srow}} \tag{437}$$

$$\widehat{PCbh}_{sRes} = 1.35 \text{ if Res} \leq 100 \tag{438}$$

$$\widehat{PCbh}_{sRes} = 1.25 \text{ if Res} > 100 \tag{439}$$

$$\widehat{PJb1}_{srow,sRes} = exp\left[-\widehat{PCbh}_{sRes}\ \widehat{PFsbp}_{srow}\left(1 - \sqrt[3]{2\widehat{Prss}_{srow}}\right)\right] \tag{440}$$

$$\widehat{PNtcw}_{srow} = \frac{0.8}{\widehat{PLpp}_{srow}}\left[\widehat{PDs}_{srow}\widehat{PBc}_{srow}\ + \left[\frac{\left(-\widehat{PDs}_{srow}+\widehat{PDctl}_{srow}\right)}{2}\right]\right] \tag{441}$$

$$\widehat{PNc}_{srow} = (\widehat{PNtcc}_{srow} + \widehat{PNtcw}_{srow})(\widehat{PNb}_{srow} + 1) \tag{442}$$

$$\widehat{PJr1}_{srow} = \left(\frac{1.51}{(\widehat{PNc}_{srow})^{0.18}}\right) \tag{443}$$

$$PJ\widehat{r2}_{srow} = \left[\left(\frac{1.51}{(PN\widehat{c}_{srow})^{0.18}}\right) + \left(\frac{20-\widehat{pRes}_{srow}}{80}\right)\left(\frac{1.51}{(PN\widehat{c}_{srow})^{0.18}} - 1\right)\right] \tag{444}$$

$$\widehat{Phi}_{srow,sRes} = \widehat{PJi}_{srow,sRes}\widehat{cps}\ \widehat{Pvs}_{srow}\ (\widehat{Prs})^{-2/3} \tag{445}$$

$$\widehat{Phs}_{srow,sRes} = \widehat{Phi}_{srow,sRes}\widehat{PJc}_{srow}\widehat{PJl}_{srow}\widehat{PJb1}_{srow,sRes}\ PJ\widehat{r1}_{srow}\ \text{if } sRes = 1 \tag{446}$$

$$\widehat{Phs}_{srow,sRes} = \widehat{Phi}_{srow,sRes}\widehat{PJc}_{srow}\widehat{PJl}_{srow}\widehat{PJb1}_{srow,sRes}PJ\widehat{r1}_{srow}\ \text{if } sRes = 2 \tag{447}$$

$$\widehat{Phs}_{srow,sRes} = \widehat{Phi}_{srow,sRes}\widehat{PJc}_{srow}\widehat{PJl}_{srow}\widehat{PJb1}_{srow,sRes}PJ\widehat{r2}_{srow}\ \text{if } sRes = 3 \tag{448}$$

$$\widehat{Phs}_{srow,sRes} = \widehat{Phi}_{srow,sRes}\widehat{PJc}_{srow}\widehat{PJl}_{srow}\widehat{PJb1}_{srow,sRes}\ \text{if } sRes = 4 \tag{449}$$

$$\widehat{Phs}_{srow,sRes} = \widehat{Phi}_{srow,sRes}\widehat{PJc}_{srow}\widehat{PJl}_{srow}\widehat{PJb1}_{srow,sRes}\ \text{if } sRes = 5 \tag{450}$$

$$\widehat{Phs}_{srow,sRes} = \widehat{Phi}_{srow,sRes}\widehat{PJc}_{srow}\widehat{PJl}_{srow}\widehat{PJb1}_{srow,sRes}\ \text{if } sRes = 6 \tag{451}$$

$$P\Delta P\widehat{bi}_{srow,sRes} = 2\ \widehat{Pfs}_{srow,sRes}PN\widehat{tcc}_{srow}\frac{(Pms\widehat{hell}_{srow})^2}{\widehat{\rho}s} \tag{452}$$

$$P\widehat{Cbp}_{sRes} = 4.5\ \text{if Res} \leq 100 \tag{453}$$

$$P\widehat{Cbp}_{sRes} = 4.5\ \text{if Res} > 100 \tag{454}$$

$$P\widehat{Rb}_{srow,sRes} = exp\left[-(P\widehat{Cbp}_{sRes})\widehat{PFsbp}_{srow}\left(1 - \sqrt[3]{2\ \widehat{Prss}_{srow}}\right)\right] \tag{455}$$

$$\widehat{PpRl}_{srow} = -0.15\left(1 + \widehat{PPrs}_{srow}\right) + 0.8 \tag{456}$$

$$\widehat{PRl}_{srow} = exp\left[-1.33(1 + P\widehat{Prs}_{srow})(P\widehat{Prlm}_{srow})^{[\widehat{PpRl}_{srow}]}\right] \tag{457}$$

$$P\Delta P\widehat{c}_{srow,sRes} = P\Delta P\widehat{bi}_{srow,sRes}(\widehat{PNb}_{srow} - 1)\widehat{PRb}_{srow,sRes}\widehat{PRl}_{srow} \tag{458}$$

$$\widehat{PNtw}_{srow} = \widehat{PNtt}_{srow}\widehat{PFw}_{srow} \tag{459}$$

$$\widehat{PSwt}_{srow} = \widehat{PNtw}_{srow}\frac{\pi}{4}(\widehat{Pdte}_{srow})^2 \tag{460}$$

$$\widehat{PSwg}_{srow} = \frac{\pi}{4}(\widehat{PDs}_{srow})^2 \left(\frac{\widehat{P\theta ds}_{srow}-\sin(\widehat{P\theta ds}_{srow})}{2\pi}\right) \tag{461}$$

$$\widehat{PSw}_{srow} = \widehat{PSwg}_{srow} - \widehat{PSwt}_{srow} \tag{462}$$

$$\widehat{PGw}_{srow} = \frac{\widehat{ms}}{\left((\widehat{PSm}_{srow}\widehat{PSw}_{srow})^{\frac{1}{2}}\right)} \tag{463}$$

$$\widehat{pDw}_{srow} = \frac{4\,\widehat{PSm}_{srow}}{(\pi\,\widehat{Pdte}_{srow}\,\widehat{PNtw}_{srow})+\left(\pi\,\widehat{PDs}_{srow}\left(\frac{\widehat{P\theta ds}_{srow}}{2\,\pi}\right)\right)} \tag{464}$$

$$P\Delta\widehat{Pwlam}_{srow} = \widehat{PNb}_{srow}\,\widehat{PRl}_{srow}\left\{\frac{26\,\widehat{PGw}_{srow}\,\widehat{\mu s}}{\widehat{\rho}s}\left[\frac{\widehat{PNtcw}_{srow}}{\widehat{Pltp}_{srow}-\widehat{Pdte}_{srow}}+\frac{\widehat{Plbc}_{srow}}{(\widehat{PDw}_{srow})^2}\right]+\right.$$
$$\left.\left[\frac{2}{\widehat{\rho}s}\left(\widehat{PGw}_{srow}\right)^2\right]\right\} \tag{465}$$

$$P\Delta\widehat{Pwturb}_{srow} = \widehat{PNb}_{srow}\,\widehat{PRl}_{srow}\left[\left(2+0.6\,\widehat{PNtcw}_{srow}\right)\frac{(1)}{2\widehat{\rho}s}\left(\widehat{PGw}_{srow}\right)^2\right] \tag{466}$$

$$P\Delta\widehat{Pw}_{srow,sRes} = P\Delta\widehat{Pwlam}_{srow} \text{ if } sRes = 1 \tag{467}$$

$$P\Delta\widehat{Pw}_{srow,sRes} = P\Delta\widehat{Pwlam}_{srow} \text{ if } sRes = 2 \tag{468}$$

$$P\Delta\widehat{Pw}_{srow,sRes} = P\Delta\widehat{Pwlam}_{srow} \text{ if } sRes = 3 \tag{469}$$

$$P\Delta\widehat{Pw}_{srow,sRes} = P\Delta\widehat{Pwturb}_{srow} \text{ if } sRes = 4 \tag{470}$$

$$P\Delta\widehat{Pw}_{srow,sRes} = P\Delta\widehat{Pwturb}_{srow} \text{ if } sRes = 5 \tag{471}$$

$$P\Delta\widehat{Pw}_{srow,sRes} = P\Delta\widehat{Pwturb}_{srow} \text{ if } sRes = 6 \tag{472}$$

$$P\Delta P\widehat{e_{srow,sRes}} = 2\ P\Delta P\widehat{bi_{srow,sRes}}PR\widehat{b_{srow,sRes}}\left(1 + \frac{PNt\widehat{cw_{srow}}}{PNt\widehat{cc_{srow}}}\right) \tag{473}$$

Binary variables

This constraint imposes that only one design alternative must be chosen:

$$\sum_{srow} yrow_{srow} = 1 \tag{474}$$

The representation of the Reynolds number ranges are:

$$\sum_{sRet} yRet_{sRet} = 1 \tag{475}$$

$$\sum_{sRes} yRes_{sRes} = 1 \tag{476}$$

Similarly, for the Nusselt number in the tube-side:

$$yNut_1 + yNut_2 = 1 \tag{477}$$

Constraints relating continuous and binary variables

The linear constraints presented below depict the relations employed to eliminate the nonlinearities associated to the product of a continuous and a binary variable.

Product of the variables $yrow_{srow}$, $yNut_1$, and $yRet_1$:

$$wyrowNut1Ret1_{srow} \leq yrow_{srow} \tag{478}$$

$$wyrowNut1Ret1_{srow} \leq yNut_1 \tag{479}$$

$$wyrowNut1Ret1_{srow} \leq yRet_1 \tag{480}$$

$$wyrowNut1Ret1_{srow} \geq yrow_{srow} + yNut_1 + yRet_1 - 2 \tag{481}$$

Product of variables $yrow_{srow}$, $yNut_2$, and $yRet_1$:

$$wyrowNut2Ret1_{srow} \leq yrow_{srow} \tag{482}$$

$$wyrowNut2Ret1_{srow} \leq yNut_2 \tag{483}$$

$$wyrowNut2Ret1_{srow} \leq yRet_1 \tag{484}$$

$$wyrowNut2Ret1_{srow} \geq yrow_{srow} + yNut_2 + yRet_1 - 2 \tag{485}$$

Product of variables $yrow_{srow}$, $yNut_1$, and $yRet_2$:

$$wyrowNut1Ret2_{srow} \leq yrow_{srow} \qquad (486)$$

$$wyrowNut1Ret2_{srow} \leq yNut_1 \qquad (487)$$

$$wyrowNut1Ret2_{srow} \leq yRet_2 \qquad (488)$$

$$wyrowNut1Ret2_{srow} \geq yrow_{srow} + yNut_1 + yRet_2 - 2 \qquad (489)$$

Product of variables $yrow_{srow}$, $yNut_2$, and $yRet_2$:

$$wyrowNut2Ret2_{srow} \leq yrow_{srow} \qquad (490)$$

$$wyrowNut2Ret2_{srow} \leq yNut_2 \qquad (491)$$

$$wyrowNut2Ret2_{srow} \leq yRet_2 \qquad (492)$$

$$wyrowNut2Ret2_{srow} \geq yrow_{srow} + yNut_2 + yRet_2 - 2 \qquad (493)$$

Product of variables $yrow_{srow}$, and $yRet_3$:

$$wyrowRet3_{srow} \leq yrow_{srow} \qquad (494)$$

$$wyrowRet3_{srow} \leq yRet_3 \qquad (495)$$

$$wyrowRet3_{srow} \geq yrow_{srow} + yRet_3 - 1 \qquad (496)$$

Product of variables $yrow_{srow}$, and $yRet_4$:

$$wyrowRet4_{srow} \leq yrow_{srow} \qquad (497)$$

$$wyrowRet4_{srow} \leq yRet_4 \qquad (498)$$

$$wyrowRet4_{srow} \geq yrow_{srow} + yRet_4 - 1 \qquad (499)$$

Product of variables $yrow_{srow}$, and $yRet_{sRet}$:

$$wyrowRet_{srow,sRet} \leq yrow_{srow} \qquad (500)$$

$$wyrowRet_{srow,sRet} \leq yRet_{sRet} \qquad (501)$$

$$wyrowRet_{srow,sRet} \geq yrow_{srow} + yRet_{sRet} - 1 \qquad (502)$$

Product of variables $yrow_{srow}$, and $yRes_{sRes}$:

$$wyrowRes_{srow,sRes} \leq yrow_{srow} \qquad (503)$$

$$wyrowRes_{srow,sRes} \leq yRes_{sRes} \tag{504}$$

$$wyrowRes_{srow,sRes} \geq yrow_{srow} + \ yRes_{sRes} - 1 \tag{505}$$

Constraints associated to the Reynolds and Nusselt numbers ranges

The formulation developed involving different flow regimes in the tube-side and in the shell-side yields the constraints represented as follows:

$$\sum_{srow=1}^{srowmax} \widehat{PRes}_{srow}yrow_{srow} \ \leq 10 \ yRes_1 + 20 \ yRes_2 + \ 10^2 yRes_3 + 10^3 yRes_4 + 10^4 yRes_5 + 10^5 yRes_6 \tag{506}$$

$$\sum_{srow=1}^{srowmax} \widehat{PRes}_{srow}yrow_{srow} \ \geq 10 \ yRes_2 + 20 \ yRes_3 + 10^2 yRes_4 + 10^3 yRes_5 + 10^4 yRes_6 + \hat{\varepsilon} \tag{507}$$

$$\sum_{srow=1}^{srowmax} \widehat{PRet}_{srow}yrow_{srow} \leq 1311 \ yRet_1 + \ 2300 \ yRet_2 + 3380 \ yRet_3 + \ \widehat{URet} \ yRet_4 \tag{508}$$

$$\sum_{srow=1}^{srowmax} \widehat{PRet}_{srow}yrow_{srow} \geq 1311 \ yRet_2 + 2300 \ yRet_3 + 3380 \ yRet_4 + \hat{\varepsilon} \tag{509}$$

$$\sum_{srow=1}^{srowmax} \widehat{PNut2}_{srow}yrow_{srow} < 3.66 \ yNut_1 + \ \widehat{UNut} \ yNut_2 \tag{510}$$

$$\sum_{srow=1}^{srowmax} \widehat{PNut2}_{srow}yrow_{srow} \ \geq 3.66 \ yNut_2 + \hat{\varepsilon} \tag{511}$$

Bounds on pressure drops and flow velocities

The set of constraints presented as follows represents bounds on pressure drops and velocities. Instead of representing the velocity bounds in a conventional way, we have rewritten it based on an analysis of the search space, where it is possible to delimit the design alternatives that violate these constraints. Souza et al. (2018) have concluded that this form of representation allows to reach a better computational performance (i.e. differently from the previous chapters, the original constraints are not included).

Shell-side pressure upper bound:

$$\sum_{sRes=1}^{sResmax} \sum_{srow=1}^{srowmax} \widehat{P\Delta Ps}_{srow,sRes}wyrowRes_{srow,sRes} \leq \widehat{\Delta Psdisp} \tag{512}$$

where $P\Delta P\widehat{s_{srow,sRes}} = P\Delta P\widehat{c_{srow,sRes}} + P\Delta P\widehat{w_{srow,sRes}} + P\Delta P\widehat{e_{srow,sRes}}$.

Tube-side pressure upper bound:

$$\sum_{sRet=1}^{sRetmax} \sum_{srow=1}^{srowmax} \widehat{P\Delta Pt}_{srow,sRet} \, wyrowRet_{srow,sRet} \leq \widehat{\Delta Ptdisp} \tag{513}$$

where $\widehat{P\Delta Pt}_{srow,sRet} = P\widehat{\Delta Ptube}_{srow,sRet} + P\widehat{\Delta Phead}_{srow,sRet}$.

Flow velocities bounds:

$$yrow_{srow} = 0 \text{ for } srow \in (Svsminout \cup Svsmaxout) \tag{514}$$

$$yrow_{srow} = 0 \text{ for } srow \in (Svtminout \cup Svtmaxout) \tag{515}$$

where the sets *Svsminout, Svsmaxout, Svtminout,* and *Svtmaxout* are given by:

$$Svsminout = \{srow \, / \widehat{Pvs}_{srow} \leq \widehat{vsmin} - \hat{\varepsilon}\} \tag{516}$$

$$Svsmaxout = \{srow \, / \, \widehat{Pvs}_{srow} \geq \widehat{vsmax} + \hat{\varepsilon}\} \tag{517}$$

$$Svtminout = \{srow \, / \, \widehat{Pvt}_{srow} \leq \widehat{vtmin} - \hat{\varepsilon}\} \tag{518}$$

$$Svtmaxout = \{srow \, / \widehat{Pvt}_{srow} \geq \widehat{vtmax} + \hat{\varepsilon}\} \tag{519}$$

where $\hat{\varepsilon}$ is a small positive number.

Geometric constraints

The same approach described before is applied to the geometric constraints, as follows:

Baffle spacing:

$$yrow_{srow} = 0 \text{ for } srow \in (SLNbminout \cup SLNbmaxout) \tag{520}$$

where the sets *SLNbminout* and *SLNbmaxout* are given by:

$$SLNbminout = \{srow \, / \, \widehat{Plbc}_{srow} \leq 0.2\widehat{PDs}_{srow} - \hat{\varepsilon}\} \tag{521}$$

$$SLNbmaxout = \{srow \, / \, \widehat{Plbc}_{srow} \geq 1.0\widehat{PDs}_{srow} + \hat{\varepsilon}\} \tag{522}$$

The constraint related to *lbcmax* is:

$$\sum_{srow=1}^{srowmax}(\widehat{Plbc}_{srow})yrow_{srow} \le 0.5 \sum_{srow=1}^{srowmax}(\widehat{plbmax1}\,\widehat{Pdte}_{srow} + \widehat{plbmax2})yrow_{srow}$$

(523)

Tube length / shell diameter ratio:

$$yrow_{srow} = 0 \text{ for } srow \in (SLDminout \cup SLDmaxout)$$

(524)

where the sets *SLDminout* and *SLDmaxout* are given by:

$$SLDminout = \{srow \,/\, \widehat{PL}_{srow} \le 3\widehat{PDs}_{srow} - \hat{\varepsilon}\}$$

(525)

$$SLDmaxout = \{srow \,/\, \widehat{PL}_{srow} \ge 15\widehat{PDs}_{srow} + \hat{\varepsilon}\}$$

(526)

Objective function

The heat transfer area when reformulated into the linear model is given by:

$$\text{Min}\ \pi \sum_{srow} \widehat{PNtt}_{srow}\widehat{Pdte}_{srow}\widehat{PL}_{srow}yrow_{srow}$$

(527)

The corresponding linear form of the total annualized cost is given by:

$$\text{Min}\ \widehat{acost}\ \sum_{srow}\left(\pi\widehat{PNtt}_{srow}\widehat{Pdte}_{srow}\widehat{PL}_{srow}\right)^{\widehat{bcost}}yrow_{srow}\ +$$

$$\widehat{ccost} \sum_{srow,sRet}\frac{\widehat{P\Delta Pt}_{srow,sRet}\widehat{mt}}{\widehat{\rho t}}wyrowRet_{srow,sRet}\ +$$

$$\widehat{ccost} \sum_{srow,sRes}\frac{\widehat{P\Delta Ps}_{srow,sRes}\widehat{ms}}{\widehat{\rho s}}wyrowRes_{srow,sRes}$$

(528)

4.4   **Model Validation**

The MILP model presented above was implemented in the GAMS software using the solver CPLEX. The example described and solved by Taborek (2008d) (section B of chapter 3.3.9) was used to validate this MILP model by fixing the geometric choices and then comparing different results. We fix the carrying error effect of rounding in the example by

using a larger number of significant figures. Results differ lower than 0.012% (corresponding

to *Sb*), as shown in Table 17.

Table 17 - Validation results

Variable	Handbook	Our revision	Our Numerical Model	Deviation (%)
hi (W/m^2 ^{o}C)	2133.50	2130.6418	2130.6418	0
hs (W/m^2 ^{o}C)	1252.00	1249.3178	1249.3178	0
ΔPc (kPa)	3.90	3.9173	3.9173	0.0011
ΔPw (kPa)	6.40	6.3726	6.3727	0.0007
ΔPe (kPa)	3.40	3.5014	3.5014	0.0011
ΔPs (kPa)	13.70	13.7915	13.7915	0.0009

Source: The author.

4.5 Comparison with Results from the Literature

Example 1, originally proposed by Shenoy (1995), is based on the minimization of

heat transfer area, and Example 2, originally presented by Mizutani et al. (2003), involves the

minimization of the total annualized cost. Both examples were solved by Ravagnani and

Caballero (2007) and Onishi et al. (2013) using an MINLP formulation. The comparison of

our results and Ravagnani and Caballero (2007) and Onishi et al. (2013) must consider some

differences:

- The tube-side correlations in our model are different from the correlations used by

    Ravagnani and Caballero (2007) and Onishi et al. (2013). Our model for the evaluation

    of the tube-side convective heat transfer coefficient encompasses all flow regimes. In

    particular, in the turbulent regime, we use the Gnielinski correlation, but Ravagnani and

    Caballero (2007) as well as Onishi et al. (2013), limited their analysis to turbulent flow

    and employed the Sieder and Tate correlation. According to Incropera and De Witt

    (2006), the Sieder and Tate correlation may yield errors up to 25%, while the errors of

    the Gnielinski correlation are lower than 10%;

- There are some differences between the equations used by Ravagnani and Caballero

    (2007) and Onishi et al. (2013) and the equations used by Taborek (2008d);

- Ravagnani and Caballero (2007) and Onishi et al. (2013) used baffle spacing as a variable, while we use the number of baffles as an integer variable. As a result, they obtain a spacing that leads to a non-integer number of baffles, which they round up to the nearest integer afterwards. They also include tube thickness as an optimization variable, but in our approach the tube thickness is defined by the user prior to the optimization;

- Ravagnani and Caballero (2007) and Onishi et al. (2013) formulations are nonconvex MINLP problems and they use a local solver that does not guarantee global optimality. Instead, our linear formulation guarantees the identification of the global optimum.

We compare the results from the original references of the corresponding examples (MIZUTANI et al., 2003; SHENOY, 1995) with the solutions found by Ravagnani and Caballero (2007) and Onishi et al. (2013) and two sets of results generated with our model. The first set of our results corresponds to the rating of the previous solutions using our model and the second set contains the optimization results obtained using our MILP formulation. Table 18 describes the search space. All the results were generated considering tube-side velocities between 1 m/s and 3 m/s and shell-side velocities between 0.5 m/s and 2 m/s. All elapsed times reported here associated to the optimization runs were measured using a computer with a processor Intel Core i7 3.41 GHz with 16.6 GB RAM memory.

Table 18 - Standard values of the discrete design variables

Variable	Values
Outer tube diameter, $\widehat{pdte}_{sd}$ (m)	0.01590, 0.01905, 0.02540
Tube length, $\widehat{pL}_{sL}$ (m)	2.438, 3.658,4.877,6.096,6.706
Number of baffles, $\widehat{pNb}_{sNb}$	7, 8, ... , 25
Number of tube passes, $\widehat{pNpt}_{sNpt}$	1, 2, 4, 6, 8
Tube pitch ratio, $\widehat{prp}_{srp}$	1.25, 1.33, 1.50
Shell diameter, $\widehat{pDs}_{sDs}$ (m)	0.2050, 0.3048, 0.3366, 0.3874, 0.4382, 0.4890, 0.5398, 0.5906, 0.6350, 0.6858, 0.7366, 0.7874, 0.8382, 0.8890, 0.9398, 0.9906, 1.0668, 1.1430, 1.2192, 1.3716, 1.5240
Tube layout, $\widehat{play}_{slay}$	1 = triangular 30°, 2 = square 90°
Baffle cut ratio, $\widehat{pBc}_{sBc}$	0.20, 0.25, 0.30

Source: The author.

Example 1

This problem was first presented by Shenoy (1995). The data of the problem streams are presented in Table 19. The thermal conductivity of the tube material is 50 W/m°C, both fouling resistances are 0.00015 m²°C/W, and the available pressure drops are 42 kPa and 7 kPa for the cold and hot streams, respectively. The minimum excess area is 0%. The allocation of the streams and the determination of the tube thickness are not variables in our optimization procedure, so we employed the values reported in the Ravagnani and Caballero solution (2007): the cold stream flows in the tube-side and the tube thickness is 1.225 mm. The rating of the results of Shenoy (1995) and Caballero and Ravagnani (2007) employed the reported values of shell-bundle clearances: 33 mm and 44 mm, respectively, but in the optimization using our model, this dimension was modelled according to Equation 309. The other clearances were determined according to Equation 310 and Equation 314.

Table 19 - Example 1 - Streams data

Stream	$\widehat{m}$ (kg/s)	Inlet $\widehat{T}$ (°C)	Outlet $\widehat{T}$ (°C)	$\widehat{\rho}$ (kg/m^3)	$\widehat{\mu}$ (mPa·s)	$\widehat{Cp}$ (J/kg°C)	$\widehat{k}$ (W/m°C)
Hot	14.90	98.0	65.0	777	0.23	2684	0.11
Cold	31.58	15.0	25.0	998	1.00	4180	0.60

Source: The author.

The comparison of the results is displayed in Table 20 and 21. The most relevant deviations in the rating of the literature solutions are for the pressure drops in the shell-side in relation to Ravagnani and Caballero (2007) and the pressure drop in the tube-side in relation to Shenoy (1995). The optimal solution of our model, using a fixed baffle cut ratio equal to the previous references (0.25), has an area 16.8% lower than Shenoy (1995) and 38.6.1% lower than Ravagnani and Caballero (2007). When including the baffle cut ratio in the optimization, the same value fixed in the previous reference was obtained. The elapsed time of the optimization using our model was 24 minutes. However, when the same problem was solved using a fixed baffle cut ratio the computational time was reduced to 4.1 minutes.

The same problem was also solved by Onishi et al. (2013), using available pressure drops of 45 kPa for the cold stream and 10 kPa for the hot stream. Table 21 contains the solution reported by Onishi et al. (2013), the rating of this solution using our model with a shell bundle clearance of 31 mm, and the optimal solution found by our MILP formulation. Our solution obtained an optimal baffle cut ratio of 0.20 and rendered a reduction of the objective function equal to 19.91% with respect to that of Onishi et al. (2013), as shown in Table 21. The computational time to solve this problem was 22 minutes. If the baffle cut is fixed to 0.25, as it was adopted in Onishi et al. (2013), the reduction of the objective function is the same, but the computational time is reduced to 3.9 minutes.

Table 20 - Example 1 – Results comparison with Shenoy (1995) and Ravagnani and Caballero (2007)

Variable	Shenoy's (1995) solution	Shenoy (1995) Rating using our model	Ravagnani and Caballero's (2007) solution	Ravagnani and Caballero (2007) Rating using our model	Our MILP model Original available pressure drops
Area (m^2)	28.40	28.40	38.52	38.52	23.64
dte (m)	0.01910	0.01910	0.01905	0.01905	0.01905
dti (m)	0.01540	0.01540	0.01660	0.01660	0.01660
Ds (m)	0.549	0.549	0.533	0.533	0.387
lay	Square	Square	Square	Square	Square
Npt	6	6	2	2	2
rp	1.33	1.33	1.33	1.33	1.25
L (m)	1.286	1.286	2.438	2.438	2.438
Nb	6	6	19	19	7
Ntt	368	368	264	264	162
vt (m/s)	-	2.770	1.108	1.108	1.805
vs (m/s)	-	0.668	1.162	0.980	0.737
ht (W/m^2°C)	8649.6	10145.8	4087.1	5484.6	8506.8
hs (W/m^2°C)	1364.5	1321.4	1308.4	1418.4	1700.3
ΔPt (kPa)	42.000	86.637	7.706	7.551	18.540
ΔPs (kPa)	3.600	3.195	7.000	10.434	6.491

Source: The author.

Table 21 - Example 1 – Results comparison with Onish et al. (2013)

Variable	Onishi et al. (2013) solution	Onishi et al. (2013) Rating using our model	Our MILP model Higher available pressure drops
Area (m^2)	28.89	28.90	23.14
dte (m)	0.01905	0.01905	0.01590
dti (m)	0.01660	0.01660	0.01345
Ds (m)	0.387	0.387	0.387
lay	Square	Square	Triangular
Npt	2	2	2
rp	1.33	1.33	1.50
L (m)	3.658	3.658	2.438
Nb	9	9	9
Ntt	132	132	190
vt (m/s)	2.215	2.215	2.344
vs (m/s)	0.517	0.457	0.589
ht (W/m^{2}ºC)	7283.9	10216.3	10989.2
hs (W/m^{2}ºC)	2096.0	1249.0	1762.8
ΔPt (kPa)	43.040	36.738	36.249
ΔPs (kPa)	10.000	4.233	8.856

Source: The author.

We conclude that the differences in results are for the most part due to the fact that all previous works find local solutions whereas our is the global one. The differences do not stem from the usage of different correlations.

Example 2

This problem was first presented by Mizutani et al. (2003). The data of the problem streams are presented in Table 22. The thermal conductivity of the tube material is 50 W/mºC, the fouling resistance of both streams is 0.00017 m^{2}ºC/W, and the maximum pressure drops are 68.95 kPa for both fluids. The minimum excess area is 0%. The economic parameters of the objective function are $\widehat{a_{cost}} = 123$, $\widehat{b_{cost}} = 0.59$, and $\widehat{c_{cost}} = 1.31$. The allocation of the streams assumes that the cold stream flows in the tube-side and the tube thickness is equal to 1.675 mm. The rating of the results of Mizutani et al.,[18] Caballero and Ravagnani[19] and

Onishi et al. (2013) employed the reported values of shell-bundle clearances: 15 mm, 42 mm

and 41 mm, respectively, but in the optimization this dimension was calculated accordingly.

Table 22 - Example 2 - Streams data

Stream	$\widehat{m}$ (kg/s)	Inlet $\widehat{T}$ (°C)	Outlet $\widehat{T}$ (°C)	$\widehat{\rho}$ (kg/m³)	$\widehat{\mu}$ (mPa·s)	$\widehat{cp}$ (J/kgºC)	$\widehat{k}$ (W/mºC)
Hot	27.78	95.0	40.0	750	0.34	2840	0.19
Cold	68.88	25.0	40.0	995	0.80	4200	0.59

Source: The author.

Table 23 and 24 presents the results. The costs found by Mizutani et al. (2003),

Ravagnani and Caballero (2007) and Onishi et al. (2013) are similar, but the tradeoff between

capital and operating costs is considerably different in each case: the capital cost found by

Mizutani et al. (2003) corresponds to 53.8% of the total cost, while according to Ravagnani

and Caballero (2007) it is 70.5%. The total annualized cost of Onishi et al. (2013) is slightly

smaller than Mizutani et al. (2003) and Ravagnani and Caballero (2007). The rating of the

solution found by Ravagnani and Caballero (2007) using our model yielded similar results.

The differences in relation to the pressure drops and heat transfer coefficients are not higher

than 10%. The solution of Onishi et al. (2013) and Mizutani et al. (2003) showed maximum

deviations of 20%, except the shell-side pressure drop. The optimal solutions of Mizutani et

al. (2003), Ravagnani and Caballero (2007), and Onishi et al. (2013) are based on a fixed

baffle cut ratio of 0.25 and the inclusion of this parameter as a variable in our model yielded

an optimal baffle cut ratio of 0.30. The elapsed time of the optimization was 48 minutes.

Our MILP solution presents a total annualized cost that is considerably lower when

compared to the results of Mizutani et al. (2003), Ravagnani and Caballero (2007), and Onishi

et al. (2013). When comparing our solution to the other cited works, we find that the main

reason for this large cost reduction is the decrease of the total number of tube passes to 1,

which allowed a reduction of the pumping costs, through the decrease of the total length of

the hydraulic path, and an increase of the mean temperature difference (the correction factor for the multipass configuration is 0.812 and is increased to 1 in the countercurrent configuration).

As in Example 1, we believe the large differences in results are mostly due to the fact that the solutions obtained in previous work are local solutions. Since we checked the issue, we think that they are not attributable to the differences in correlations and/or modeling.

Table 23 - Example 2 – Results comparison with Mizutani et al. (2003) and Ravagnani and Caballero (2007)

Variable	Mizutani et al.'s (2003) solution	Mizutani et al. (2003) Rating using our model	Ravagnani and Caballero's (2007) solution	Ravagnani and Caballero (2007) Rating using our model
Total cost ($/y)	5250.00	5279.56	5191.47	5137.78
Area cost ($/y)	2826.00	2825.45	3663.23	3461.77
Pumping cost($/y)	2424.00	2454.11	1528.24	1676.02
Area (m^2)	202.00	202.81	286.15	286.15
dte (m)	0.01590	0.01590	0.01905	0.01905
dti (m)	0.01260	0.01260	0.01570	0.01570
Ds (m)	0.687	0.687	0.838	0.838
lay	Square	Square	Square	Square
Npt	2	2	2	2
rp	1.25	1.25	1.33	1.33
L (m)	4.877	4.877	6.706	6.706
Nb	8	8	18	18
Ntt	832	832	713	713
vt (m/s)	-	1.334	1.003	1.003
vs (m/s)	-	0.467	0.500	0.447
ht (W/m^2°C)	6480.0	7400.0	4186.2	5599.4
hs (W/m^2°C)	1829.0	1951.7	1516.5	1558.8
ΔPt (kPa)	22.676	23.553	13.404	14.701
ΔPs (kPa)	7.494	6.558	6.445	7.065

Source: The author.

Table 24 - Example 2 – Results comparison with Onishi et al. (2013)

Variable	Onishi et al. (2013) solution	Onishi et al. (2013) Rating using our model	Our MILP Model
Total cost ($/y)	5134.21	4853.40	3754.01
Area cost ($/y)	3175.61	3175.61	2510.14
Pumping cost($/y)	1958.59	1677.79	1243.86
Area (m^2)	247.22	247.22	165.95
dte (m)	0.01905	0.01905	0.01590
dti (m)	0.01660	0.01660	0.01255
Ds (m)	0.787	0.787	0.591
lay	Square	Square	Square
Npt	2	2	1
rp	1.33	1.33	1.33
L (m)	6.706	6.706	6.096
Nb	17	17	12
Ntt	616	616	545
vt (m/s)	1.039	1.039	1.027
vs (m/s)	0.500	0.449	0.512
ht (W/m^2°C)	4356.7	5743.4	5846.7
hs (W/m^2°C)	1880.2	1591.6	1972.0
ΔPt (kPa)	15.921	14.729	8.650
ΔPs (kPa)	10.609	7.049	9.467

Source: The author.

4.6 Partial Conclusions

By recognizing that the geometric variables have discrete representations, we rigorously reformulated the entire MINLP problem of the design optimization of shell-and-tube heat exchangers using the Bell-Delaware method in a form of a MILP problem. Our reformulation is not an approximation or a linearization by truncating Taylor series. Rather, it is rigorous, in the sense that the feasible solutions of the MINLP model are also feasible in the MILP model and vice-versa. We validated our implemented approach through its comparison with a literature result (TABOREK, 2008d). The proposed approach can identify solutions that are significantly better, the most relevant reason for the significant improvement is the local nature of the optimum found by other approaches.

CONCLUSIONS

A MILP model for the design of shell and tube heat exchangers was presented. The comparison of the MILP model with an MINLP formulation through the solution of the same sample of heat exchanger design problems shows drawbacks in the MINLP approach in relation to non-convergence and local optima. Due to its linear nature, the MILP model proposed here is immune to these obstacles, always reaching the global optimum.

It is explored alternative techniques to reduce the computational effort. Several linear formulations were proposed based on different alternatives of aggregation of the discrete values of the design variables in relation to the binary variables. The results showed that the aggregation of the binary variables allows a considerable reduction of the computational effort to solve the MILP problem. Considering a sample of 10 design problems, the best aggregation alternative demanded only 0.21% of the total solver time in comparison of the original MILP.

This performance gain is important because it allows further investigations for the inclusion of this model into more complex problems, such as, the insertion of the detailed heat exchanger design into the heat exchanger network synthesis problem.

The entire MINLP problem of the design optimization of shell-and-tube heat exchangers using the Bell-Delaware method was rigorously reformulated in a form of a MILP problem. Our reformulation is not an approximation or a linearization by truncating Taylor series. Rather, it is rigorous, in the sense that the feasible solutions of the MINLP model are also feasible in the MILP model and vice-versa. The proposed approach can identify solutions that are significantly better, the most relevant reason for the significant improvement is the local nature of the optimum found by other approaches and the global nature of the optimum found.

SUGGESTIONS FOR FUTURE WORKS

- Apply this linear model developed for series of heat exchanger and the synthesis of heat exchanger networks;
- Investigation of different objective function alternatives to solve the problem of optimum design of heat exchangers;
- Insertion of the uncertainty issue regarding the information about the project in the optimization.

REFERENCES

ASADI, M.; SONG, Y.; SUNDEN, B.; XIE, G. Economic optimization design of shell-and-tube heat exchangers by a cuckoo-search-algorithm. *Appl Therm Eng.*, v.73, p.1032-1040, 2014.

BELL, K. J. Exchanger design: based on the Delaware research report. *Petro/Chem*, v. 32, 1960.

BELL, K. J. Logic of the design process. In: *Heat Exchanger Design Handbook*. Ed. G.F. Hewitt, Begell House, New York, 2008.

CAO, E. *Heat transfer in process engineering*. McGraw-Hill, New York, 2010.

CHAUDHURI, P. D.; DIWEKAR, U. M. An automated approach for the optimal design of heat exchangers. *Ind Eng Chem Res.* v.36, p.3685-3693, 1997.

COSTA, A. L. H.; QUEIROZ, E. M. Design optimization of shell-and-tube heat exchangers. *Appl Therm Eng*. v28, p.1798-1805, 2008.

ERYENER, D. Thermoeconomic optimization of baffle spacing for shell and tube heat exchangers. *Energy Convers Manage.* v 47, p.1478-1489, 2006.

GONÇALVES, C. O.; COSTA, A. L. H.; BAGAJEWICZ, M. J. Alternative MILP formulations for shell and tube heat exchanger optimal design. *Ind. Eng. Chem. Res.*, v. 56, p. 5970-5979, 2017.

GONÇALVES, C. O.; COSTA, A. L. H.; BAGAJEWICZ, M. J. Shell and tube heat exchanger design using mixed-integer linear programming. *AIChE J.*, v. 63, p. 1907-1922, 2016.

HADIDI, A.; HADIDI, M.; NAZARI, A. A new design approach for shell-and-tube heat exchangers using imperialist competitive algorithm (ICA) from economic point of view. *Energy Convers Manage.* v.67, p.66-74, 2013.

INCROPERA, F. P. D.; WITT, D. P. *Fundamentals of heat and mass transfer*. 6th.ed. New York: John Wiley & Sons, 2006.

JEGEDE, F. O.; POLLEY, G. T. Optimum heat exchanger design. *Chem. Eng. Res. Des.* v.70(A2), p.133-141, 1992.

KAKAÇ, S.; LIU, H. *Heat Exchanger Selection, Rating and Thermal Design*. 3 ed. Boca Raton, FL: CRC Press, 2012.

KERN, D. Q. *Process heat transfer*. New York: McGraw-Hill, 1950.

LUDWIG, E. *Applied process design for chemical and petrochemical plants*. Gulf Professional Publishing: Oxford. 3, 3rd ed, 2001.

MIZUTANI, F. T.; et al. Mathematical Programming Model for Heat-Exchanger Network Synthesis Including Detailed Heat-Exchanger Designs. 1. Shell-and-Tube Heat-Exchanger Design. *Ind. Eng. Chem. Res,* v. 42, n.17, p. 4009-4018, 2003.

MOHANTY, D. K. Application of firefly algorithm for design optimization of a shell and tube heat exchanger from economic point of view. *Int J Therm Sci*. v.102, p.228-238, 2016.

MURALIKRISHNA, K.; SHENOY, U. V. Heat exchanger design targets for minimum area and cost. *Trans IChemE*. V.78(Part A), p.161-167, 2000.

ONISHI, V. C.; RAVAGNANI, M., CABALLERO, J. A. Mathematical programming model for heat exchanger design through optimization of partial objectives. *Energy Convers. Manage.* v.74, p.60-69, 2013.

PATEL, V. K.; RAO, R. V. Design optimization of shell-and-tube heat exchanger using particle swarm optimization technique. *Appl Therm Eng.* v.30, p.1417-1425, 2010.

PONCE-ORTEGA, J. M.; SERNA-GONZÁLEZ, M.; JIMÉNEZ-GUTIÉRREZ, A. Use of genetic algorithms for the optimal design of shell-and-tube heat exchangers. *Appl Therm Eng*. v.29, p.203-209, 2009.

PONCE-ORTEGA, J. M.; SERNA-GONZÁLEZ, M.; SALCEDO-ESTRADA, L. I.; JIMÉNEZ-GUTIÉRREZ, A. A minimum-investment design of multiple shell and tube heat exchangers using a MINLP formulation. *Chem Eng Res Des*. v.84, p.905-910, 2006.

RAVAGNANI, M.; SILVA, A. P.; BISCAIA, E. C.; CABALLERO, J. A. Optimal design of shell-and-tube heat exchangers using particle swarm optimization. *Ind Eng Chem Res*. v.48, p.2927-2935, 2009.

RAVAGNANI, M.; SILVA, A. P., Andrade AL. Detailed equipment design in heat exchanger networks synthesis and optimization. *Appl. Thermal Eng.* v.23, p.141-151, 2003.

RAVAGNANI, M.; CABALLERO, J. A. A MINLP model for the rigorous design of shell and tube heat exchangers using the TEMA standards. *Chem Eng Res Des.* v.85, p.1423:1435, 2007.

SAUNDERS, E. A. D. *Heat exchangers: selection, design and construction*. New York: John Wiley and Sons Inc., 1988.

SERTH, R. W. *Process heat transfer*: principles and applications. Oxford: Elsevier, 2007.

SHENOY, U. V. *Heat exchanger network synthesis – Process optimization by energy and resource analysis* (Gulf Publishing Company), USA. 1995.

SOUZA, P. A.; COSTA, A. L. H.; BAGAJEWICZ, M. J. Globally optimal linear approach for the design of process equipment: The case of air coolers. *AIChE J.*, v. 64, p. 886-903, 2018.

TABOREK, J. Shell-and-tube heat exchangers: single-phase flow. In: Hewitt, G. F. (Ed.) *Heat exchanger design handbook*. New York: Begell House, 2008a.

TABOREK, J. Performance evaluation of a geometry specified exchanger. In: *Heat Exchanger Design Handbook*. Ed. G.F. Hewitt, Begell House, New York, 2008b.

TABOREK, J. Calculation of shell-side heat transfer coefficient and pressure drop. In: *Heat Exchanger Design Handbook*. Ed. G.F. Hewitt, Begell House, New York, 2008c.

TABOREK, J. Input data and recommended practices. In: *Heat Exchanger Design Handbook*. Ed. G.F. Hewitt, Begell House, New York, 2008d.

TAYAL, M. C.; FU, Y; DIWEKAR, U. M. Optimal design of heat exchangers: a genetic algorithm framework. *Ind Eng Chem Res.* v.3, p.457-467, 1999.

TEMA. Standards of the tubular exchangers manufactures association. Tubular Exchanger Manufacturers Association, 9th ed., New York, 2007

TINKER, T., Shell-side Heat Transfer Characteristics of Segmentally Baffled Shell-and-tube Exchangers, *American Society of Mechanical Engineers*, ASME Paper n. 47-A-130, 1947.

TOWLER, G.; SINNOT, R. *Chemical engineering design – principles, practice and economics of plant and process design*, Elsevier, 2008.

WILDI-TREMBLAY, P., GOSSELIN, L. Minimizing shell-and-tube heat exchanger cost with genetic algorithms and considering maintenance. *Int J Energy Res.* v.31, p.867-885, 2007.

WILLS, M. J. N.; JOHNSTON, D. A New and Accurate Hand Calculation Method for Shell-side Pressure Drop and Flow Distribution, Proc. 22nd National Heat Transfer Conference, HTD v. 36*, American Society of Mechanical Engineers*, pp. 67-79, 1984.

APPENDIX A – **Alternative MILP formulations with different aggregations of the binary variables.**

We describe here the alternative MILP formulations with different aggregations of the binary variables.

Alternative 1. This alternative is described in detail in Chapter 2.

Alternative 2.

Binary Variables Equality Constraints. This constraint imposes tree binary variables:

$$\sum_{srow=1}^{srowmax} yrow_{srow} = 1 \tag{A1}$$

$$\sum_{sL=1}^{sLmax} yL_{sL} = 1 \tag{A2}$$

$$\sum_{sNb=1}^{sNbmax} yNb_{sNb} = 1 \tag{A3}$$

Heat Transfer Rate Equation. The expressions of all heat transfer coefficients and the heat transfer area are inserted into the heat transfer equation, thus yielding:

$$\hat{Q}\left(\sum_{srow=1}^{srowmax} \frac{\widehat{Pdte}_{srow}}{\widehat{Pht}_{srow}\,\widehat{Pdtι}_{srow}} yrow_{srow} + \widehat{Rft}\sum_{srow=1}^{srowmax} \frac{\widehat{Pdte}_{srow}}{\widehat{Pdtι}_{srow}} yrow_{srow} + \right.$$
$$\frac{\sum_{srow=1}^{srowmax} \widehat{Pdte}_{srow}\ln(\frac{\widehat{Pdte}_{srow}}{\widehat{Pdtι}_{srow}})yrow_{srow}}{2\,\widehat{Ktube}} + \widehat{Rfs} +$$
$$\left. \sum_{srow=1}^{srowmax}\sum_{sL=1}^{sLmax}\sum_{sNb=1}^{sNbmax} \frac{1}{\widehat{Phs}_{srow,sL,sNb}} whs_{srow,sL,sNb}\right) \le$$
$$\left(\pi \sum_{srow=1}^{srowmax}\sum_{sL=1}^{sLmax} \widehat{PNtt}_{srow}\,\widehat{Pdte}_{srow}\,\widehat{PL}_{sL}\, wA_{srow,sL}\right)\left(\frac{100}{100+\widehat{Aexc}}\right)\widehat{\varDelta Tlm}\,\hat{F}_{srow} \tag{A4}$$

where $\widehat{PNtt}_{srow}$ is the total number of tubes and:

$$\widehat{Pht}_{srow} = \frac{\widehat{kt}\, 0.023 \left(\frac{4\,\widehat{mt}}{\pi\,\widehat{\mu t}}\right)^{0.8} \widehat{Prt}^{n}}{\widehat{Pdti}_{srow}^{1.8}} \left(\frac{\widehat{PNpt}_{srow}}{\widehat{PNtt}_{srow}}\right)^{0.8} \tag{A5}$$

$$\widehat{Phs}_{srow,sL,sNb} = \frac{\widehat{ks}\, 0.36 \left(\frac{\widehat{ms}}{\widehat{\mu s}}\right)^{0.55} \widehat{Prs}^{1/3}}{\widehat{PDeq}_{srow}^{0.45}} \left(\frac{(\widehat{PNb}_{sNb}+1)}{\widehat{PDs}_{srow}\, \widehat{PFAR}_{srow}\, \widehat{PL}_{sL}}\right)^{0.55} \tag{A6}$$

$$\widehat{PFAR}_{srow} = 1 - \frac{1}{\widehat{Prp}_{srow}} \tag{A7}$$

$$\widehat{PDeq}_{srow} = \frac{\widehat{aDeq}_{srow}\widehat{Prp}_{srow}^{2}\widehat{Pdte}_{srow}^{2}}{\pi \widehat{Pdte}_{srow}} - \widehat{Pdte}_{srow} \tag{A8}$$

$$\widehat{aDeq}_{srow} = \begin{cases} 4 & \text{if } \widehat{Play}_{srow} = 1 \\[2em] 3.46 & \text{if } \widehat{Play}_{srow} = 2 \end{cases} \tag{A9}$$

$$\widehat{F}_{srow} = \begin{cases} \dfrac{(\widehat{R}^2+1)^{0.5}\, \ln\left(\frac{(1-\widehat{P})}{(1-\widehat{R}\,\widehat{P})}\right)}{(\widehat{R}-1)\ln\left(\frac{2-\widehat{P}\left(\widehat{R}+1-(\widehat{R}^2+1)^{0.5}\right)}{2-\widehat{P}\left(\widehat{R}+1+(\widehat{R}^2+1)^{0.5}\right)}\right)} & \text{if } \widehat{PNpt}_{srow} \neq 1 \\[1em] 1 & \text{if } \widehat{PNpt}_{srow} = 1 \end{cases} \tag{A10}$$

The constraint in Equation (A4) has continuous variable: $whs_{srow,sL,sNb}$ and $wA_{srow,sL}$. The relations of these variables and the corresponding binary variable are:

$$whs_{srow,sL,sNb} \leq yrow_{srow} \tag{A11}$$

$$whs_{srow,sL,sNb} \leq yL_{sL} \tag{A12}$$

$$whs_{srow,sL,sNb} \leq yNb_{sNb} \tag{A13}$$

$$whs_{srow,sL,sNb} \geq yrow_{srow} + yL_{sL} + yNb_{sNb} - 2 \tag{A14}$$

$$wA_{srow,sL} \leq yrow_{srow} \tag{A15}$$

$$wA_{srow,sL} \leq yL_{sL} \tag{A16}$$

$$wA_{srow,sL} \geq yrow_{srow} + yL_{sL} - 1 \tag{A17}$$

Bounds on Pressure Drops, Flow Velocities and Reynolds Numbers. The bounds on the shell-side and tube-side pressure drops are expressed by:

$$\left(\sum_{srow=1}^{srowmax} \sum_{sNb=1}^{sNbmax} \sum_{sL=1}^{sLmax} \widehat{P\varDelta Ps}_{srow,sL,sNb}\, whs_{srow,sL,sNb}\right) \leq \widehat{\varDelta Psdisp} \qquad (A18)$$

$$\sum_{srow=1}^{srowmax} \sum_{sL=1}^{sLmax} \widehat{P\varDelta Ptturb1}_{srow,sL}\, wA_{srow,sL} \; +$$

$$\sum_{srow=1}^{srowmax} \sum_{sL=1}^{sLmax} \widehat{P\varDelta Ptturb2}_{srow.sL}\, wA_{srow,sL} \; +$$

$$\sum_{srow=1}^{srowmax} \widehat{P\varDelta Ptcab}_{srow}\, \widehat{K}_{srow}\, yrow_{srow} \; \leq \widehat{\varDelta Ptdisp} \qquad (A19)$$

where:

$$\widehat{P\varDelta Ps}_{srow,sL,sNb} = 0.864 \frac{\widehat{ms}^{1.812}\widehat{\mu s}^{0.188}}{\widehat{\rho s}}\left(\frac{(\widehat{PNb}_{sNb}+1)^{2.812}}{\widehat{PDs}_{srow}^{0.812}(\widehat{PFAR}_{srow}\widehat{PL}_{sL})^{1.812}(\widehat{PDeq}_{srow})^{1.188}}\right) \qquad (A20)$$

$$P\widehat{\varDelta Ptturb1}_{srow,sL} = \left(\frac{0.112\,\widehat{mt}^2}{\pi^2\rho t}\right)\left(\frac{\widehat{PNpt}_{srow}^3\widehat{PL}_{sL}}{\widehat{PNtt}_{srow}^2\,\widehat{Pdti}_{srow}^5}\right) \qquad (A21)$$

$$P\widehat{\varDelta Ptturb2}_{srow,sL} = (0.528)\left(\frac{4^{1.58}\,\widehat{mt}^{1.58}\widehat{\mu t}^{0.42}}{\pi^{1.58}\,\widehat{\rho t}}\right)\frac{\widehat{PNpt}_{srow}^{2.58}\widehat{PL}_{sL}}{\widehat{PNtt}_{srow}^{1.58}\widehat{Pdti}_{srow}^{4.58}} \qquad (A22)$$

$$P\widehat{\varDelta Ptcab}_{srow} = \left(\frac{8\,\widehat{mt}^2}{\pi^2\,\widehat{\rho t}}\right)\frac{\widehat{PNpt}_{srow}^3}{\widehat{PNtt}_{srow}^2\widehat{Pdti}_{srow}^4} \qquad (A23)$$

The bounds on the shell-side and tube-side flow velocities are:

$$\widehat{vsmin} \leq \frac{\widehat{ms}}{\widehat{\rho s}}\sum_{srow=1}^{srowmax}\sum_{sL=1}^{sLmax}\sum_{sNb=1}^{sNbmax}\frac{(\widehat{PNb}_{sNb}+1)}{\widehat{PDs}_{srow}\,\widehat{PFAR}_{srow}\,\widehat{PL}_{sL}}whs_{srow,sL,sNb} \qquad (A24)$$

$$\widehat{vsmax} \geq \frac{\widehat{ms}}{\widehat{\rho s}}\sum_{srow=1}^{srowmax}\sum_{sL=1}^{sLmax}\sum_{sNb=1}^{sNbmax}\frac{(\widehat{PNb}_{sNb}+1)}{\widehat{PDs}_{srow}\,\widehat{PFAR}_{srow}\,\widehat{PL}_{sL}}whs_{srow,sL,sNb} \qquad (A25)$$

$$\widehat{vtmin} \leq \frac{4\,\widehat{mt}}{\pi\,\widehat{\rho t}}\sum_{srow=1}^{srowmax}\frac{\widehat{PNpt}_{srow}}{\widehat{PNtt}_{srow}\,\widehat{Pdti}_{srow}^2}yrow_{srow} \qquad (A26)$$

$$\widehat{vtmax} \geq \frac{4\,\widehat{mt}}{\pi\,\widehat{\rho t}}\sum_{srow=1}^{srowmax}\frac{\widehat{PNpt}_{srow}}{\widehat{PNtt}_{srow}\,\widehat{Pdti}_{srow}^2}yrow_{srow} \qquad (A27)$$

The bounds on the Reynolds numbers are:

$$\frac{\widehat{ms}}{\widehat{\mu s}}\left(\sum_{srow=1}^{srowmax}\sum_{sL=1}^{sLmax}\sum_{sNb=1}^{sNbmax}\frac{\widehat{PDeq}_{srow}(\widehat{PNb}_{sNb}+1)}{\widehat{PDs}_{srow}\,\widehat{PFAR}_{srow}\,\widehat{PL}_{sL}}whs_{srow,sL,sNb}\right) \geq 2\cdot10^3 \qquad (A28)$$

$$\frac{4\,\widehat{mt}}{\pi\,\widehat{\mu t}}\sum_{srow=1}^{srowmax}\frac{\widehat{PNpt}_{srow}}{\widehat{PNtt}_{srow}\,\widehat{Pdti}_{srow}}yrow_{srow} \geq 10^4 \qquad (A29)$$

Geometric Constraints. The maximum and minimum baffle spacing constraints are:

$$\sum_{sL=1}^{sLmax}\sum_{sNb=1}^{sNbmax}\frac{\widehat{PL}_{sL}}{(\widehat{PNb}_{sNb}+1)}wlbc_{sL,sNb} \leq 1{,}0 \sum_{srow=1}^{srowmax}\widehat{PDs}_{srow}\,yrow_{srow} \qquad (A30)$$

$$\sum_{sL=1}^{sLmax}\sum_{sNb=1}^{sNbmax}\frac{\widehat{PL}_{sL}}{(\widehat{PNb}_{sNb}+1)}wlbc_{sL,sNb} \geq 0{,}2 \sum_{srow=1}^{srowmax}\widehat{PDs}_{srow}\,yrow_{srow} \qquad (A31)$$

The constraints in Equations (A30) and (A31) has continuous variable: $wlbc_{sL,sNb}$. The relations of this variable and the corresponding binary variable are:

$$wlbc_{sL,sNb} \leq yL_{sL} \tag{A32}$$

$$wlbc_{sL,sNb} \leq yNb_{sNb} \tag{A33}$$

$$wlbc_{sL,sNb} \geq yL_{sL} + yNb_{sNb} - 1 \tag{A34}$$

The constraints associating the ratio between the tube length and the shell diameter are:

$$\sum_{sL=1}^{sLmax} \widehat{PL}_{sL} \, yL_{sL} \leq 15 \sum_{srow=1}^{srowmax} \widehat{PDs}_{srow} \, yrow_{srow} \tag{A35}$$

$$\sum_{sL=1}^{sLmax} \widehat{PL}_{sL} \, yL_{sL} \geq 3 \sum_{srow=1}^{srowmax} \widehat{PDs}_{srow} \, yrow_{srow} \tag{A36}$$

Objective Function. The expression of the objective function in relation to the binary variables is given by:

$$\text{Min } \pi \sum_{srow=1}^{srowmax} \sum_{sL=1}^{sLmax} \widehat{PNtt}_{srow} \, \widehat{Pdte}_{srow} \, \widehat{PL}_{sL} \, wA_{srow,sL} \tag{A37}$$

Additional Constraints for the Reduction of the Search Space. These extra sets of constraints aim to accelerate the search and are derived from the bounds on velocities, shell-side pressure drop, and tube length/shell diameter ratio. A lower bound on the heat transfer area is also included based on maximum flow velocities (see Gonçalves et al. (2016) for further details).

Flow velocities Bounds.

$$whs_{srow,sL,sNb} = 0 \qquad \text{for } (srow, sL, sNb) \in (Svsminout \cup Svsmaxout) \tag{A38}$$

$$yrow_{srow} = 0 \qquad \text{for } (srow) \in (Svtminout \cup Svtmaxout) \tag{A39}$$

The sets *Svsminout*, *Svsmaxout*, *Svtminout*, and *Svtmaxout* are given by:

$$Svsminout = \{(srow, sL, sNb) \ / \ \frac{\widehat{ms}}{\widehat{\rho s}} \ \frac{(\widehat{PNb}_{sNb}+1)}{\widehat{PDs}_{srow} \ \widehat{PFAR}_{srow} \ \widehat{PL}_{sL}} \leq \widehat{vsmin} - \hat{\varepsilon}\} \tag{A40}$$

$$Svsmaxout = \{(srow, sL, sNb) \ / \ \frac{\widehat{ms}}{\widehat{\rho s}} \ \frac{(\widehat{PNb}_{sNb}+1)}{\widehat{PDs}_{srow} \ \widehat{PFAR}_{srow} \ \widehat{PL}_{sL}} \geq \widehat{vsmax} + \hat{\varepsilon}\} \tag{A41}$$

$$Svtminout = \{(srow) \ / \ \frac{4 \ \widehat{mt}}{\pi \ \widehat{\rho t}} \ \frac{\widehat{PNpt}_{srow}}{\widehat{PNtt}_{srow} \ \widehat{Pdt}_{srow}^{2}} \leq \widehat{vtmin} - \hat{\varepsilon}\} \tag{A42}$$

$$Svtmaxout = \{(srow) \ / \ \frac{4 \ \widehat{mt}}{\pi \ \widehat{\rho t}} \ \frac{\widehat{PNpt}_{srow}}{\widehat{PNtt}_{srow} \ \widehat{Pdt}_{srow}^{2}} \geq \widehat{vsmax} + \hat{\varepsilon}\} \tag{A43}$$

where ε is a small positive number.

Shell-side Pressure Upper Bound.

$$whs_{srow,sL,sNb} = 0 \qquad \text{for } (srow, sL, sNb) \in SDPsmaxout \tag{A44}$$

where the set *SDPsmaxout* is given by:

$$SDPsmaxout = \{(srow, sL, sNb) \ / \ \widehat{P\Delta Ps}_{srow,sL,sNb} \geq \widehat{\Delta Psdisp} + \hat{\varepsilon}\} \tag{A45}$$

Baffle Spacing.

$$yL_{sL} + yNb_{sNb} + yrow_{srow} \leq 2 \qquad \text{for } (srow, sL, sNb) \in (SLNbminout \cup SLNbmaxout) \tag{A46}$$

where the sets *SLNbminout* and *SLNbmaxout* are given by:

$$SLNbminout = \{(srow, sL, sNb) \ / \ \frac{\widehat{PL}_{sL}}{\widehat{PNb}_{sNb}+1} \leq 0.2\widehat{PDs}_{srow} - \hat{\varepsilon}\} \tag{A47}$$

$$SLNbmaxout = \{(srow, sL, sNb) \ / \ \frac{\widehat{PL}_{sL}}{\widehat{PNb}_{sNb}+1} \geq 1.0\widehat{PDs}_{srow} + \hat{\varepsilon}\} \tag{A48}$$

Tube length / shell diameter ratio.

$$yrow_{srow} + yL_{sL} \leq 1 \qquad \text{for } (srow, sL) \in (SLDminout \cup SLDmaxout) \tag{A49}$$

where the sets *SLDminout* and *SLDmaxout* are given by:

$$SLDminout = \{(srow, sL) \ / \ \widehat{PL}_{sL} \leq 3\widehat{PDs}_{srow} - \hat{\varepsilon}\} \tag{A50}$$

$$SLDmaxout = \{(srow, sL) \ / \ \widehat{PL}_{sL} \geq 15\widehat{PDs}_{srow} + \hat{\varepsilon}\} \tag{A51}$$

Heat Transfer Area.

$$wA_{srow,sL} = 0 \qquad \text{for } (srow, sL) \in SAminout \tag{A52}$$

where the set of heat exchangers with area lower than the minimum possible is:

$$SAminout = \{(srow, sL) \ / \pi \ \widehat{PNtt}_{srow}\widehat{Pdte}_{srow}\widehat{PL}_{sL} \leq \widehat{Amin} - \hat{\varepsilon}\} \tag{A53}$$

The lower bound on the heat transfer area can be determined by:

$$\widehat{Amin} = \frac{\hat{Q}}{\widehat{Umax}\Delta \widehat{Tlm}} \tag{A54}$$

$$\widehat{Umax} = \frac{1}{\frac{1}{\widehat{htmax}}\widehat{drmin} + \widehat{Rft} \cdot \widehat{drmin} + \frac{\widehat{Pdte}_{srow}\ln(\widehat{drmin})}{2\,\widehat{ktube}} + \widehat{Rfs} + \frac{1}{\widehat{hsmax}}} \tag{A55}$$

$$\widehat{htmax} = \max(\widehat{Pht}_{srow}) \tag{A56}$$

$$\widehat{hsmax} = \max(\widehat{Phs}_{srow,sL,sNb}) \tag{A57}$$

$$\widehat{drmin} = \min(\widehat{Pdte}_{srow}/\widehat{Pdti}_{srow}) \tag{A58}$$

Alternative 3.

Binary Variables Equality Constraints. This constraint imposes two binary variables:

$$\sum_{srow1=1}^{srow1max} yrow1_{srow1} = 1 \tag{A59}$$

$$\sum_{srow2=1}^{srow2max} yrow2_{srow2} = 1 \tag{A60}$$

Heat Transfer Rate Equation. The expressions of all heat transfer coefficients and the heat transfer area are inserted into the heat transfer equation, thus yielding:

$$\hat{Q} \left(\sum_{srow1=1}^{srow1max} \frac{\widehat{Pdte}_{srow1}}{\widehat{Pht}_{srow1} \, \widehat{Pdti}_{srow1}} yrow1_{srow1} + \widehat{Rft} \sum_{srow1=1}^{srow1max} \frac{\widehat{Pdte}_{srow1}}{\widehat{Pdti}_{srow1}} \, yrow1_{srow1} + \right.$$

$$\frac{\sum_{srow1=1}^{srow1max} \widehat{Pdte}_{srow1} \ln(\frac{\widehat{Pdte}_{srow1}}{\widehat{Pdti}_{srow1}}) yrow1_{srow1}}{2 \, \widehat{Ktube}} + \widehat{Rfs} +$$

$$\left. \sum_{srow1=1}^{srow1max} \sum_{srow2=1}^{srow2max} \frac{1}{\widehat{Phs}_{srow1,srow2}} whs_{srow1,srow2} \right) \le$$

$$\left(\pi \sum_{srow1=1}^{srow1max} \sum_{srow2=1}^{srow2max} \widehat{PNtt}_{srow1} \, \widehat{Pdte}_{srow1} \, \widehat{PL}_{srow2} \, whs_{srow1,srow2} \right) \cdot$$

$$\left(\frac{100}{100+\widehat{Aexc}} \right) \widehat{\Delta Tlm} \, \hat{F}_{srow1} \qquad \text{(A61)}$$

where $\widehat{PNtt}_{srow1}$ is the total number of tubes and:

$$\widehat{Pht}_{srow1} = \frac{\widehat{kt} \, 0.023 \left(\frac{4 \, \widehat{mt}}{\pi \, \widehat{\mu t}} \right)^{0.8} \widehat{Prt}^n}{\widehat{Pdti}_{srow1}^{1.8}} \left(\frac{\widehat{PNpt}_{srow1}}{\widehat{PNtt}_{srow1}} \right)^{0.8} \qquad \text{(A62)}$$

$$\widehat{Phs}_{srow1,srow2} = \frac{\widehat{ks} \, 0.36 \left(\frac{\widehat{ms}}{\widehat{\mu s}} \right)^{0.55} \widehat{Prs}^{1/3}}{\widehat{PDeq}_{srow1}^{0.45}} \left(\frac{(\widehat{PNb}_{srow2}+1)}{\widehat{PDs}_{srow1} \, \widehat{PFAR}_{srow1} \, \widehat{PL}_{srow2}} \right)^{0.55} \qquad \text{(A63)}$$

$$\widehat{PFAR}_{srow1} = 1 - \frac{1}{\widehat{Prp}_{srow1}} \qquad \text{(A64)}$$

$$\widehat{PDeq}_{srow1} = \frac{\widehat{aDeq}_{srow1} \widehat{Prp}_{srow1}^2 \widehat{Pdte}_{srow1}^2}{\pi \widehat{Pdte}_{srow1}} - \widehat{Pdte}_{srow1} \qquad \text{(A65)}$$

$$\widehat{aDeq}_{srow1} = \begin{cases} 4 & \text{if } \widehat{Play}_{srow1} = 1 \\ \\ 3.46 & \text{if } \widehat{Play}_{srow1} = 2 \end{cases} \qquad \text{(A66)}$$

$$\hat{F}_{srow1} = \begin{cases} \dfrac{(\hat{R}^2+1)^{0.5} \ln\left(\frac{(1-\hat{P})}{(1-\hat{R}\hat{P})} \right)}{(\hat{R}-1) \ln\left(\frac{2-\hat{P}\left(\hat{R}+1-(\hat{R}^2+1)^{0.5} \right)}{2-\hat{P}\left(\hat{R}+1+(\hat{R}^2+1)^{0.5} \right)} \right)} & \text{if } \widehat{PNpt}_{srow1} \ne 1 \\ \\ 1 & \text{if } \widehat{PNpt}_{srow1} = 1 \end{cases} \qquad \text{(A67)}$$

The constraint in Equation (A61) has continuous variable: $whs_{srow1,srow2}$. The relations of this variable and the corresponding binary variable are:

$$whs_{srow1,srow2} \le yrow1_{srow1} \qquad \text{(A68)}$$

$$whs_{srow1,srow2} \le yrow2_{srow2} \qquad \text{(A69)}$$

$$whs_{srow1,srow2} \ge yrow1_{srow1} + yrow2_{srow2} - 1 \qquad \text{(A70)}$$

Bounds on Pressure Drops, Flow Velocities and Reynolds Numbers. The

bounds on the shell-side and tube-side pressure drops are expressed by:

$$\left(\sum_{srow1=1}^{srow1max} \sum_{sroW2=1}^{srow2max} \widehat{P\Delta Ps}_{srow1,srow2} whs_{srow1,srow2} \right) \leq \widehat{\Delta Psdisp} \tag{A71}$$

$$\sum_{srow1=1}^{srow1max} \sum_{srow2=1}^{srow2max} P\widehat{\Delta Ptturb1}_{srow1,srow2} \, whs_{srow1,srow2} \, +$$

$$\sum_{srow1=1}^{srow1max} \sum_{srow2=1}^{srow2max} P\widehat{\Delta Ptturb2}_{srow1.srow2} \, whs_{srow1,srow2} \, +$$

$$\sum_{srow1=1}^{srow1max} P\widehat{\Delta Ptcab}_{srow1} \, \widehat{K}_{srow1} \, yrow1_{srow1} \leq \widehat{\Delta Ptdisp} \tag{A72}$$

where:

$$\widehat{P\Delta Ps}_{srow1,srow2} = 0.864 \frac{\widehat{ms}^{1.812} \widehat{\mu s}^{0.188}}{\widehat{\rho s}} \left(\frac{(\widehat{PNb}_{srow2}+1)^{2.812}}{\widehat{PDs}_{srow1}^{0.812} (\widehat{PFAR}_{srow1} \widehat{PL}_{srow2})^{1.812} (\widehat{PDeq}_{srow1})^{1.188}} \right) \tag{A73}$$

$$P\widehat{\Delta Ptturb1}_{srow1,srow2} = \left(\frac{0.112 \, \widehat{mt}^2}{\pi^2 \rho t} \right) \left(\frac{\widehat{PNpt}_{srow1}^3 \widehat{PL}_{srow2}}{\widehat{PNtt}_{srow1}^2 \widehat{Pdti}_{srow1}^5} \right) \tag{A74}$$

$$P\widehat{\Delta Ptturb2}_{srow1,srow2} = (0.528) \left(\frac{4^{1.58} \, \widehat{mt}^{1.58} \, \widehat{\mu t}^{0.42}}{\pi^{1.58} \, \widehat{\rho t}} \right) \frac{\widehat{PNpt}_{srow1}^{2.58} \widehat{PL}_{srow2}}{\widehat{PNtt}_{srow1}^{1.58} \widehat{Pdti}_{srow1}^{4.58}} \tag{A75}$$

$$P\widehat{\Delta Ptcab}_{srow1} = \left(\frac{8 \, \widehat{mt}^2}{\pi^2 \, \widehat{\rho t}} \right) \frac{\widehat{PNpt}_{srow1}^3}{\widehat{PNtt}_{srow1}^2 \widehat{Pdti}_{srow1}^4} \tag{A76}$$

The bounds on the shell-side and tube-side flow velocities are:

$$\widehat{vsmin} \leq \frac{\widehat{ms}}{\widehat{\rho s}} \sum_{srow1=1}^{srow1max} \sum_{srow2=1}^{srow2max} \frac{(\widehat{pNb}_{srow2}+1)}{\widehat{pDs}_{srow1} \, p\widehat{FAR}_{srow1} \, \widehat{pL}_{srow2}} whs_{srow1,srow2} \tag{A77}$$

$$\widehat{vsmax} \geq \frac{\widehat{ms}}{\widehat{\rho s}} \sum_{srow1=1}^{srow1max} \sum_{srow2=1}^{srow2max} \frac{(\widehat{pNb}_{srow2}+1)}{\widehat{pDs}_{srow1} \, p\widehat{FAR}_{srow1} \, \widehat{pL}_{srow2}} whs_{srow1,srow2} \tag{A78}$$

$$\widehat{vtmin} \leq \frac{4 \, \widehat{mt}}{\pi \, \widehat{\rho t}} \sum_{srow1=1}^{srow1max} \frac{\widehat{PNpt}_{srow1}}{\widehat{PNtt}_{srow1} \, \widehat{Pdti}_{srow1}^2} yrow1_{srow1} \tag{A79}$$

$$\widehat{vtmax} \geq \frac{4 \, \widehat{mt}}{\pi \, \widehat{\rho t}} \sum_{srow1=1}^{srow1max} \frac{\widehat{PNpt}_{srow1}}{\widehat{PNtt}_{srow1} \, \widehat{Pdti}_{srow1}^2} yrow1_{srow1} \tag{A80}$$

The bounds on the Reynolds numbers are:

$$\frac{\widehat{ms}}{\widehat{\mu s}} \left(\sum_{srow1=1}^{srow1max} \sum_{srow2=1}^{srow2max} \frac{\widehat{PDeq}_{srow1}(\widehat{PNb}_{srow2}+1)}{\widehat{PDs}_{srow1} \, \widehat{PFAR}_{srow1} \, \widehat{PL}_{srow2}} whs_{srow1,srow2} \right) \geq 2 \cdot 10^3 \tag{A81}$$

$$\frac{4 \, \widehat{mt}}{\pi \, \widehat{\mu t}} \sum_{srow1=1}^{srow1max} \frac{\widehat{PNpt}_{srow1}}{\widehat{PNtt}_{srow1} \, \widehat{Pdti}_{srow1}} yrow1_{srow1} \geq 10^4 \tag{A82}$$

Geometric Constraints. The maximum and minimum baffle spacing constraints are:

$$\sum_{srow2=1}^{srow2max} \frac{\widehat{PL}_{srow2}}{(\widehat{PNb}_{srow2}+1)} yrow2_{srow2} \leq 1{,}0 \sum_{srow1=1}^{srow1max} \widehat{PDs}_{srow1} yrow1_{srow1} \qquad (A83)$$

$$\sum_{srow2=1}^{srow2max} \frac{\widehat{PL}_{srow2}}{(\widehat{PNb}_{srow2}+1)} yrow2_{srow2} \geq 0{,}2 \sum_{srow1=1}^{srow1max} \widehat{PDs}_{srow1} yrow1_{srow1} \qquad (A84)$$

The constraints associating the ratio between the tube length and the shell diameter are:

$$\sum_{srow2=1}^{srow2max} \widehat{PL}_{srow2} yrow2_{srow2} \leq 15 \sum_{srow1=1}^{srow1max} \widehat{PDs}_{srow1} yrow1_{srow1} \qquad (A85)$$

$$\sum_{srow2=1}^{srow2max} \widehat{PL}_{srow2} yrow2_{srow2} \geq 3 \sum_{srow1=1}^{srow1max} \widehat{PDs}_{srow1} yrow1_{srow1} \qquad (A86)$$

Objective Function. The expression of the objective function in relation to the binary variables is given by:

$$\text{Min } \pi \sum_{srow1=1}^{srow1max} \sum_{srow2=1}^{srow2max} \widehat{PNtt}_{srow1} \widehat{Pdte}_{srow1} \widehat{PL}_{srow2} whs_{srow1,srow2} \qquad (A87)$$

Additional Constraints for the Reduction of the Search Space. These extra sets of constraints aim to accelerate the search and are derived from the bounds on velocities, shell-side pressure drop, and tube length/shell diameter ratio. A lower bound on the heat transfer area is also included based on maximum flow velocities (see Gonçalves et al. (2016) for further details).

Flow velocities Bounds.

$$whs_{srow1,srow2} = 0 \qquad \text{for } (srow1, srow2) \in (Svsminout \cup Svsmaxout) \qquad (A88)$$

$$yrow1_{srow1} = 0 \qquad \text{for } (srow1) \in (Svtminout \cup Svtmaxout) \qquad (A89)$$

The sets *Svsminout*, *Svsmaxout*, *Svtminout*, and *Svtmaxout* are given by:

$$Svsminout = \{(srow1, srow2) \, / \, \frac{\widehat{ms}}{\widehat{\rho s}} \frac{(\widehat{PNb}_{srow2}+1)}{\widehat{PDs}_{srow1} \, \widehat{PFAR}_{srow1} \, \widehat{PL}_{srow2}} \leq \widehat{vsmin} - \hat{\varepsilon}\} \tag{A90}$$

$$Svsmaxout = \{(srow1, srow2) \, / \, \frac{\widehat{ms}}{\widehat{\rho s}} \frac{(\widehat{PNb}_{srow2}+1)}{\widehat{PDs}_{srow1} \, \widehat{PFAR}_{srow1} \, \widehat{PL}_{srow2}} \geq \widehat{vsmax} + \hat{\varepsilon}\} \tag{A91}$$

$$Svtminout = \{(srow1) \, / \, \frac{4 \, \widehat{mt}}{\pi \, \widehat{\rho t}} \frac{\widehat{PNpt}_{srow1}}{\widehat{PNtt}_{srow1} \, \widehat{Pdti}_{srow1}^{\,2}} \leq \widehat{vtmin} - \hat{\varepsilon}\} \tag{A92}$$

$$Svtmaxout = \{(srow1) \, / \, \frac{4 \, \widehat{mt}}{\pi \, \widehat{\rho t}} \frac{\widehat{PNpt}_{srow1}}{\widehat{PNtt}_{srow1} \, \widehat{Pdti}_{srow1}^{\,2}} \geq \widehat{vsmax} + \hat{\varepsilon}\} \tag{A93}$$

where $\hat{\varepsilon}$ is a small positive number.

Shell-side Pressure Upper Bound.

$$whs_{srow1,srow2} = 0 \qquad \text{for } (srow1, srow2) \in SDPsmaxout \tag{A94}$$

where the set *SDPsmaxout* is given by:

$$SDPsmaxout = \{(srow1, srow2) \, / \, \widehat{P\Delta Ps}_{srow1,srow2} \geq \widehat{\Delta Psdisp} + \hat{\varepsilon}\} \tag{A95}$$

Baffle Spacing.

$$yrow1_{srow1} + yrow2_{srow2} \leq 1 \quad \text{for } (srow1, srow2) \in (SLNbminout \cup SLNbmaxout) \tag{A96}$$

where the sets *SLNbminout* and *SLNbmaxout* are given by:

$$SLNbminout = \{(srow1, srow2) \, / \, \frac{\widehat{PL}_{srow2}}{\widehat{PNb}_{srow2}+1} \leq 0.2\widehat{PDs}_{srow1} - \hat{\varepsilon}\} \tag{A97}$$

$$SLNbmaxout = \{(srow1, srow2) \, / \, \frac{\widehat{PL}_{srow2}}{\widehat{PNb}_{srow2}+1} \geq 1.0\widehat{PDs}_{srow1} + \hat{\varepsilon}\} \tag{A98}$$

Tube length / shell diameter ratio.

$$yrow1_{srow1} + yrow2_{srow2} \leq 1 \quad \text{for } (srow1, srow2) \in (SLDminout \cup SLDmaxout) \tag{A99}$$

where the sets *SLDminout* and *SLDmaxout* are given by:

$$SLDminout = \{(srow1, srow2) \,/\, \widehat{PL}_{srow2} \leq 3\widehat{PDs}_{srow1} - \hat{\varepsilon}\} \tag{A100}$$

$$SLDmaxout = \{(srow1, srow2) \,/\, \widehat{PL}_{srow2} \geq 15\widehat{PDs}_{srow1} + \hat{\varepsilon}\} \tag{A101}$$

Heat Transfer Area.

$$whs_{srow1,srow2} = 0 \qquad \text{for } (srow1, srow2) \in SAminout \tag{A102}$$

where the set of heat exchangers with area lower than the minimum possible is:

$$SAminout = \{(srow1, srow2) \,/\, \pi\, \widehat{PNtt}_{srow1}\widehat{Pdte}_{srow1}\widehat{PL}_{srow2} \leq \widehat{Amin} - \hat{\varepsilon}\} \tag{A103}$$

The lower bound on the heat transfer area can be determined by:

$$\widehat{Amin} = \frac{\hat{Q}}{\widehat{Umax}\,\widehat{\Delta Tlm}} \tag{A104}$$

$$\widehat{Umax} = \frac{1}{\frac{1}{\widehat{htmax}}\widehat{drmin} + \widehat{Rft}\cdot\widehat{drmin} + \frac{\widehat{Pdte}_{srow1}\ln(\widehat{drmin})}{2\,ktube} + \widehat{Rfs} + \frac{1}{\widehat{hsmax}}} \tag{A105}$$

$$\widehat{htmax} = \max(\widehat{Pht}_{srow1}) \tag{A106}$$

$$\widehat{hsmax} = \max(\widehat{Phs}_{srow1,srow2}) \tag{A107}$$

$$\widehat{drmin} = \min(\widehat{Pdte}_{srow1}/\widehat{Pdti}_{srow1}) \tag{A108}$$

Alternative 4.

Binary Variables Equality Constraints. This constraint imposes two binary variables:

$$\sum_{srow=1}^{srowmax} yrow_{srow} = 1 \tag{A109}$$

$$\sum_{sNb=1}^{sNbmax} yNb_{sNb} = 1 \tag{A110}$$

Heat Transfer Rate Equation. The expressions of all heat transfer coefficients and the heat transfer area are inserted into the heat transfer equation, thus yielding:

$$\hat{Q}\left(\sum_{srow=1}^{srowmax}\frac{\widehat{Pdte}_{srow}}{\widehat{Pht}_{srow}\,\widehat{Pdti}_{srow}}yrow_{srow} + \widehat{Rft}\sum_{srow=1}^{srowmax}\frac{\widehat{Pdte}_{srow}}{\widehat{Pdti}_{srow}}yrow_{srow} + \right.$$

$$\left.\frac{\sum_{srow=1}^{srowmax}\widehat{Pdte}_{srow}\ln(\frac{\widehat{Pdte}_{srow}}{\widehat{Pdti}_{srow}})yrow_{srow}}{2\,\widehat{Ktube}} + \widehat{Rfs} + \sum_{srow=1}^{srowmax}\sum_{sNb=1}^{sNbmax}\frac{1}{\widehat{Phs}_{srow,sNb}}whs_{srow,sNb}\right) \le$$

$$\left(\pi\,\sum_{srow=1}^{srowmax}\widehat{PNtt}_{srow}\,\widehat{Pdte}_{srow}\,\widehat{PL}_{srow}yrow_{srow}\,\right)\left(\frac{100}{100+\widehat{Aexc}}\right)\widehat{\Delta Tlm}\,\hat{F}_{srow}$$

$$\text{(A111)}$$

where $\widehat{PNtt}_{srow}$ is the total number of tubes and:

$$\widehat{Pht}_{srow} = \frac{\widehat{kt}\,0.023\left(\frac{4\,\widehat{mt}}{\pi\,\widehat{\mu t}}\right)^{0.8}\widehat{Prt}^{n}}{\widehat{Pdti}_{srow}^{1.8}}\left(\frac{\widehat{PNpt}_{srow}}{\widehat{PNtt}_{srow}}\right)^{0.8} \qquad\qquad\text{(A112)}$$

$$\widehat{Phs}_{srow,sNb} = \frac{\widehat{ks}\,0.36\left(\frac{\widehat{ms}}{\widehat{\mu s}}\right)^{0.55}\widehat{Prs}^{1/3}}{\widehat{PDeq}_{srow}^{0.45}}\left(\frac{(\widehat{PNb}_{sNb}+1)}{\widehat{PDs}_{srow}\,\widehat{PFAR}_{srow}\,\widehat{PL}_{srow}}\right)^{0.55} \qquad\text{(A113)}$$

$$\widehat{PFAR}_{srow} = 1 - \frac{1}{\widehat{Prp}_{srow}} \qquad\qquad\text{(A114)}$$

$$\widehat{PDeq}_{srow} = \frac{\widehat{aDeq}_{srow}\widehat{Prp}_{srow}^{2}\widehat{Pdte}_{srow}^{2}}{\pi\widehat{Pdte}_{srow}} - \widehat{Pdte}_{srow} \qquad\qquad\text{(A115)}$$

$$\widehat{aDeq}_{srow} = \begin{cases} 4 & \text{if } \widehat{Play}_{srow} = 1 \\ \\ 3.46 & \text{if } \widehat{Play}_{srow} = 2 \end{cases} \qquad\qquad\text{(A116)}$$

$$\hat{F}_{srow} = \begin{cases} \dfrac{(\hat{R}^{2}+1)^{0.5}\,\ln\left(\frac{(1-\hat{P})}{(1-\hat{R}\hat{P})}\right)}{(\hat{R}-1)\ln\left(\frac{2-\hat{P}\left(\hat{R}+1-(\hat{R}^{2}+1)^{0.5}\right)}{2-\hat{P}\left(\hat{R}+1+(\hat{R}^{2}+1)^{0.5}\right)}\right)} & \text{if } \widehat{PNpt}_{srow} \ne 1 \\ \\ 1 & \text{if } \widehat{PNpt}_{srow} = 1 \end{cases} \qquad\text{(A117)}$$

The constraint in Equation (A111) has continuous variable: $whs_{srow,sNb}$. The relations of this variable and the corresponding binary variable are:

$$whs_{srow,sNb} \le yrow_{srow} \qquad\qquad\qquad\text{(A118)}$$

$$whs_{srow,sNb} \le yNb_{sNb} \qquad\qquad\qquad\text{(A119)}$$

$$whs_{srow,sNb} \ge yrow_{srow} + yNb_{sNb} - 1 \qquad\qquad\qquad\text{(A120)}$$

Bounds on Pressure Drops, Flow Velocities and Reynolds Numbers. The

bounds on the shell-side and tube-side pressure drops are expressed by:

$$\left(\sum_{srow=1}^{srowmax} \sum_{sNb=1}^{sNbmax} \widehat{P\Delta Ps}_{srow,sNb}\, whs_{srow,sNb}\right) \leq \Delta\widehat{Psdisp} \tag{A121}$$

$$\sum_{srow=1}^{srowmax} P\Delta\widehat{Ptturb1}_{srow}\, yrow_{srow} + \sum_{srow=1}^{srowmax} P\Delta\widehat{Ptturb2}_{srow}\, yrow_{srow} +$$
$$\sum_{srow=1}^{srowmax} P\Delta\widehat{Ptcab}_{srow}\, \widehat{K}_{srow}\, yrow_{srow} \leq \Delta\widehat{Ptdisp} \tag{A122}$$

where:

$$\widehat{P\Delta Ps}_{srow,sNb} = 0.864\,\frac{\widehat{ms}^{1.812}\,\widehat{\mu s}^{0.188}}{\widehat{\rho s}}\left(\frac{(\widehat{PNb}_{sNb}+1)^{2.812}}{\widehat{PDs}_{srow}^{0.812}(\widehat{PFAR}_{srow}\widehat{PL}_{srow})^{1.812}(\widehat{PDeq}_{srow})^{1.188}}\right) \tag{A123}$$

$$P\Delta\widehat{Ptturb1}_{srow} = \left(\frac{0.112\,\widehat{mt}^2}{\pi^2 \rho t}\right)\left(\frac{\widehat{PNpt}_{srow}^3\widehat{PL}_{srow}}{\widehat{PNtt}_{srow}^2\widehat{Pdti}_{srow}^5}\right) \tag{A124}$$

$$P\Delta\widehat{Ptturb2}_{srow} = (0.528)\left(\frac{4^{1.58}\,\widehat{mt}^{1.58}\,\widehat{\mu t}^{0.42}}{\pi^{1.58}\,\widehat{\rho t}}\right)\frac{\widehat{PNpt}_{srow}^{2.58}\widehat{PL}_{srow}}{\widehat{PNtt}_{srow}^{1.58}\widehat{Pdti}_{srow}^{4.58}} \tag{A125}$$

$$P\Delta\widehat{Ptcab}_{srow} = \left(\frac{8\,\widehat{mt}^2}{\pi^2\,\widehat{\rho t}}\right)\frac{\widehat{PNpt}_{srow}^3}{\widehat{PNtt}_{srow}^2\widehat{Pdti}_{srow}^4} \tag{A126}$$

The bounds on the shell-side and tube-side flow velocities are:

$$\widehat{vsmin} \leq \frac{\widehat{ms}}{\widehat{\rho s}}\sum_{srow=1}^{srowmax}\sum_{sNb=1}^{sNbmax}\frac{(\widehat{PNb}_{sNb}+1)}{\widehat{PDs}_{srow}\,\widehat{PFAR}_{srow}\,\widehat{PL}_{srow}}whs_{srow,sNb} \tag{A127}$$

$$\widehat{vsmax} \geq \frac{\widehat{ms}}{\widehat{\rho s}}\sum_{srow=1}^{srowmax}\sum_{sNb=1}^{sNbmax}\frac{(\widehat{PNb}_{sNb}+1)}{\widehat{PDs}_{srow}\,\widehat{PFAR}_{srow}\,\widehat{PL}_{srow}}whs_{srow,sNb} \tag{A128}$$

$$\widehat{vtmin} \leq \frac{4\,\widehat{mt}}{\pi\,\widehat{\rho t}}\sum_{srow=1}^{srowmax}\frac{\widehat{PNpt}_{srow}}{\widehat{PNtt}_{srow}\,\widehat{Pdti}_{srow}^2}yrow_{srow} \tag{A129}$$

$$\widehat{vtmax} \geq \frac{4\,\widehat{mt}}{\pi\,\widehat{\rho t}}\sum_{srow=1}^{srowmax}\frac{\widehat{PNpt}_{srow}}{\widehat{PNtt}_{srow}\,\widehat{Pdti}_{srow}^2}yrow_{srow} \tag{A130}$$

The bounds on the Reynolds numbers are:

$$\frac{\widehat{ms}}{\widehat{\mu s}}\left(\sum_{srow=1}^{srowmax}\sum_{sNb=1}^{sNbmax}\frac{\widehat{PDeq}_{srow}(\widehat{PNb}_{sNb}+1)}{\widehat{PDs}_{srow}\,\widehat{PFAR}_{srow}\,\widehat{PL}_{srow}}whs_{srow,sNb}\right) \geq 2\cdot10^3 \tag{A131}$$

$$\frac{4\,\widehat{mt}}{\pi\,\widehat{\mu t}}\sum_{srow=1}^{srowmax}\frac{\widehat{PNpt}_{srow}}{\widehat{PNtt}_{srow}\,\widehat{Pdti}_{srow}}yrow_{srow} \geq 10^4 \tag{A132}$$

Geometric Constraints. The maximum and minimum baffle spacing constraints are:

$$\sum_{srow=1}^{srowmax} \sum_{sNb=1}^{sNbmax} \frac{\widehat{PL}_{srow}}{(\widehat{PNb}_{sNb}+1)} whs_{srow,sNb} \leq 1{,}0 \sum_{srow=1}^{srowmax} \widehat{PDs}_{srow} yrow_{srow} \qquad (A133)$$

$$\sum_{srow=1}^{srowmax} \sum_{sNb=1}^{sNbmax} \frac{\widehat{PL}_{srow}}{(\widehat{PNb}_{sNb}+1)} whs_{srow,sNb} \geq 0{,}2 \sum_{srow=1}^{srowmax} \widehat{PDs}_{srow} yrow_{srow} \qquad (A134)$$

The constraints associating the ratio between the tube length and the shell diameter are:

$$\sum_{srow=1}^{srowmax} \widehat{PL}_{srow} \, yrow_{srow} \leq 15 \sum_{srow=1}^{srowmax} \widehat{PDs}_{srow} \, yrow_{srow} \qquad (A135)$$

$$\sum_{srow=1}^{srowmax} \widehat{PL}_{srow} \, yrow_{srow} \geq 3 \sum_{srow=1}^{srowmax} \widehat{PDs}_{srow} \, yrow_{srow} \qquad (A136)$$

Objective Function. The expression of the objective function in relation to the binary variables is given by:

$$\text{Min } \pi \sum_{srow=1}^{srowmax} \widehat{PNtt}_{srow} \, \widehat{Pdte}_{srow} \, \widehat{PL}_{srow} yrow_{srow} \qquad (A137)$$

Additional Constraints for the Reduction of the Search Space. These extra sets of constraints aim to accelerate the search and are derived from the bounds on velocities, shell-side pressure drop, and tube length/shell diameter ratio. A lower bound on the heat transfer area is also included based on maximum flow velocities (see Gonçalves et al. (2016) for further details).

Flow velocities Bounds.

$$whs_{srow,sNb} = 0 \qquad \text{for } (srow, sNb) \in (Svsminout \cup Svsmaxout) \qquad (A138)$$

$$yrow_{srow} = 0 \qquad \text{for } (srow) \in (Svtminout \cup Svtmaxout) \qquad (A139)$$

The sets *Svsminout*, *Svsmaxout*, *Svtminout*, and *Svtmaxout* are given by:

$$Svsminout = \{(srow, sNb) \ / \ \frac{\widehat{ms}}{\widehat{\rho s}} \ \frac{(\widehat{PNb}_{sNb}+1)}{\widehat{PDs}_{srow} \ \widehat{PFAR}_{srow} \ \widehat{PL}_{srow}} \ \leq \ \widehat{vsmin} - \hat{\varepsilon}\} \tag{A140}$$

$$Svsmaxout = \{(srow, sNb) \ / \ \frac{\widehat{ms}}{\widehat{\rho s}} \ \frac{(\widehat{PNb}_{sNb}+1)}{\widehat{PDs}_{srow} \ \widehat{PFAR}_{srow} \ \widehat{PL}_{srow}} \ \geq \ \widehat{vsmax} + \hat{\varepsilon}\} \tag{A141}$$

$$Svtminout = \{(srow) \ / \ \frac{4}{\pi} \frac{\widehat{mt}}{\widehat{\rho t}} \ \frac{\widehat{PNpt}_{srow}}{\widehat{PNtt}_{srow} \ \widehat{Pdt}_{srow}^{2}} \ \leq \ \widehat{vtmin} - \hat{\varepsilon}\} \tag{A142}$$

$$Svtmaxout = \{(srow) \ / \ \frac{4}{\pi} \frac{\widehat{mt}}{\widehat{\rho t}} \ \frac{\widehat{PNpt}_{srow}}{\widehat{PNtt}_{srow} \ \widehat{Pdt}_{srow}^{2}} \ \geq \ \widehat{vsmax} + \hat{\varepsilon}\} \tag{A143}$$

where $\hat{\varepsilon}$ is a small positive number.

Shell-side Pressure Upper Bound.

$$whs_{srow,sNb} = 0 \qquad \text{for } (srow, sNb) \in SDPsmaxout \tag{A144}$$

where the set *SDPsmaxout* is given by:

$$SDPsmaxout = \{(srow, sNb) \ / \ \widehat{P\Delta Ps}_{srow,sNb} \ \geq \ \widehat{\Delta Psdisp} + \hat{\varepsilon}\} \tag{A145}$$

Baffle Spacing.

$$yNb_{sNb} + yrow_{srow} \ \leq 1 \quad \text{for } (srow, sNb) \in (SLNbminout \cup SLNbmaxout) \tag{A146}$$

where the sets *SLNbminout* and *SLNbmaxout* are given by:

$$SLNbminout = \{(srow, sNb) \ / \ \frac{\widehat{PL}_{srow}}{\widehat{PNb}_{sNb}+1} \ \leq 0.2\widehat{PDs}_{srow} - \hat{\varepsilon}\} \tag{A147}$$

$$SLNbmaxout = \{(srow, sNb) \ / \ \frac{\widehat{PL}_{srow}}{\widehat{PNb}_{sNb}+1} \ \geq 1.0\widehat{PDs}_{srow} + \hat{\varepsilon}\} \tag{A148}$$

Tube length / shell diameter ratio.

$$yrow_{srow} \ \leq 0 \quad \text{for } (srow) \in (SLDminout \cup SLDmaxout) \tag{A149}$$

where the sets *SLDminout* and *SLDmaxout* are given by:

$$SLDminout = \{(srow) \ / \ \widehat{PL}_{srow} \ \leq 3\widehat{PDs}_{srow} - \hat{\varepsilon}\} \tag{A150}$$

$$SLDmaxout = \{(srow) \ / \ \widehat{PL}_{srow} \ \geq 15\widehat{PDs}_{srow} + \hat{\varepsilon}\} \tag{A151}$$

Heat Transfer Area.

$$yrow_{srow} = 0 \qquad \text{for } (srow) \in SAminout \tag{A152}$$

where the set of heat exchangers with area lower than the minimum possible is:

$$SAminout = \{(srow) / \pi \widehat{PNtt}_{srow} \widehat{Pdte}_{srow} \widehat{PL}_{srow} \leq \widehat{Amin} - \hat{\varepsilon}\} \tag{A153}$$

The lower bound on the heat transfer area can be determined by:

$$\widehat{Amin} = \frac{\hat{Q}}{\widehat{Umax}\,\widehat{\Delta Tlm}} \tag{A154}$$

$$\widehat{Umax} = \frac{1}{\frac{1}{\widehat{htmax}}\widehat{drmin} + \widehat{Rft}\cdot\widehat{drmin} + \frac{\widehat{Pdte}_{srow}\ln(\widehat{drmin})}{2\,\widehat{ktube}} + \widehat{Rfs} + \frac{1}{\widehat{hsmax}}} \tag{A155}$$

$$\widehat{htmax} = \max(\widehat{Pht}_{srow}) \tag{A156}$$

$$\widehat{hsmax} = \max(\widehat{Phs}_{srow,sNb}) \tag{A157}$$

$$\widehat{drmin} = \min(\widehat{Pdte}_{srow}/\widehat{Pdti}_{srow}) \tag{A158}$$

Alternative 5. This alternative was described in detail in the main text.

APPENDIX B – **Parameters of the Bell-Delaware method.**

Table B 1 - Values of the parameter ψ_n

Npt (number of tube passes)	Ds (m)	ψ_n
2	0.2050	0.18
2	0.3048	0.09
2	0.3366	0.075
2	0.3874	0.06
2	0.4382	0.048
2	0.4890	0.046
2	0.5398	0.044
2	0.5906	0.042
2	0.6350	0.038
2	0.6858	0.036
2	0.7366	0.035
2	0.7874	0.034
2	0.8382	0.033
2	0.8890	0.032
2	0.9398	0.03
2	0.9906	0.028
2	1.0668	0.025
2	1.1430	0.024
2	1.2192	0.0235
2	1.3716	0.02
2	1.5240	0.018
4	0.2050	0.30
4	0.3048	0.20
4	0.3366	0.18
4	0.3874	0.16
4	0.4382	0.13
4	0.4890	0.125
4	0.5398	0.12
4	0.5906	0.118
4	0.6350	0.114
4	0.6858	0.11
4	0.7366	0.10
4	0.7874	0.095
4	0.8382	0.09
4	0.8890	0.085
4	0.9398	0.08
4	0.9906	0.075
4	1.0668	0.073
4	1.1430	0.071
4	1.2192	0.065
4	1.3716	0.06
4	1.5240	0.05

6	0.2050	0.40
6	0.3048	0.22
6	0.3366	0.20
6	0.3874	0.18
6	0.4382	0.17
6	0.4890	0.168
6	0.5398	0.16
6	0.5906	0.158
6	0.6350	0.15
6	0.6858	0.148
6	0.7366	0.135
6	0.7874	0.122
6	0.8382	0.118
6	0.8890	0.11
6	0.9398	0.105
6	0.9906	0.098
6	1.0668	0.09
6	1.1430	0.088
6	1.2192	0.087
6	1.3716	0.08
6	1.5240	0.074
8	0.2050	0.80
8	0.3048	0.30
8	0.3366	0.22
8	0.3874	0.20
8	0.4382	0.20
8	0.4890	0.18
8	0.5398	0.17
8	0.5906	0.16
8	0.6350	0.15
8	0.6858	0.14
8	0.7366	0.13
8	0.7874	0.125
8	0.8382	0.12
8	0.8890	0.115
8	0.9398	0.11
8	0.9906	0.105
8	1.0668	0.10
8	1.1430	0.098
8	1.2192	0.095
8	1.3716	0.09
8	1.5240	0.08

Note 1: The value of ψ_n for $Npt = 1$ is equal to 0 for any Ds

Note 2: This table was evaluated considering for the sake of simplification the utilization of a fixed tube diameter of 0.01905 m, however these values can be employed for any tube diameter without significant loss of accuracy.

Table B 2 - Values of the parameters of the Bell-Delaware method for evaluation of the convective heat transfer coefficient for an ideal tube bank

Layout angle	Reynolds Number	$\widehat{Pa1}_{sRes,slay}$	$\widehat{Pa2}_{sRes,slay}$	$\widehat{Pa3}_{sRes,slay}$	$\widehat{Pa4}_{sRes,slay}$
30°	<10	1.400	-0.667	1.450	0.519
	10-20	1.360	-0.657		
	$20\text{-}10^2$	1.360	-0.657		
	$10^2\text{-}10^3$	0.593	-0.477		
	$10^3\text{-}10^4$	0.321	-0.388		
	$10^4\text{-}10^5$	0.321	-0.388		
45°	<10	1.550	-0.667	1.930	0.500
	10-20	0.498	-0.656		
	$20\text{-}10^2$	0.498	-0.656		
	$10^2\text{-}10^3$	0.730	-0.500		
	$10^3\text{-}10^4$	0.370	-0.396		
	$10^4\text{-}10^5$	0.370	-0.396		
90°	<10	0.970	-0.667	1.187	0.370
	10-20	0.900	-0.631		
	$20\text{-}10^2$	0.900	-0.631		
	$10^2\text{-}10^3$	0.408	-0.460		
	$10^3\text{-}10^4$	0.107	-0.266		
	$10^4\text{-}10^5$	0.370	-0.395		

Table B 3 - Values of the parameters of the Bell-Delaware method for evaluation of the friction factor for an ideal tube bank

Layout angle	Reynolds Number	$\widehat{Pb1}_{sRes,slay}$	$\widehat{Pb2}_{sRes,slay}$	$\widehat{Pb3}_{sRes,slay}$	$\widehat{Pb4}_{sRes,slay}$
30°	<10	35.000	-1.000	7.00	0.500
	10-20	32.1000	-0.973		
	$20\text{-}10^2$	32.1000	-0.973		
	$10^2\text{-}10^3$	6.0900	-0.476		
	$10^3\text{-}10^4$	0.0815	-0.152		
	$10^4\text{-}10^5$	0.391	-0.123		
45°	<10	32.000	-1.000	6.59	0.520
	10-20	26.200	-0.913		
	$20\text{-}10^2$	26.200	-0.913		
	$10^2\text{-}10^3$	3.500	-0.476		
	$10^3\text{-}10^4$	0.333	-0.136		
	$10^4\text{-}10^5$	0.303	-0.126		
90°	<10	35.000	-1.000	6.30	0.378
	10-20	32.1000	-0.963		
	$20\text{-}10^2$	32.1000	-0.963		
	$10^2\text{-}10^3$	6.0900	-0.602		
	$10^3\text{-}10^4$	0.0815	-0.022		
	$10^4\text{-}10^5$	0.391	-0.148		

APPENDIX C – **SCIENTIFIC PRODUCTION**

The scientific production developed during the period of this thesis is showed in this section. Only the first page of the works will be displayed in the same order they are listed.

Conference: XX Congresso Brasileiro de Engenharia Química – COBEQ 2014. October 19th -22th, 2014. Florianópolis, SC, Brasil.

⇒ Title: Otimização da limpeza de redes de trocadores de calor empregando os algoritmos genéticos. Authors: Caroline de O. Gonçalves, Eduardo M. Queiroz, Fernando L. P. Pessoa, Fábio S. Liporace, Sérgio G. Oliveira, André L. H. Costa.

Conference: XXII Congresso Brasileiro de Engenharia Química – COBEQ 2018. September 23th -26th, 2018. Florianópolis, SC, Brasil.

⇒ Title: Comparação de diferentes alternativas de função objetivo na formulação do problema de projeto ótimo de trocadores de calor casco-e-tubo: massa X área. Authors: Caroline de O. Gonçalves, N. R. Martins, G. A. Carvalho, André L. H. Costa, Miguel J. Bagajewicz.

Journal: AIChE-Journal, 2016.

⇒ Title: Shell and Tube Heat Exchanger Design Using Mixed-Integer Linear Programming. Authors: Caroline de O. Gonçalves, André L. H. Costa, Miguel J. Bagajewicz.

Journal: I&EC Research, 2017.

⇒ Title: Alternative Mixed-Integer Linear Programming Formulations for Shell and Tube Heat Exchanger Optimal Design. Authors: Caroline de O. Gonçalves, André L. H. Costa, Miguel J. Bagajewicz.

Journal: AIChE-Journal, 2019. (Accepted for publication)

⇒ Title: Linear Method for the Design of Shell and Tube Heat Exchangers using the Bell-Delaware Method. Authors: Caroline de O. Gonçalves, André L. H. Costa, Miguel J. Bagajewicz.

COBEQ 2014
XX Congresso Brasileiro de Engenharia Química

19 a 22 de outubro de 2014
Florianópolis/SC

OTIMIZAÇÃO DA LIMPEZA DE REDES DE TROCADORES DE CALOR EMPREGANDO OS ALGORITMOS GENÉTICOS

C. de O. GONÇALVES[1], E. M. QUEIROZ[2], F. L. P. PESSOA[2], F. S. LIPORACE[3], S. G. OLIVEIRA[3] e A. L. H. COSTA[1]

[1] Universidade do Estado do Rio de Janeiro, Departamento de Operações e Projetos Industriais
[2] Universidade Federal do Rio de Janeiro, Departamento de Engenharia Química
[3] Petrobras, CENPES
E-mail para contato: andrehc@uerj.br

RESUMO – Durante a operação de redes de trocadores de calor, é usual ocorrer a deposição sobre a superfície de troca térmica nestes equipamentos, diminuindo assim a sua efetividade. Uma abordagem possível para mitigar esse problema é baseada no estabelecimento de uma programação de limpeza dos trocadores capaz de reduzir o impacto da deposição. Nesse contexto, o presente trabalho tem como objetivo explorar uma alternativa de otimização baseada em algoritmos genéticos para identificar a programação ótima das paradas para limpeza. Como solução para esse problema tem-se qual trocador de calor da rede deverá ser limpo em cada período de tempo. O desempenho da abordagem proposta é ilustrado usando um exemplo baseado numa refinaria real brasileira.

1. INTRODUÇÃO

Na medida em que as redes de trocadores de calor são utilizadas, frequentemente ocorre o fenômeno da deposição. Esse é um grande problema presente nas indústrias de processo, pois as incrustações nos trocadores de calor reduzem a efetividade térmica e aumentam a queda de pressão, aumentando o consumo de energia e os custos de operação.

Uma forma de mitigação que pode ser empregada para reduzir o impacto da deposição implica na parada periódica dos trocadores para a limpeza. Entretanto, esta abordagem envolve um *trade-off*, pois se por um lado as limpezas são capazes de restaurar a efetividade dos trocadores, por outro implicam em custos e também em um aumento no consumo de energia durante o período que o trocador está parado. Vários autores na literatura estudaram o problema de identificação da programação ótima das limpezas em redes (Smaili *et al.*, 2002; Lavaja e Bagajewicz, 2004; Rodriguez e Smith, 2007).

Neste contexto, este trabalho apresenta a aplicação de uma metodologia estocástica para a identificação da melhor programação de limpeza de redes de trocadores de calor. O método de otimização estocástica utilizado foi baseado nos algoritmos genéticos (Linden, 2008). A utilização desta abordagem pode ser justificada pela sua flexibilidade para lidar com problemas complexos, tais

COMPARAÇÃO DE DIFERENTES ALTERNATIVAS DE FUNÇÃO OBJETIVO NA FORMULAÇÃO DO PROBLEMA DE PROJETO ÓTIMO DE TROCADORES DE CALOR CASCO-E-TUBO: MASSA X ÁREA

GONÇALVES CO[1], MARTINS NR[1], CARVALHO GA[1],
COSTA ALH[1] e BAGAJEWICZ MJ[2]

[1] Universidade do Estado do Rio de Janeiro, Programa de Pós-graduação em Engenharia Química (PPG-EQ/UERJ)
[2] University of Oklahoma, School of Chemical, Biological and Materials Engineering
E-mail para contato: andrehc@uerj.br

RESUMO – Este trabalho apresenta uma comparação da massa e da área de troca térmica como alternativas de função objetivo do problema de projeto ótimo de trocadores de calor. A análise é baseada em uma formulação linear do problema de otimização do projeto capaz de identificar o ótimo global. Os resultados mostram que, em boa parte dos problemas investigados, o trocador otimizado considerando as duas funções objetivos não são os mesmos, sendo registrados casos onde esta diferença pode ser considerável.

1. INTRODUÇÃO

Atualmente, a crescente competitividade a nível mundial impulsiona uma busca permanente por redução de custos, seja na fase de projeto de uma planta de processo ou durante a sua operação. Uma vez que equipamentos de troca térmica são responsáveis por boa parte do investimento necessário em um novo empreendimento no contexto da indústria de processos químicos, há um grande esforço na literatura para o desenvolvimento de ferramentas computacionais baseadas na aplicação de técnicas de otimização para o projeto deste tipo de equipamento. Em função da sua importância, boa parte deste esforço é direcionado para trocadores de calor casco-e-tubo, foco do presente trabalho.

A formulação do problema de projeto ótimo pode se basear na minimização do custo total anualizado englobando o investimento no trocador associado ao custo operacional relativo ao escoamento das correntes através do equipamento. Considerando um trocador isolado, esta função objetivo é capaz de descrever o trade-off típico associado ao problema de projeto de trocadores de calor, ou seja, maiores velocidades permitem aumentar os coeficientes de convecção, o que leva a uma redução da área de troca térmica e, por conseguinte, do investimento. Entretanto, maiores velocidades também são responsáveis por aumentar a queda de pressão no escoamento, o que implica em um aumento do custo operacional.

Entretanto, em um processo completo, a análise do consumo de energia necessário ao

AIChE

Shell and Tube Heat Exchanger Design Using Mixed-Integer Linear Programming

Caroline de O. Gonçalves and André L. H. Costa

Institute of Chemistry, Rio de Janeiro State University (UERJ) Rua São Francisco Xavier, 524, Maracanã, Rio de Janeiro, RJ, CEP 20550-900 Brazil

Miguel J. Bagajewicz

School of Chemical, Biological and Materials Engineering, University of Oklahoma, Norman Oklahoma 73019

The design of heat exchangers, especially shell and tube heat exchangers was originally proposed as a trial and error procedure where guesses of the heat transfer coefficient were made and then verified after the design was finished. This traditional approach is highly dependent of the experience of a skilled engineer and it usually results in oversizing. Later, optimization techniques were proposed for the automatic generation of the best design alternative. Among these methods, there are heuristic and stochastic approaches as well as mathematical programming. In all cases, the models are mixed integer non-linear and non-convex. In the case of mathematical programming solution procedures, all the solution approaches were likely to be trapped in a local optimum solution, unless global optimization is used. In addition, it is very well-known that local solvers need good initial values or sometimes they do not even find a feasible solution. In this article, we propose to use a robust mixed integer global optimization procedure to obtain the optimal design. Our model is linear thanks to the use of standardized and discrete geometric values of the heat exchanger main mechanical components and a reformulation of integer nonlinear expressions without losing any rigor. © 2016 American Institute of Chemical Engineers AIChE J, 63: 1907–1922, 2017

Keywords: optimization, design

Introduction

In its classical book,[1] Kern presents the design of shell and tube heat exchangers, as a guess-and-verify procedure where the overall heat transfer coefficient is guessed first and the design is performed in such a way that the final resulting heat transfer coefficient is at least larger than the one that has been guessed. Modern textbooks[2-4] also presents in essence the same trial-and-error design procedure: first an initial tentative heat exchanger is proposed, then the heat exchanger is rated, and the results are checked to verify if the heat exchanger is acceptable, considering the excess area and the allowable pressure drop. If the proposed heat exchanger does not satisfy the task demands, alterations in the design must be conducted and followed by a new rating and further examination. The procedure must be repeated until an acceptable solution is found. This traditional approach involves the direct intervention of a skilled engineer and remained somewhat unaltered for a long time. Alternatively, algorithms based on heuristic rules, which could be implemented in a computer code, were also proposed for the identification of a design solution.[5,6] However, the heuristic nature of these schemes does not guarantee that the area or the cost are optimal.

More recently, heat exchanger design was considered as an optimization problem with cost being minimized. However, for a given heat transfer task, an accurate assessment of the heat exchanger capital cost would require elaborate costing of parts as well as assembly costs. For this reason, previous works usually employed some substitutes: heat exchanger area or a simplified cost function in relation to the area. Therefore, the objective function used normally is the minimization of the heat exchanger area or the total annualized cost, including capital (area based) and operating costs (pumping costs).

The techniques for design optimization of shell and tube heat exchangers can be organized in three mains classes: heuristic rules based on thermofluidynamic relations, metaheuristic methods, and mathematical programming.

The utilization of heuristic rules involves different techniques for the exploration of the search space, such as, graphical analysis and systematic screening of the counting table. Muralikrishna and Shenoy[5] proposed the analysis of the feasible region of the design problem through a pressure drop graph using geometrical and operational constraints. The insertion of objective function curves in the proposed graph allowed the identification of the best design alternative. Ravagnani et al.[6] proposed the application of an heuristic algorithm to a crescent sequence of shell diameters in the counting table aiming to identify the smallest heat exchanger according to the pressure drop constraints. Eryener[7] presented several graphs associated to the baffle spacing aiming to identify the optimal value of

# Alternative Mixed-Integer Linear Programming Formulations for Shell and Tube Heat Exchanger Optimal Design

Caroline de O. Gonçalves,[†] André L. H. Costa,[†] and Miguel J. Bagajewicz[*,‡]

[†]Institute of Chemistry, Rio de Janeiro State University (UERJ), Rua São Francisco Xavier, 524, Maracanã, Rio de Janeiro CEP 20550-900, Brazil

[‡]School of Chemical, Biological, and Materials Engineering, University of Oklahoma, Norman, Oklahoma 73019, United States

Ⓢ Supporting Information

ABSTRACT: In a recent article (Gonçalves et al., AICHE J. 2017. DOI: 10.1002/aic.15556), we presented a mixed-integer linear programming formulation for the detailed design of shell and tube heat exchangers based on the Kern approach (Kern, D. Q. Process Heat Transfer; McGraw Hill, 1950). The formulation relies on the use of standardized values for several mechanical parts, which we express in terms of discrete choices. Because we aim at having this model used as part of more complex models (i.e., heat exchanger networks synthesis), we identified a need to improve its computational efficiency. In this article, we explore several different modeling options to speed up solutions. These options are based on different alternatives of aggregation of the discrete values in relation to the set of binary variables. Numerical results show that these procedures allow large computational effort reductions.
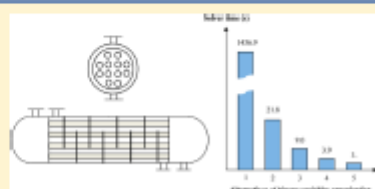
1. INTRODUCTION

Heat exchangers are equipment responsible for the modification of the temperature or physical state of process streams. They are a considerable fraction of the hardware of process industries, where a large process plant (e.g., a refinery) may involve the design of several hundreds of heat exchangers.[3]

The traditional approach for the design of heat exchangers involves the direct intervention of a skilled engineer in a trial-and-error procedure. Most often, the main target is the identification of a feasible heat exchanger candidate just able to fulfill the desired thermal service, not necessarily in an optimal manner. Since, for a given thermal task, there are different feasible alternatives, the quality of the design is highly dependent on the experience of the engineer. This aspect becomes even more important in a scenario of generational transition, where engineering teams were reduced and thermal specialists became rare in chemical and oil companies.[4] Modern textbooks present algorithms for the solution of the design problem, where some level of optimization is included, but these schemes keep the same trial-and-error logic.[5]

By aiming at circumventing the limitations of the traditional design approach, several papers formulate the design problem as an optimization problem.[6] The objective function is usually the minimization of the heat exchanger area restricted by allowable pressure drops or the minimization of the total annualized cost including capital and operating costs in a yearly basis.[7] The main constraints are the thermal and hydraulic equations of the heat exchanger model.

In general, the computational techniques employed for the solution of the design problem can be classified into three categories: heuristic, metaheuristic, and mathematical programming. The heuristic methods explore the search space based on thermo-fluid dynamic relations with the support of graphics[8] or screening tools.[9] Metaheuristic methods consist of randomized algorithms for the search of the optimal solution such as simulated annealing,[10] genetic algorithms,[11] particle swarm optimization,[12] among others. Our article is inserted into the category of mathematical programming. Mathematical programming techniques involve the utilization of deterministic algorithms, where the solution can be found based on formal optimality conditions (local or global). Newer mathematical programming solutions for the design of heat exchangers consider the discrete nature of the design variables and thus yield mixed-integer nonlinear programming (MINLP) problems.[13–15] An important aspect of MINLP alternatives is their nonconvexity, which may present nonconvergence problems and multiple local optima.

Recently, we proposed a mixed-integer linear programming (MILP) formulation for the design problem[1] aimed at the minimization of the heat transfer area. The model is based on the utilization of standard values for several mechanical parts expressed in terms of discrete choices together with one simple hydraulic and thermal model.[2] For example, tube diameters come only in certain discrete values, and their wall thickness is

A

Linear Method for the Design of Shell and Tube Heat Exchangers using the Bell-Delaware Method

Caroline de O. Gonçalves
School of Science and Technology, Unigranrio University, Av. Perimetral Prof. José de Souza Herdy, 1160 – Jardim Vinte e Cinco de Agosto, Duque de Caxias, RJ, CEP 25071-202 Brazil

André L. H. Costa
Institute of Chemistry, Rio de Janeiro State University (UERJ), Rua São Francisco Xavier, 524, Maracanã, Rio de Janeiro, RJ, CEP 20550-900 Brazil

Miguel J. Bagajewicz
School of Chemical, Biological and Materials Engineering, University of Oklahoma, Norman Oklahoma 73019 EUA

In this article, we present a rigorous reformulation of the Bell-Delaware model for the design optimization of shell and tube heat exchanger to obtain a linear model. We extend a previously presented methodology1,2 of rigorously reformulate the MINLP Kern model and we add disjunctions to automatically choose the different correlations to calculate heat transfer coefficients and pressure drop under different flow regimes. The linear character of the formulation allows the identification of the global optimum, even using conventional optimization algorithms. The proposed MILP formulation with the Bell-Delaware method is able to identify feasible solutions for the design of heat exchangers at a lower cost than those obtained through conventional design formulations in the literature. Comparisons with the Kern method also indicate an average 22% difference (usually lower) in area.